

Nonstationary, Nonparametric, Nonseparable Bayesian Spatio-Temporal Modeling Using Kernel Convolution of Order Based Dependent Dirichlet Process

Moumita Das and Sourabh Bhattacharya¹

¹Moumita Das is a postdoctoral research fellow at Basque Center for Applied Mathematics, Spain and Sourabh Bhattacharya is an Associate Professor in Interdisciplinary Statistical Research Unit, Indian Statistical Institute, 203, B. T. Road, Kolkata 700108. Corresponding e-mail: sourabh@isical.ac.in.

Abstract

Spatio-temporal processes are important modeling tools for varieties of problems in environmental science, biological science, geographical science, etc. It is generally assumed that the underlying model is parametric, typically a Gaussian process, and that the covariance function is stationary and separable. That this structure does not need to be always realistic have been perceived by many researchers and attempts have been made to construct nonparametric processes consisting of neither stationary nor separable covariance functions. But, as we elucidate, some desirable and important spatio-temporal properties are not guaranteed by the existing approaches, thus calling for further innovative ideas.

In this article, using kernel convolution of order based dependent Dirichlet process ([Griffin and Steel \(2006\)](#)) we construct a nonstationary, nonseparable, nonparametric space-time process, which, as we show, satisfies desirable properties, and includes the stationary, separable, parametric processes as special cases. We also investigate the smoothness properties of our proposed model.

Since our model entails an infinite random series, for Bayesian model fitting purpose we must either truncate the series or more appropriately consider a random number of summands, which renders the model dimension a random variable. We attack the variable dimensionality problem using Transdimensional Transformation based Markov Chain Monte Carlo introduced by [Das and Bhattacharya \(2019b\)](#), which can update all the variables and also change dimensions in a single block using essentially a single random variable drawn from some arbitrary density defined on a relevant support. For the sake of completeness we also address the problem of truncating the infinite series by providing a uniform bound on the error incurred by truncating the infinite series.

We illustrate the effectiveness of our model and methodologies on a simulated data set and demonstrate that our approach significantly outperforms that of [Fuentes and Reich \(2013\)](#) which is based on principles somewhat similar to ours. We also fit two real, spatial and spatio-temporal datasets with our approach and obtain quite encouraging results in both the cases.

Keywords: *Kernel convolution; Nonstationary; Nonseparable; Order based Dependent Dirichlet Process; Spatio-temporal data; Transdimensional Transformation based Markov Chain Monte Carlo.*

Contents

Contents	1
1 Introduction	3
2 Overview of other available nonstationary approaches	5
2.1 Parametric approaches	5
2.2 Nonparametric approaches	8
3 Kernel convolution of ODDP	10
3.1 Overview of ODDP	10
3.2 Kernel convolution of ODDP	11
4 Continuity and smoothness properties of our model	14
5 Truncation of the infinite summand	16
6 Choice of kernel, prior distributions and computational region	16
6.1 Elicitation of hyperparameters of the underlying ODDP	17
6.1.1 Choice of G_0	17
6.1.2 Prior selection for α	17
6.1.3 Prior selection for λ	18
6.2 Computational region	18
7 Joint posterior and a briefing of TTMCMC for updating parameters in our variable dimensional modeling framework	18
8 Simulation study	19
8.1 A nonstationary non-Gaussian data generating process	19
8.2 Results of fitting our model to the simulated data	20
8.2.1 Leave-one-out cross-validation	20
8.2.2 Correlation Analysis	20
8.3 Comparative study with respect to FR's approach	23
8.3.1 Correlation Analysis	23
9 Real data analysis	23
9.1 Spatial data	23
9.1.1 Calculating the W126 metric	26
9.2 Spatio-temporal data analysis	28
9.2.1 Data	28
9.2.2 Model	30
9.2.3 Implementation	31
9.2.4 Leave-one-out cross validation	31

10 Summary and conclusion	32
S-1Proof of Theorem 1	36
S-2Proof of Theorem 2	36
S-3Proof of Theorem 4	38
S-4Proof of Theorem 7	38
S-5Proof of Theorem 9	40
S-6Proof of Theorem 10	41
S-7Transdimensional transformation based Markov chain Monte Carlo (TTM- CMC)	45
S-7.1 Notation	46
S-7.2 Illustration of TTMC MC with a simple example	46
S-7.3 General TTMC MC algorithm for jumping more than one dimensions at a time when several sets of parameters are related	48
S-7.4 Detailed balance	50
S-8TTMC MC algorithm for our spatio-temporal model	51
S-9Simulation study	56
S-9.1 Algorithm for generating the synthetic data	56
S-10Real data analysis	58
S-10.1 Spatial Data	58
S-10.2 Spatio-temporal Data	60
Bibliography	62

1 Introduction

Recent years have witnessed considerable amount of research on spatial and spatio-temporal modeling. The major inferential objectives of spatio-temporal modeling are to predict a plausible value at some point in space and time, forecasting the future value at some location, and to make inference about the parameters of the spatio-temporal processes. A model must take account of spatio-temporal dependence structure of the given process. It is common practice to assume that the underlying spatial or spatio-temporal process is stationary and isotropic Gaussian process, as it facilitates prediction. In particular, the geostatistical method of kriging assumes a Gaussian process structure for the unknown spatial or spatio-temporal field and focuses on calculating the optimal linear predictor of the field. When performing kriging, researchers generally assume a stationary, often isotropic, covariance function. The covariance of responses at any two locations is assumed to be a function of the separation vector or of the distance between locations, but not a function of the actual locations. Researchers often estimate the parameters of an isotropic covariance function from the semivariogram, the estimation of which is based on the squared differences between the responses as a function of the distance between locations. The standard kriging approach allows one to flexibly estimate a smooth spatial field, with no pre-specified parametric stochastic model for the data. However, these approaches have several drawbacks. The most important is that the true covariance structure may not be stationary. This is because there may be local influences affecting the correlation structure of the random process. For instance, orographic effects influence the atmospheric transport of pollutants, and result in a correlation structure that depends on different spatial locations (Guttorp and Sampson (1994)). If one is modelling an environmental variable across the United States, the field is likely to be much more smooth in the topographically-challenged Great Plains than in the Rocky Mountains. This is manifested as different covariance structures in those two regions. Assuming a stationary covariance structure will result in oversmoothing the field in the mountains and undersmoothing the field in great plains (Paciorek (2003)).

Realizing the limitations of stationary parametric processes (almost invariably Gaussian processes) researchers have come up with many novel ideas for constructing nonstationary and/or nonparametric processes. The first significant work in the framework of nonstationary parametric processes is by Sampson and Guttorp (1992), who proposed an approach based on spatial deformation. This work is followed up by Damian *et al.* (2001) and Schmidt and O'Hagan (2003), providing the corresponding Bayesian generalizations. Nonstationarity has been induced in parametric space-time models by Haas (1995) by proposing a moving window regression residual kriging. A similar approach has been proposed by Nott and Dunsmuir (2002). Higdon (1998) (see also Higdon *et al.* (1999), Higdon (2001)) proposed a kernel convolution approach for inducing nonstationarity in Gaussian processes. Similar approaches are also proposed by Fuentes and Smith (2001) and Fuentes (2002). Approaches that attempt to model the underlying process as nonparametric, in addition to modeling the covariance structure as nonstationary are more recent in comparison, the approach of Gelfand *et al.* (2005) based on Dirichlet processes (see, for example, Ferguson (1973), Ferguson (1974)) being the first in this regard; see Duan *et al.* (2007) for a generalization. Duan *et al.* (2009) use stochastic differential equations to construct a nonstationary, non-Gaussian process. We

discuss these proposals in some detail in Section 2.

Fuentes and Reich (2013) proposed a nonparametric nonstationary model based on kernel processes mixing. In their study they showed that their proposed model outperformed all other models for several types of simulation designs (Stationary Gaussian, Nonstationary Gaussian, Stationary Non-Gaussian, Nonstationary Non-Gaussian). They illustrated their model with application to the monthly average values of ammonium and nitrate at 209 monitoring stations in the US. Their proposed nonstationary non-Gaussian model reduced the root mean square error (RMSE) by 24% for ammonium and 18% for nitrate when compared to the nonstationary Gaussian approach. RMSE also reduced compared to stationary Gaussian and stationary non-Gaussian approaches, although the gain is more moderate in these cases.

Griffin and Steel (2006) (henceforth, GS) proposed the novel order-based dependent Dirichlet processes (ODDP). They introduced a framework for nonparametric modeling with dependence on continuous covariates. Dependence is induced through relevant weights utilizing similarities in the covariate information. Each weight is a transformation of independently and identically distributed (*iid*) random variables. GS derived an ordering π of these random variables at each covariate value such that distributions for similar covariate values are associated with similar orderings and thus will be close. These orderings combined with Poisson point process give a simple analytical expression for the correlation function of the distributions, which ensures that if two points are similar in the covariate space they will get higher correlation compared to the points that are not. Furthermore when the distance between two points is large enough in the covariate space, the correlation approaches zero. In spatial/spatio-temporal context, it translates into the fact that when two observations are widely separated in space/space-time, the model based correlations tend to zero. But the ODDP process suffers from the limitation of being stationary.

Preserving all the desirable properties of the correlation function of ODDP, we attempt to incorporate further flexibility in our spatial/temporal/spatio-temporal model in terms of nonstationarity and nonseparability through our proposed kernel convolution based methodology. Specifically, we propose a new class of spatial/temporal/spatio-temporal models that is nonparametric, nonstationary, nonseparable, and such that the correlation tends to zero if either of spatial and temporal distance tends to infinity. All these properties are desirable in real data scenarios, and hence any effective, realistic model must satisfy these properties. Unfortunately, such a wholesome model does not seem to exist in the current literature, as we point out in our review. Hence, this paper is an attempt to create one class of such realistic stochastic processes. We illustrate our ideas not only with simulation study, but also with a real spatial data on ozone and a real spatio-temporal data on particulate matters. That these data sets are both strictly and weakly nonstationary, are inferred in a separate paper by Roy and Bhattacharya (2020) using novel Bayesian methodologies. In this article, we further show that the empirical correlations for the spatio-temporal data tend to zero as the spatio-temporal lags increase. A similar property is also expected of the spatial ozone data, but the small size of the data did not permit such rigorous analysis. Moreover, these data sets are far from Gaussianity, as simple quantile-quantile plots indicate. As we argued, these properties are expected in reality, and the general class of nonparametric spatio-temporal models that we propose, provides adequate fits to both these data sets. Moreover, comparison of our analyses with one of the most competent existing models, shows that our model is possibly

indeed worth pursuing.

The rest of our paper is structured as follows. In Section 2 we provide a brief overview of the existing approaches to construction of nonstationary, nonseparable space-time processes in both parametric and nonparametric frameworks, arguing that not all desirable properties are necessarily accounted for in these approaches. Such issues necessitate development of new approaches to construction of nonstationary, nonparametric, nonseparable space-time models. In Section 3 we introduce our proposed space-time model based on kernel convolution of ODDP and show that it satisfies the properties that are not guaranteed by the existing models. We investigate continuity and smoothness properties of our model in Section 4. Since our proposed model involves a random infinite series, for model fitting one needs to either truncate the series or assume a random number of summands and adopt variable dimensional Markov Chain Monte Carlo (MCMC) approaches. Although we adopt the latter framework for our applications, and implement the recently developed Transdimensional Transformation based Markov Chain Monte Carlo (TTMCMC) (Das and Bhattacharya (2019b)) for simulating from our variable dimensional model, for the sake of completeness we also investigate the truncation approach. Indeed, in Section 5 we consider the difference between the prior predictive models with and without truncation of the random infinite series, providing a bound that depends upon the truncation parameter. Thus, the truncation parameter can be chosen so that the bound falls below any desired level. In Section 6 we discuss the choice of suitable kernels, prior distributions and choice of the spatio-temporal domain that is relevant for computational purpose. We describe the joint posterior distribution associated with our model, and provide a brief discussion of TTMCMC in Section 7. We detail a simulation study illustrating the performance of our model and comparison with Fuentes and Reich (2013) in Section 8. Indeed, the model of Fuentes and Reich (2013), in spite of being very different from our ideas, comes closest to our model conceptually, among the existing models. In Section 9 we consider application of our ideas to two real datasets: a spatial ozone dataset, and a spatio-temporal dataset on particulate matters. Finally, we summarize our contributions and provide concluding remarks in Section 10.

Proofs of our results and requisite details of TTMCMC, particularly in the context of our spatio-temporal model, and details regarding generation of the data for the simulation experiment, are provided in the supplement Das and Bhattacharya (2019a), whose sections and algorithms have the prefix “S-” when referred to in this paper.

2 Overview of other available nonstationary approaches

2.1 Parametric approaches

The deformation approaches of Sampson and Guttorp (1992), Damian *et al.* (2001), and Schmidt and O’Hagan (2003) are based on Gaussian processes. In these approaches replications of the data are necessary, which the authors relate to temporal independence of the data. This also means that space-time data can not be modeled using these approaches, unless all the temporal dependence can be captured through a trend term in the mean structure. Moreover, in the deformation-based approaches model based theoretical correlations between

random observations separated by large enough distances need not necessarily tend to zero. Letting $Y(\mathbf{s}, t)$ denote the response at spatial location \mathbf{s} and time t , [Sampson and Guttorp \(1992\)](#) deal with the variogram of the following form:

$$\text{Var}(Y(\mathbf{s}_1, t) - Y(\mathbf{s}_2, t)) = f(\|\mathbf{d}(\mathbf{s}_1, t) - \mathbf{d}(\mathbf{s}_2, t)\|), \quad (2.1)$$

for any $\mathbf{s}_1, \mathbf{s}_2, t$, where f is an appropriate monotone function and \mathbf{d} is a one-to-one nonlinear mapping. The technique of [Sampson and Guttorp \(1992\)](#) involves appropriately approximating f by \hat{f} using the multidimensional scaling method, and obtaining a configuration of points $\{\mathbf{u}_1, \dots, \mathbf{u}_n\}$ in a “deformed” space where the process is assumed isotropic. Then, using thin-plate splines, a nonlinear approximation of \mathbf{d} , which we denote by $\hat{\mathbf{d}}$, is determined such that $\hat{\mathbf{d}}(\mathbf{s}_i) \approx \mathbf{u}_i$, for $i = 1, \dots, n$. Bayesian versions of the key idea have been described in [Damian *et al.* \(2001\)](#), who use random thin-plate splines and [Schmidt and O’Hagan \(2003\)](#), who use Gaussian process to implement the nonlinear transformation \mathbf{d} . Rather than estimate f nonparametrically, both specify a parametric functional form from a valid class of such monotone functions.

As is clear, since large differences $\|\mathbf{s}_1 - \mathbf{s}_2\|$ does not imply that $\|\mathbf{d}(\mathbf{s}_1) - \mathbf{d}(\mathbf{s}_2)\|$ is also large, the model based correlations between two observations widely separated need not necessarily tend to zero, in either of the aforementioned deformation-based approaches.

The kernel convolution approaches of [Higdon *et al.* \(1999\)](#), [Higdon \(2001\)](#), and [Fuentes and Smith \(2001\)](#) overcome some of the difficulties of the deformation approach. In these approaches data replication is not necessary, and for appropriate choices of the kernel, stationarity, nonstationarity, separability, and nonseparability can be achieved with respect to spatio-temporal data. In the approach of [Higdon *et al.* \(1999\)](#), [Higdon \(2001\)](#),

$$Y(\mathbf{x}) = \int K(\mathbf{x}, \mathbf{u})Z(\mathbf{u})d\mathbf{u}, \quad (2.2)$$

where K is a kernel function and $Z(\cdot)$ is a white noise process. Then the covariance between $Y(\mathbf{x}_1)$ and $Y(\mathbf{x}_2)$ is given by

$$C(\mathbf{x}_1, \mathbf{x}_2) = \int K(\mathbf{x}_1, \mathbf{u})K(\mathbf{x}_2, \mathbf{u})d\mathbf{u}. \quad (2.3)$$

In general, this does not depend upon \mathbf{x}_1 and \mathbf{x}_2 only through $\mathbf{x}_1 - \mathbf{x}_2$, thus achieving nonstationarity. However, it is clear from the covariance structure (2.3) that $C(\mathbf{x}_1, \mathbf{x}_2)$ does not generally tend to zero as $d = \|\mathbf{x}_1 - \mathbf{x}_2\| \rightarrow \infty$. But for separable space-time processes (see, for example, [Cressie and Wikle \(2011\)](#) for various illustrations) related to representation (2.2) this property holds under the additional assumption of isotropy with respect to either space or time. We elaborate this below.

Although representation (2.2) can not achieve separability with respect to space and time, a modified representation of the following form does:

$$Y(\mathbf{s}, t) = \int K_1(\mathbf{s}, \mathbf{u})K_2(t, \mathbf{v})Z_1(\mathbf{u})Z_2(\mathbf{v})d\mathbf{u}d\mathbf{v}. \quad (2.4)$$

In (2.4), K_1, K_2 are two kernel functions, and $Z_1(\mathbf{x}), Z_2(\mathbf{x})$ are independent white noise processes. Now the covariance is given by

$$\begin{aligned} C((\mathbf{s}_1, t_1), (\mathbf{s}_2, t_2)) &= \int K_1(\mathbf{s}_1, \mathbf{u})K_1(\mathbf{s}_2, \mathbf{u})K_2(t_1, \mathbf{v})K_2(t_2, \mathbf{v})d\mathbf{u}d\mathbf{v} \\ &= C_1(\mathbf{s}_1, \mathbf{s}_2) \times C_2(t_1, t_2), \end{aligned} \quad (2.5)$$

where

$$C_1(\mathbf{s}_1, \mathbf{s}_2) = \int K_1(\mathbf{s}_1, \mathbf{u})K_1(\mathbf{s}_2, \mathbf{u})d\mathbf{u}, \quad (2.6)$$

$$C_2(t_1, t_2) = \int K_2(t_1, \mathbf{v})K_2(t_2, \mathbf{v})d\mathbf{v}, \quad (2.7)$$

exhibiting separability. Further assuming that either of C_1 or C_2 is isotropic, it follows that if either of $d_1 = \|\mathbf{s}_1 - \mathbf{s}_2\|$ or $d_2 = |t_1 - t_2|$ tends to infinity, the covariance given by (2.5) tends to zero even though either of C_1 or C_2 is nonstationary. But if both C_1 and C_2 are nonstationary, then this result need not hold.

The approach of Fuentes and Smith (2001) comes close towards solving the problem of zero covariance in the limit with large enough separation between observations, which we now explain. They model the underlying process as

$$Y(\mathbf{x}) = \int K(\mathbf{x} - \mathbf{u})Z_{\theta(\mathbf{u})}d\mathbf{u}, \quad (2.8)$$

where $Z_{\theta}(\mathbf{x}); \mathbf{x} \in D$ is a family of independent, stationary Gaussian processes indexed by θ , where the covariance of $Z_{\theta(\mathbf{u})}$ is given by

$$\text{Cov}(Z_{\theta(\mathbf{u})}(\mathbf{x}_1), Z_{\theta(\mathbf{u})}(\mathbf{x}_2)) = C_{\theta(\mathbf{u})}(\mathbf{x}_1 - \mathbf{x}_2). \quad (2.9)$$

Then, the covariance between $Y(\mathbf{x}_1)$ and $Y(\mathbf{x}_2)$ is given by

$$C(\mathbf{x}_1, \mathbf{x}_2; \theta) = \int K(\mathbf{x}_1 - \mathbf{u})K(\mathbf{x}_2 - \mathbf{u})C_{\theta(\mathbf{u})}(\mathbf{x}_1 - \mathbf{x}_2)d\mathbf{u}. \quad (2.10)$$

For practical purposes, Fuentes and Smith (2001) approximate $Y(\mathbf{x})$ with

$$\hat{Y}(\mathbf{x}) = \frac{1}{M} \sum_{m=1}^M K(\mathbf{x} - \mathbf{u}_m)Z_{\theta(\mathbf{u}_m)}(\mathbf{x}), \quad (2.11)$$

and $C(\mathbf{x}_1, \mathbf{x}_2; \theta)$ by

$$\hat{C}(\mathbf{x}_1, \mathbf{x}_2; \theta) = \frac{1}{M} \sum_{m=1}^M K(\mathbf{x}_1 - \mathbf{u}_m)K(\mathbf{x}_2 - \mathbf{u}_m)C_{\theta(\mathbf{u}_m)}(\mathbf{x}_1 - \mathbf{x}_2), \quad (2.12)$$

where $\{\mathbf{u}_1, \dots, \mathbf{u}_M\}$ can be thought of as a set of locations drawn independently from the domain D . Assuming that the family of independent Gaussian processes $Z_{\theta}(\mathbf{x}); \mathbf{x} \in D$ is also isotropic, it follows, using the fact that M is finite, that $\hat{C}(\mathbf{x}_1, \mathbf{x}_2; \theta) \rightarrow 0$ as $\|\mathbf{x}_1 - \mathbf{x}_2\| \rightarrow \infty$

since $C_{\theta(u_m)}(\mathbf{x}_1 - \mathbf{x}_2) \rightarrow 0$ for each $m = 1, \dots, M$. However, this of course does not guarantee that $\hat{C}(\mathbf{x}_1, \mathbf{x}_2; \boldsymbol{\theta}) \rightarrow 0$ as $M \rightarrow \infty$. That is, this does not necessarily imply that $C(\mathbf{x}_1, \mathbf{x}_2; \boldsymbol{\theta}) \rightarrow 0$.

A nonstationary process has been constructed by [Chang et al. \(2011\)](#), by representing the underlying process as a linear combination of basis functions and stationary Gaussian processes. This approach also does not guarantee that the correlation tends to zero if $\|\mathbf{x}_1 - \mathbf{x}_2\| \rightarrow \infty$. For other available parametric approaches to nonstationarity we refer to the references provided in [Chang et al. \(2011\)](#).

2.2 Nonparametric approaches

[Gelfand et al. \(2005\)](#) seem to be the first to propose a nonstationary, nonparametric Bayesian model based on Dirichlet process mixing. They represent the random field $\mathbf{Y}_D = \{Y(\mathbf{x}); \mathbf{x} \in D\}$ as $\sum_{\ell=1}^{\infty} w_{\ell} \delta_{\boldsymbol{\theta}_{\ell, D}}$, where $\boldsymbol{\theta}_{\ell, D} = \{\theta_{\ell}(\mathbf{x}); \mathbf{x} \in D\}$ are realizations from a specified stationary Gaussian process, which we denote as \mathbf{G}_0 , $w_1 = V_1$, $w_{\ell} = V_{\ell} \prod_{r=1}^{\ell-1} (1 - V_r)$ for $\ell \geq 2$, where $V_r \stackrel{iid}{\sim} \text{Beta}(1, \alpha)$; $r = 1, 2, \dots$. Thus, a random process \mathbf{G} is induced on the space of processes of \mathbf{Y}_D with \mathbf{G}_0 being the ‘‘central’’ process. [Gelfand et al. \(2005\)](#) assume the space-time data $\mathbf{Y}_t = (Y(\mathbf{s}_1, t), \dots, Y(\mathbf{s}_n, t))'$ to be time-independent for $t = 1, \dots, T$, which is the same assumption of data replication used in the deformation-based approaches. The temporal-independence assumption allows [Gelfand et al. \(2005\)](#) to model the data as follows: for $t = 1, \dots, T$, $\mathbf{Y}_t \stackrel{iid}{\sim} \mathbf{G}^{(n)}$ and $\mathbf{G}^{(n)} \sim DP(\mathbf{G}_0^{(n)})$, where $\mathbf{G}^{(n)}$ and $\mathbf{G}_0^{(n)}$ denote the n -variate distributions corresponding to the processes \mathbf{G} and \mathbf{G}_0 . The development leads to the following covariance structure: for any $\mathbf{s}_1, \mathbf{s}_2, t$,

$$\text{Cov}(Y(\mathbf{s}_1, t), Y(\mathbf{s}_2, t) \mid \mathbf{G}) = \sum_{\ell=1}^{\infty} w_{\ell} \theta_{\ell}(\mathbf{s}_1) \theta_{\ell}(\mathbf{s}_2) - \left\{ \sum_{\ell=1}^{\infty} w_{\ell} \theta_{\ell}(\mathbf{s}_1) \right\} \left\{ \sum_{\ell=1}^{\infty} w_{\ell} \theta_{\ell}(\mathbf{s}_2) \right\}, \quad (2.13)$$

which is nonstationary. However, marginalized over \mathbf{G} , the covariance between $Y(\mathbf{s}_1, t)$ and $Y(\mathbf{s}_2, t)$ turns out to be stationary. Since, in [Gelfand et al. \(2005\)](#), the Bayesian inference of the data $\mathbf{Y}_1, \dots, \mathbf{Y}_n$ proceeds by integrating out $\mathbf{G}^{(n)}$, the entire flavour of nonstationarity is lost. Also, given \mathbf{G} , (2.13) is nonstationary but does not necessarily converge to zero if $\|\mathbf{s}_1 - \mathbf{s}_2\| \rightarrow \infty$.

[Duan et al. \(2007\)](#) attempt to generalize the model of [Gelfand et al. \(2005\)](#) by specifying \mathbf{G} as

$$Pr\{Y(\mathbf{x}_1) \in A_1, \dots, Y(\mathbf{x}_n) \in A_n\} = \sum_{i_1=1}^{\infty} \cdots \sum_{i_n=1}^{\infty} p_{i_1, \dots, i_n} \delta_{\theta_{i_1}(\mathbf{x}_1)}(A_1) \cdots \delta_{\theta_{i_n}(\mathbf{x}_n)}(A_n), \quad (2.14)$$

where θ_j 's are *iid* \mathbf{G}_0 as in [Gelfand et al. \(2005\)](#), and $\{p_{i_1, \dots, i_n} \geq 0 : \sum_{i_1=1}^{\infty} \cdots \sum_{i_n=1}^{\infty} p_{i_1, \dots, i_n} = 1\}$ determine the site-specific joint selection probabilities, which also must satisfy simple constraints to ensure consistency. The resulting conditional covariance (conditional on \mathbf{G}) and the marginal covariance are somewhat modified versions of those of [Gelfand et al. \(2005\)](#), but now even the marginal covariance is nonstationary. By choosing \mathbf{G}_0 to be an isotropic Gaussian process it can be ensured that the marginal covariance tends to zero as

two observations are widely separated, but the same can not be ensured for the conditional covariance. Moreover, replications of the data is necessary even for this generalized version of [Gelfand *et al.* \(2005\)](#), and modeling temporal dependence is precluded as before. A methodology very similar to that of [Duan *et al.* \(2007\)](#) is proposed in [Petrone *et al.* \(2009\)](#).

Although the aforementioned approaches are temporally independent, [Kottas *et al.* \(2007\)](#) have considered a first order autoregressive setup to model temporal dependence as a simple parametric temporal extension of the temporally independent model proposed in [Gelfand *et al.* \(2005\)](#).

A nonstationary, nonseparable non-Gaussian spatiotemporal process has been constructed by [Duan *et al.* \(2009\)](#) using discretized versions of stochastic differential equations, but again, the correlations between largely separated observations do not necessarily tend to zero under their model. Also, stationarity or separability can not be derived as special cases of this approach.

A flexible approach using kernel convolution of Lévy random measures has been detailed in [Wolpert *et al.* \(2011\)](#), but even this approach does not guarantee that correlations tend to zero for largely separated distances for arbitrarily chosen kernels.

An univariate and multivariate nonparametric spatial model based on kernel process mixing has been proposed by [Fuentes and Reich \(2013\)](#) (henceforth, FR). In this work, the idea of stick-breaking prior of [Sethuraman \(1994\)](#) was extended to a spatial set up. A different, unknown distribution was assigned to each location, with a series of space-dependent kernel functions that have a space-varying bandwidth parameter. Essentially, the Beta-distributed sequence $\{V_r : r = 1, 2, \dots\}$ in the stick-breaking construction of the traditional Dirichlet process are multiplied with a sequence of space-dependent kernels $\{K_r(\mathbf{s}) : r = 1, 2, \dots\}$, and the \mathbf{G}_0 -distributed sequence is replaced with an isotropic Gaussian process with nonstationary variance. The kernel functions attempt to impose a natural ranking for the different mixture components based on distances of locations to knots, which seems to be an alternative way to mimic the role of the orderings imposed in GS. As the bandwidths of the kernels tend to zero uniformly, the covariance conditional on $\{V_r : r = 1, 2, \dots\}$ tends to the isotropic covariance of the underlying Gaussian process. Marginally, the covariance structure, albeit nonstationary, need not yield zero covariance even if the distance between the locations tend to infinity. Moreover, this idea has been considered only for spatial modeling. Although it is simple to extend the method to spatio-temporal situations, enforcing separability is needed, does not seem to be as straightforward.

Compared to the vast literature on continuous nonstationary spatio temporal processes, there are very few methods available to model non-smooth covariance structures over the space or both space-time ([Guttorp *et al.* \(2013\)](#)). Among them, [Kim *et al.* \(2005\)](#) developed a method based on a Bayesian approach to Voronoi tessellation. Since our approach hinges upon the idea of GS, and smoothness properties of the ODDP depends on the order generating process, it is discontinuous in nature. We will discuss in details the smoothness properties of our model in Section 4. Another possible source of nonstationarity is the local influence of some covariates on the spatial process of interest. Recently, there have been some proposals in the literature that account for covariate information in the covariance structure of spatial and spatio-temporal processes; see, for example, [Reich *et al.* \(2011\)](#), [Schmidt *et al.* \(2011\)](#), [Neto *et al.* \(2014\)](#), [Ingebrigtsen *et al.* \(2014\)](#), [Risser and Calder \(2015\)](#), [Gilani *et al.* \(2016\)](#), [Risser *et al.* \(2019\)](#). Since in our model we introduce dependence via the ODDP, where

weights in the Sethuraman representation are dependent on the covariate information, we can efficiently incorporate the local influence of covariate information into our model. The covariate information can also be incorporated in the kernel that we convolve the ODDP with.

In the next section we introduce our idea based on kernel convolution of ODDP and show that it overcomes the issues faced by the traditional approaches to construction of flexible space-time models.

3 Kernel convolution of ODDP

Before introducing our proposal, it is necessary to first provide an overview of ODDP.

3.1 Overview of ODDP

In order to induce spatial dependence between observations at different locations GS modify the nonparametric stick-breaking construction of Sethuraman (1994) in the following way: for each point $\mathbf{x} \in D$, where D is some specified domain, they define the distribution:

$$G_{\mathbf{x}} \stackrel{\mathcal{D}}{=} \sum_{i=1}^{\infty} p_i(\mathbf{x}) \delta_{\boldsymbol{\theta}_{\pi_i(\mathbf{x})}}, \quad (3.1)$$

where

$$p_i(\mathbf{x}) = V_{\pi_i(\mathbf{x})} \prod_{j < i} (1 - V_{\pi_j(\mathbf{x})}). \quad (3.2)$$

In (3.1) and (3.2), $\boldsymbol{\pi}(\mathbf{x}) = (\pi_1(\mathbf{x}), \pi_2(\mathbf{x}), \dots)$ denotes the ordering at \mathbf{x} , where $\pi_i(\mathbf{x}) \in \{1, 2, \dots\}$ and $\pi_i(\mathbf{x}) = \pi_j(\mathbf{x})$ if and only if $i = j$. For $j = 1, 2, \dots$, the parameters $\boldsymbol{\theta}_j \stackrel{iid}{\sim} G_0$, where G_0 is some specified parametric centering distribution, and $V_j \stackrel{iid}{\sim} \text{Beta}(1, \alpha)$, where $\alpha > 0$ is a specified parameter. The process associated with specification (3.1) is the ODDP. Clearly, if $\pi_i(\mathbf{x}) = i$ for each \mathbf{x} and i , then the Dirichlet process (DP) results at all locations.

GS construct $\boldsymbol{\pi}(\mathbf{x})$ in a way such that it is associated with the realization of a point process. Specifically, they consider a stationary Poisson process Φ and a sequence of sets $U(\mathbf{x})$ for $\mathbf{x} \in D$, the latter determining the relevant region for the ordering purpose. In the case of only spatial problems, if $\mathbf{x} \in D \subset \mathbb{R}^d$, for $d \geq 1$, then GS suggest $U(\mathbf{x}) = D$ for all $\mathbf{x} \in D$ as a suitable construction of $U(\mathbf{x})$. For time series problems they suggest $D = \mathbb{R}$ and $U(x) = (-\infty, x]$. When $\mathbf{x} = (\mathbf{s}', t)'$, that is, when \mathbf{x} consists of both spatial and temporal co-ordinates, for our modeling purpose, we use $U(\mathbf{x}) = D \times (-\infty, t]$.

Letting $\{\mathbf{z}_1, \mathbf{z}_2, \dots\}$ denote a realization of the stationary Poisson point process, the ordering $\boldsymbol{\pi}(\mathbf{x})$ is chosen to satisfy $\|\mathbf{x} - \mathbf{z}_{\pi_1(\mathbf{x})}\| < \|\mathbf{x} - \mathbf{z}_{\pi_2(\mathbf{x})}\| < \|\mathbf{x} - \mathbf{z}_{\pi_3(\mathbf{x})}\| < \dots$, where $\|\cdot\|$ is a distance measure and $\mathbf{z}_{\pi(\mathbf{x})} \in \Phi \cap U(\mathbf{x})$. Thus, although the set of probabilities $\{p_i(\mathbf{x}); i = 1, 2, \dots\}$ remains same for all locations, they are randomly permuted. This random permutation, in turn, induces spatial dependence. Assuming a homogeneous Poisson point process with intensity λ , ODDP is characterized by G_0 , α , and λ . We express dependence of ODDP on these parameters by $\text{ODDP}(\alpha G_0, \lambda)$.

Assuming that data $\{y_1, \dots, y_n\}$ are available at sites $\{\mathbf{x}_1, \dots, \mathbf{x}_n\}$, GS embed the ODDP in a hierarchical Bayesian model:

$$\begin{aligned} y_i &\sim f_{\boldsymbol{\theta}_i}(\cdot) \\ \boldsymbol{\theta}_i &\sim G_{\mathbf{x}_i} \\ G_{\mathbf{x}_i} &\sim \text{ODDP}(\alpha G_0, \lambda). \end{aligned}$$

Note that the same theory can be extended to space-time situations with $\mathbf{x} = (\mathbf{s}', t)'$, where \mathbf{s} stands for the spatial location and t stands for the time point.

Next, we introduce our proposed idea of kernel convolution of ODDP.

3.2 Kernel convolution of ODDP

We consider the following model for the data $\mathbf{Y} = \{y_1, \dots, y_n\}$ at locations/times $\{\mathbf{x}_i = (\mathbf{s}'_i, t_i)'; i = 1, \dots, n\}$:

$$y_i = f(\mathbf{x}_i) + \epsilon_i, \quad (3.3)$$

where $\epsilon_i \stackrel{iid}{\sim} N(0, \sigma^2)$, for unknown σ^2 . We represent the spatio-temporal process $f(\mathbf{x})$ as a convolution of ODDP $G_{\mathbf{x}}$ with a smoothing kernel $K(\mathbf{x}, \cdot)$:

$$f(\mathbf{x}) = \int K(\mathbf{x}, \boldsymbol{\theta}) dG_{\mathbf{x}}(\boldsymbol{\theta}) = \sum_{i=1}^{\infty} K(\mathbf{x}, \boldsymbol{\theta}_{\pi_i(\mathbf{x})}) p_i(\mathbf{x}) \quad \forall \mathbf{x} \in D \subseteq \mathbb{R}^d, \quad (3.4)$$

$d (\geq 1)$ being the dimension of \mathbf{x} . Thus, given $\mathbf{G}_{\mathbf{x}_i}$,

$$y_i \sim N(f(\mathbf{x}_i), \sigma^2), \quad (3.5)$$

the normal distribution with mean $f(\mathbf{x}_i)$ of the form (3.4) and variance σ^2 . Thus, given $\mathbf{G}_{\mathbf{x}_i}$ and $\mathbf{G}_{\mathbf{x}_j}$, y_i and y_j are independent.

Since the ODDP model of GS can also be viewed as a convolution, it is important to clarify its differences with (3.4) and (3.5). Indeed, note that with respect to GS, the response data y_i has the following distribution:

$$y_i \sim \int f_{\boldsymbol{\theta}}(\cdot) dG_{\mathbf{x}_i}(\boldsymbol{\theta}) = \sum_{j=1}^{\infty} f_{\boldsymbol{\theta}_{\pi_j(\mathbf{x}_i)}}(\cdot) p_j(\mathbf{x}_i). \quad (3.6)$$

Thus, under (3.6) (that is, under the model proposed by GS), for any choice of $f_{\boldsymbol{\theta}}$, y_i arises from an infinite mixture with mixture density components $f_{\boldsymbol{\theta}_{\pi_j(\mathbf{x}_i)}}(\cdot)$ and corresponding mixture probabilities $p_j(\mathbf{x}_i)$. On the other hand, our model postulates a normal distribution for y_i via (3.4) and (3.5), where the mean is the kernel convolution given by (3.4). The convolutions given by (3.4) and (3.6) also have different interpretations. The latter is a density, whereas, the former is any real-valued function. Note that unlike the case of (3.3), given $\mathbf{G}_{\mathbf{x}_i}$ and $\mathbf{G}_{\mathbf{x}_j}$, y_i and y_j are not independent if $f_{\boldsymbol{\theta}}(\cdot) = \delta_{\boldsymbol{\theta}}(\cdot)$, that is, when $y_i \sim \mathbf{G}_{\mathbf{x}_i}$. Further implications, with respect to nonstationarity and correlation structure tending to zero with widely separated distances, are discussed following Theorem 5.

In spatio-temporal processes we have to specify the joint distribution for an uncountable number of random variables. But, in practice we observe the process at a finite number of locations only. To infer about the process, it is better to have finite moments, that ensures existence of the posterior distribution. It also facilitates the prediction of the process at an arbitrary unobserved location. The following theorem, the proof of which is presented in Section S-1 of the supplement, gives an expression of the expectation of $f(\mathbf{x})$.

Theorem 1. *Let $\int |K(\mathbf{x}, \boldsymbol{\theta})| dG_0(\boldsymbol{\theta}) < \infty$. Then $\int |K(\mathbf{x}, \boldsymbol{\theta})| dG_{\mathbf{x}}(\boldsymbol{\theta}) < \infty$ with probability one, and*

$$E(f(\mathbf{x})) = E \int K(\mathbf{x}, \boldsymbol{\theta}) dG_{\mathbf{x}}(\boldsymbol{\theta}) = \int K(\mathbf{x}, \boldsymbol{\theta}) dEG_{\mathbf{x}}(\boldsymbol{\theta}) = \int K(\mathbf{x}, \boldsymbol{\theta}) dG_0(\boldsymbol{\theta}) = E_{G_0} K(\mathbf{x}, \boldsymbol{\theta}).$$

Before deriving the covariance structure of $f(\cdot)$, we define the necessary notation following GS. Let

$$T(\mathbf{x}_1, \mathbf{x}_2) = \{k : \text{there exists } i, j \text{ such that } \pi_i(\mathbf{x}_1) = \pi_j(\mathbf{x}_2) = k\}.$$

For $k \in T(\mathbf{x}_1, \mathbf{x}_2)$, we further define $A_{lk} = \{\pi_j(\mathbf{x}_l) : j < i \text{ where } \pi_i(\mathbf{x}_l) = k\}$, $S_k = A_{1k} \cap A_{2k}$ and $S'_k = A_{1k} \cup A_{2k} - S_k$. Then, the following theorem, the proof of which is deferred to Section S-2 of the supplement, provides an expression for the covariance structure of $f(\cdot)$, which will be our reference point for arguments regarding nonstationarity and other desirable spatial properties in comparison with the existing methods.

Theorem 2. *If $\int |K(\mathbf{x}, \boldsymbol{\theta})| dG_0(\boldsymbol{\theta}) < \infty$ and $\int |K(\mathbf{x}_1, \boldsymbol{\theta})K(\mathbf{x}_2, \boldsymbol{\theta})| dG_0(\boldsymbol{\theta}) < \infty$, then for a fixed ordering at \mathbf{x}_1 and \mathbf{x}_2 ,*

$$\begin{aligned} \text{Cov}(f(\mathbf{x}_1), f(\mathbf{x}_2)) &= \text{Cov}_{G_0}(K(\mathbf{x}_1, \boldsymbol{\theta}), K(\mathbf{x}_2, \boldsymbol{\theta})) \\ &\times \frac{2}{(\alpha + 1)(\alpha + 2)} \sum_{k \in T(\mathbf{x}_1, \mathbf{x}_2)} \left(\frac{\alpha}{\alpha + 2}\right)^{\#S_k} \left(\frac{\alpha}{\alpha + 1}\right)^{\#S'_k}. \end{aligned} \quad (3.7)$$

where

$$\text{Cov}_{G_0}(K(\mathbf{x}_1, \boldsymbol{\theta}), K(\mathbf{x}_2, \boldsymbol{\theta})) = \int K(\mathbf{x}_1, \boldsymbol{\theta})K(\mathbf{x}_2, \boldsymbol{\theta}) dG_0(\boldsymbol{\theta}) - E_{G_0}(K(\mathbf{x}_1, \boldsymbol{\theta}))E_{G_0}(K(\mathbf{x}_2, \boldsymbol{\theta})). \quad (3.8)$$

Corollary 3. *It follows from the above theorem that for $i = 1, 2$, if $\int K^2(\mathbf{x}_i, \boldsymbol{\theta}) dG_0(\boldsymbol{\theta}) < \infty$, then*

$$\text{Var}(f(\mathbf{x}_i)) = \frac{\text{Var}_{G_0}(K(\mathbf{x}_i, \boldsymbol{\theta}))}{\alpha + 1} \quad (3.9)$$

and

$$\text{Corr}(f(\mathbf{x}_1), f(\mathbf{x}_2)) = \text{Corr}_{G_0}(K(\mathbf{x}_1, \boldsymbol{\theta}), K(\mathbf{x}_2, \boldsymbol{\theta})) \times \text{Corr}(G_{\mathbf{x}_1}, G_{\mathbf{x}_2}), \quad (3.10)$$

where

$$\text{Corr}(G_{\mathbf{x}_1}, G_{\mathbf{x}_2}) = \frac{2}{\alpha + 2} \sum_{k \in T(\mathbf{x}_1, \mathbf{x}_2)} \left(\frac{\alpha}{\alpha + 2}\right)^{\#S_k} \left(\frac{\alpha}{\alpha + 1}\right)^{\#S'_k}. \quad (3.11)$$

The expression for the correlation in (3.11) has been obtained by GS.

The above results provide an expression for the correlation conditional on a fixed ordering. To obtain the unconditional correlation it is necessary to marginalize the conditional correlation over the point process Φ . Following GS we also modify the notation as follows: we now let $T(\mathbf{x}_1, \mathbf{x}_2) = \Phi \cap U(\mathbf{x}_1) \cap U(\mathbf{x}_2)$, $A_{\ell k} = A_\ell(\mathbf{z}_k)$, where $A_\ell(\mathbf{z}) = \{\mathbf{w} \in \Phi \cap U(\mathbf{x}_\ell) : \|\mathbf{w} - \mathbf{x}_\ell\| < \|\mathbf{z} - \mathbf{x}_\ell\|\}$, for $\mathbf{z} \in \Phi \cap U(\mathbf{x}_\ell)$. As already mentioned in Section 3.1, when $\mathbf{x} = (\mathbf{s}', t)'$, we define $U(\mathbf{x}) = D \times (-\infty, t]$.

Also, for $\mathbf{z} \in T(\mathbf{x}_1, \mathbf{x}_2)$, we let $S(\mathbf{z}) = A_1(\mathbf{z}) \cap A_2(\mathbf{z})$ and $S'(\mathbf{z}) = A_1(\mathbf{z}) \cup A_2(\mathbf{z}) - S(\mathbf{z})$, which imply that $S(\mathbf{z}) = \{\mathbf{w} \in T(\mathbf{x}_1, \mathbf{x}_2) : \|\mathbf{w} - \mathbf{x}_1\| < \|\mathbf{z} - \mathbf{x}_1\| \text{ and } \|\mathbf{w} - \mathbf{x}_2\| < \|\mathbf{z} - \mathbf{x}_2\|\}$.

We further define, as in GS, $S_{-\mathbf{z}}(\mathbf{z})$ and $S'_{-\mathbf{z}}(\mathbf{z})$ to be translations of $S(\mathbf{z})$ and $S'(\mathbf{z})$, respectively, by $-\mathbf{z}$. Then, the refined Campbell theorem yields, in the case where Φ is a stationary point process with intensity λ :

$$\begin{aligned} \text{Corr}(f(\mathbf{x}_1), f(\mathbf{x}_2)) &= \text{Corr}_{G_0}(K(\mathbf{x}_1, \boldsymbol{\theta}), K(\mathbf{x}_2, \boldsymbol{\theta})) \\ &\times \frac{2\lambda}{\alpha + 2} \int_{U(\mathbf{x}_1) \cap U(\mathbf{x}_2)} \int \left(\frac{\alpha}{\alpha + 2} \right)^{\phi_{-\mathbf{z}}(S_{-\mathbf{z}})} \left(\frac{\alpha}{\alpha + 1} \right)^{\phi_{-\mathbf{z}}(S'_{-\mathbf{z}})} P_0(d\phi) d\mathbf{z} \end{aligned} \quad (3.12)$$

In (3.12), $P_0(d\phi)$ is the Palm distribution of Φ at the origin, and $\phi_{-\mathbf{z}}$ is the realization of Φ translated by $-\mathbf{z}$. Note also that the second factor of the above correlation is the unconditional correlation between $G_{\mathbf{x}_1}$ and $G_{\mathbf{x}_2}$ (see GS).

Remark 4. *It is worth pointing out that unlike Gelfand et al. (2005) who obtained covariance structure conditional on the random process \mathbf{G} , in our case, the covariance structures conditional on the random measures $\mathbf{G}_{\mathbf{x}}$ are not relevant, since it follows from (3.5) and the subsequent discussion that $\text{Cov}(y_1, y_2 | \mathbf{G}_{\mathbf{x}_1}, \mathbf{G}_{\mathbf{x}_2}) = 0$. Indeed, dependence among the responses is induced through dependence among $\mathbf{G}_{\mathbf{x}}$.*

The following theorem, the proof of which is provided in Section S-3 of the supplement, shows that the above correlation structure of our kernel convolution based ODDP satisfies desirable properties.

Theorem 5. *$\text{Corr}(f(\mathbf{x}_1), f(\mathbf{x}_2)) \rightarrow 1$ as $\|\mathbf{x}_1 - \mathbf{x}_2\| \rightarrow 0$ and $\text{Corr}(f(\mathbf{x}_1), f(\mathbf{x}_2)) \rightarrow 0$ as $\|\mathbf{x}_1 - \mathbf{x}_2\| \rightarrow \infty$.*

It is clear from the above theorem and model (3.3) that $\text{Corr}(y_i, y_j) \rightarrow 1$ as $\|\mathbf{x}_i - \mathbf{x}_j\| \rightarrow 0$ and $\text{Corr}(y_i, y_j) \rightarrow 0$ as $\|\mathbf{x}_i - \mathbf{x}_j\| \rightarrow \infty$.

Under a stationary Poisson process assumption for Φ , and for particular specifications of $U(\mathbf{x})$ mentioned in Section 3.1, the calculations of GS show that the second factor of (3.12) depends upon \mathbf{x}_1 and \mathbf{x}_2 only through $\|\mathbf{x}_1 - \mathbf{x}_2\|$, leading to isotropy of the process. There does not seem to exist any result analogous to the refined Campbell theorem in the context of nonstationary Poisson process which might allow one to construct a nonstationary correlation structure in this case. The analytic form of the ODDP correlation structure need not be available for other constructions of $U(\mathbf{x})$ either. Isotropy results even in the case of the more flexible Cox processes. Note that the correlations between any two responses y_i and y_j may correspond to nonstationarity if their expectations under the density $f_{\boldsymbol{\theta}}(\cdot)$

are nonlinear in $\boldsymbol{\theta}$. However, there is no guarantee that the correlation tends to zero as $\|\mathbf{x}_i - \mathbf{x}_j\| \rightarrow \infty$.

On the other hand, our kernel convolution idea neatly solves this problem of attainment of nonstationarity via the first factor of our correlation structure given in (3.12). Indeed, the kernel $K(\mathbf{x}, \boldsymbol{\theta})$ can be chosen in the spirit of Higdon *et al.* (1999), for instance, such that $\text{Corr}_{G_0}(K(\mathbf{x}_1, \boldsymbol{\theta}), K(\mathbf{x}_2, \boldsymbol{\theta}))$ does not depend upon $\mathbf{x}_1 - \mathbf{x}_2$ alone. In other words, by simply controlling the kernel we can ensure nonstationarity of our process $f(\cdot)$ even if the underlying ODDP is stationary or even isotropic. Of course, our process can be made stationary as well by choosing the kernel, say, in the spirit of Higdon (1998), and setting $U(\mathbf{x})$ to be of the forms specified by GS, when \mathbf{x} consists of either only spatial co-ordinates or only temporal co-ordinate. When $\mathbf{x} = (\mathbf{s}', t)'$, then we set $U(\mathbf{x}) = D \times (-\infty, t]$, as already mentioned before.

We further note that our general space-time correlation structure given by (3.10) is nonseparable, that is, in general, $\text{Corr}(f(\mathbf{s}_1, t_1), f(\mathbf{s}_2, t_2)) \neq \text{Corr}_1(\mathbf{s}_1, \mathbf{s}_2) \times \text{Corr}_2(t_1, t_2)$, where Corr_1 and Corr_2 are spatial and temporal structures respectively. However, if desired, separability can be easily induced by allowing the kernel to depend upon only the spatial location and by allowing the ordering $\boldsymbol{\pi}$ to depend only upon time, or the vice versa. Specifically, letting $K(\mathbf{x}, \boldsymbol{\theta}) = K(\mathbf{s}, \boldsymbol{\theta})$ and $\boldsymbol{\pi}(\mathbf{x}) = \boldsymbol{\pi}(t)$, we obtain

$$\text{Corr}(f(\mathbf{s}_1, t_1), f(\mathbf{s}_2, t_2)) = \text{Corr}_{G_0}(K(\mathbf{s}_1, \boldsymbol{\theta}), K(\mathbf{s}_2, \boldsymbol{\theta})) \times \text{Corr}(G_{t_1}, G_{t_2}), \quad (3.13)$$

and letting $K(\mathbf{x}, \boldsymbol{\theta}) = K(t, \boldsymbol{\theta})$ and $\boldsymbol{\pi}(\mathbf{x}) = \boldsymbol{\pi}(\mathbf{s})$, we obtain

$$\text{Corr}(f(\mathbf{s}_1, t_1), f(\mathbf{s}_2, t_2)) = \text{Corr}_{G_0}(K(t_1, \boldsymbol{\theta}), K(t_2, \boldsymbol{\theta})) \times \text{Corr}(G_{\mathbf{s}_1}, G_{\mathbf{s}_2}), \quad (3.14)$$

In contrast, under the ODDP approach of GS, it is clear from the correlation structure that $\text{Corr}(G_{\mathbf{x}_1}, G_{\mathbf{x}_2}) \neq \text{Corr}_1(\mathbf{s}_1, \mathbf{s}_2) \times \text{Corr}_2(t_1, t_2)$, showing that separability can not be enforced if desired.

Thus, following our approach it is easy to construct nonparametric covariance structures that are either stationary or nonstationary, which, in turn, can be constructed as either separable or nonseparable, as desired. These illustrate the considerable flexibility inherent in our approach, while satisfying at the same time the desirable conditions that the correlation between $f(\mathbf{x}_1)$ and $f(\mathbf{x}_2)$ tends to 1 or zero accordingly as the distance between \mathbf{x}_1 and \mathbf{x}_2 tends to zero or infinity.

4 Continuity and smoothness properties of our model

For stationary models, properties like continuity and smoothness can be quite generally characterized by the continuity and smoothness of the correlation function. In particular, continuity and smoothness of stationary processes typically depend upon the behaviour of the correlation function at zero; see Yaglom (1987a) and Yaglom (1987b) for details. For nonstationary processes, however, such elegant theory is not available. Indeed, the structure of the correlation function itself may be difficult to get hold of, rendering it difficult to investigate the properties of the underlying nonstationary stochastic process. For our purpose, we utilize the notions of almost sure continuity, mean square continuity and mean

square differentiability of stochastic processes (see, for example, [Stein \(1999\)](#), [Banerjee and Gelfand \(2003\)](#)) to study the properties of our nonstationary spatio-temporal process.

Definition 6. A process $\{X(\mathbf{x}), \mathbf{x} \in \mathbb{R}^d\}$ is L_2 continuous at \mathbf{x}_0 if $\lim_{\mathbf{x} \rightarrow \mathbf{x}_0} E[X(\mathbf{x}) - X(\mathbf{x}_0)]^2 = 0$. Continuity in the L_2 sense is also referred to as mean square continuity and will be denoted by $X(\mathbf{x}) \xrightarrow{L_2} X(\mathbf{x}_0)$.

Definition 7. A process $\{X(\mathbf{x}), \mathbf{x} \in \mathbb{R}^d\}$ is almost surely continuous at \mathbf{x}_0 if $X(\mathbf{x}) \rightarrow X(\mathbf{x}_0)$ a.s. as $\mathbf{x} \rightarrow \mathbf{x}_0$. If the process is almost surely continuous for every $\mathbf{x}_0 \in \mathbb{R}^d$ then the process is said to have continuous realizations.

Theorem 8. Assume the following conditions:

(A1) For all \mathbf{x} and $\boldsymbol{\theta}$, $|K(\mathbf{x}, \boldsymbol{\theta})| < M$ for some $M < \infty$.

(A2) Given any $\boldsymbol{\theta}$, $K(\mathbf{x}, \boldsymbol{\theta})$ is a continuous function of \mathbf{x} .

Then $f(\cdot)$ is both almost surely continuous and mean square continuous in the interior of $\bigcap_{k=1}^{\infty} A_{ki_k}$, where $A_{ki_k} = \{\mathbf{x} : \pi_k(\mathbf{x}) = i_k\}$, and for each $k = 1, 2, \dots$, $i_k \in \{1, 2, \dots\}$; $i_k \neq i_{k'}$ for any $k \neq k'$. On the other hand, $f(\cdot)$ is almost surely discontinuous at any point $\mathbf{x}_0 \in \bigcap_{k=1}^{\infty} A_{ki_k}$ lying on the boundary of A_{ki_k} , for any i_k .

See Section S-4 for a proof of this result. Now we examine mean square differentiability of our process.

Definition 9. A process $\{X(\mathbf{x}), \mathbf{x} \in \mathbb{R}^d\}$ is said to be mean square differentiable at \mathbf{x}_0 if for any direction \mathbf{u} , there exists a process $L_{\mathbf{x}_0}(\mathbf{u})$, linear in \mathbf{u} such that

$$X(\mathbf{x}_0 + \mathbf{u}) = X(\mathbf{x}_0) + L_{\mathbf{x}_0}(\mathbf{u}) + R(\mathbf{x}_0, \mathbf{u}), \text{ where } \frac{R(\mathbf{x}_0, \mathbf{u})}{\|\mathbf{u}\|} \xrightarrow{L_2} 0.$$

Theorem 10. Assume the following conditions:

(B1) For all \mathbf{x} and $\boldsymbol{\theta}$, $|K(\mathbf{x}, \boldsymbol{\theta})| < M$ for some $M < \infty$.

(B2) Given any $\boldsymbol{\theta}$, $K(\mathbf{x}, \boldsymbol{\theta})$ is a continuously differentiable function of \mathbf{x} .

Then $f(\cdot)$ is mean square differentiable in the interior of $\bigcap_{k=1}^{\infty} A_{ki_k}$.

See Section S-5 for a proof of this theorem.

In real life applications most of the spatio-temporal processes are expected to be irregular in nature. One of the desirable properties of a spatio-temporal model is that, it allows the different degrees of smoothness across space than across time. Our model has achieved this property regarding smoothness. For example, if we associate the ODDP prior only to the spatial locations, then the process becomes smoother across time than across space depending on the choice of the kernel.

5 Truncation of the infinite summand

Since our proposed model $f(\mathbf{x}) = \sum_{k=1}^{\infty} K(\mathbf{x}, \boldsymbol{\theta}_{\pi(\mathbf{x})})p_i(\mathbf{x})$ is an infinite (random) series, for model-fitting purpose it is necessary to truncate the series to $f(\mathbf{x}) = \sum_{k=1}^N K(\mathbf{x}, \boldsymbol{\theta}_{\pi(\mathbf{x})})p_i(\mathbf{x})$, where N is to be determined, or to implement variable-dimensional Markov chain methods where N is to be considered a random variable so that the number of parameters associated with $f(\mathbf{x})$ is also a random variable.

Although we will describe and implement TTMC, we first prove a theorem with respect to truncation of the infinite random series. Note that in the context of traditional Dirichlet process characterized by Sethuraman's stick breaking construction (Sethuraman (1994)) which involves infinite random series, Ishwaran and James (2001) proposed a method of truncating the infinite series.

We now state our theorem on truncation, the proof of which is provided in Section S-6 of the supplement. But before stating the theorem it is necessary to define some required notation. Let

$$P_N(\mathbf{x}_i) = \sum_{i=1}^N K(\mathbf{x}_i, \boldsymbol{\theta}_i)p_i, \quad \text{and} \quad P(\mathbf{x}_i) = \sum_{i=1}^{\infty} K(\mathbf{x}_i, \boldsymbol{\theta}_i)p_i,$$

where N needs to be determined. Also let

$$P_N = (P_N(\mathbf{x}_1), \dots, P_N(\mathbf{x}_n))' \quad \text{and} \quad P = (P(\mathbf{x}_1), \dots, P(\mathbf{x}_n))',$$

and denote by Θ_N and Θ the sets of random quantities $(V_i, \boldsymbol{\theta}_i)$ associated with P_N and P respectively. We define the following marginal densities of the vector of observations $\mathbf{y} = \{y_1, \dots, y_n\}$, where $[\cdot|\cdot]$ and $[\cdot]$ denote conditional and marginal densities, respectively:

$$\begin{aligned} m_N(\mathbf{y}) &= \int_{\Theta_N} [\mathbf{y}|P_N][P_N]d\Theta_N \\ &= \int_{\Theta} [\mathbf{y}|P_N][P]d\Theta, \end{aligned}$$

and

$$m_{\infty}(\mathbf{y}) = \int_{\Theta} [\mathbf{y}|P][P]d\Theta.$$

Theorem 11. *Under the assumption that $\sup_{\boldsymbol{\theta}} K(x_i, \boldsymbol{\theta}) \leq M$ for $i = 1, \dots, n$, where $M > 0$ is a finite constant, we have*

$$\int_{\mathbb{R}^n} |m_N(\mathbf{y}) - m_{\infty}(\mathbf{y})| d\mathbf{y} \leq 4M^2n \left(\frac{\alpha}{\alpha + 2} \right)^N + 2\sqrt{\frac{2}{\pi}}Mn \left(\frac{\alpha}{\alpha + 1} \right)^N.$$

6 Choice of kernel, prior distributions and computational region

The choice of kernel $K(\cdot, \cdot)$ plays a crucial role in nonstationary spatio-temporal data analysis. For instance, if $K(\mathbf{x}, \boldsymbol{\theta}) = K(\mathbf{x} - \boldsymbol{\theta})$, then the correlation between $Y(\mathbf{x}_1)$ and $Y(\mathbf{x}_2)$ turns

out to be a function of $\mathbf{x}_1 - \mathbf{x}_2$, thus inducing stationarity. For the purpose of nonstationarity, it is necessary to make the parameters of the kernel depend upon space and time. In the spatial context such nonstationary kernels are considered in [Higdon *et al.* \(1999\)](#). In this paper, we consider a nonstationary space-time kernel; for the spatial part of the kernel we essentially adopt the dependence structure and the associated prior distributions proposed by [Higdon *et al.* \(1999\)](#) and for the temporal part we allow the relevant coefficient to be time varying, modeled by a stationary Gaussian process.

In particular, we consider the following kernel for our applications:

$$K(\mathbf{s}, t, \boldsymbol{\theta}, \tau) = \exp \left\{ -\frac{1}{2}(\mathbf{s} - \boldsymbol{\theta})^T \Sigma(\mathbf{s})(\mathbf{s} - \boldsymbol{\theta}) - \delta(t)|t - \tau| \right\},$$

where $\Sigma(\mathbf{s})$ is a 2×2 positive definite dispersion matrix depending upon \mathbf{s} , and $\delta(t) > 0$ depends upon time t . We assume that $\log(\delta(t))$ is a zero mean Gaussian process with covariance $c_\delta(t_1, t_2) = \sigma_\delta^2 \exp \{(t_1 - t_2)^2/a_\delta\}$. We set

$$\Sigma(\mathbf{s})^{\frac{1}{2}} = \varphi \begin{pmatrix} \left[\frac{\sqrt{4A^2 + \|\psi(\mathbf{s})\|^4 \pi^2}}{2\pi} + \frac{\|\psi(\mathbf{s})\|^2}{2} \right]^{\frac{1}{2}} & 0 \\ 0 & \left[\frac{\sqrt{4A^2 + \|\psi(\mathbf{s})\|^4 \pi^2}}{2\pi} - \frac{\|\psi(\mathbf{s})\|^2}{2} \right]^{\frac{1}{2}} \end{pmatrix} \begin{pmatrix} \cos \alpha(\mathbf{s}) & \sin \alpha(\mathbf{s}) \\ -\sin \alpha(\mathbf{s}) & \cos \alpha(\mathbf{s}) \end{pmatrix},$$

where $\|\psi(\mathbf{s})\|^2 = \psi_1^2(\mathbf{s}) + \psi_2^2(\mathbf{s})$ and $\alpha(\mathbf{s}) = \tan^{-1} \left(\frac{\psi_2(\mathbf{s})}{\psi_1(\mathbf{s})} \right)$. We assume that $\psi_1(\cdot)$ and $\psi_2(\cdot)$ are independent and identical zero mean Gaussian processes with covariance $c_\psi(\mathbf{s}_1, \mathbf{s}_2) = \sigma_\psi^2 \exp \{-\|\mathbf{s}_1 - \mathbf{s}_2\|^2/b_\psi\}$. We put the $U(3, 200)$ prior on φ , a_δ , and b_ψ ; we set $\sigma_\delta^2 = \sigma_\psi^2 = 1$. Also, we set $A = 3.5$. Since in our applications we center and scale the observed time points, for τ we specify the $N(0, 1)$ prior.

6.1 Elicitation of hyperparameters of the underlying ODDP

6.1.1 Choice of G_0

In our applications, we center and scale each of the two components $\{s_{1i}; i = 1, \dots, n\}$ and $\{s_{2i}; i = 1, \dots, n\}$ of the available spatial locations $\{\mathbf{s}_i = (s_{1i}, s_{2i}); i = 1, \dots, n\}$. Consequently, the choosing G_0 to be the bivariate normal distribution with both means zero, both variances equal to one, and correlation ρ appears to be reasonable. We estimate ρ by the empirical correlation between $\{s_{1i}; i = 1, \dots, n\}$ and $\{s_{2i}; i = 1, \dots, n\}$.

6.1.2 Prior selection for α

For the choice of prior distributions of the parameters associated with the ODDP we follow [Griffin and Steel \(2004\)](#) and GS. In particular, we put the inverted Beta distribution prior on α , given by

$$p(\alpha) = \frac{n_0^\eta \Gamma(2\eta) \alpha^{\eta-1}}{\Gamma(\eta)^2 (\alpha + n_0)^{2\eta}},$$

where the hyperparameter n_0 is the prior median of α . Note that the prior variance exists if $\eta > 2$ and is a decreasing function of η . This prior implies that $\frac{\alpha}{\alpha + n_0}$ follows a $Beta(\eta, \eta)$ distribution.

6.1.3 Prior selection for λ

Note that, for small α , only the first few elements of stick breaking representation are important, so fewer number of points from the underlying Poisson process is needed to induce the second factor of the correlation structure (3.12) which roughly depends upon the ratio $\lambda/(\alpha+1)$ for $U(\mathbf{x}) = D$ (spatial problem) and $U(x) = (-\infty, x]$ (temporal problem); see GS for the details. Thus a relatively small value of λ suffices in such cases. Similarly, when α is larger, larger λ is necessary to obtain the same correlation. Keeping these in mind, we select the log-normal prior for λ with mean $\log(\alpha)$ and variance b_λ , say. For our applications, we choose $b_\lambda = 20$, so that we obtain a reasonably vague prior.

6.2 Computational region

Following GS, we consider a truncated region for the point process Z which includes the range of the observed \mathbf{x} . This truncated region has been referred to as the computational region by GS. In particular, we choose a bounding box of the form $(a_1, b_1) \times (a_2, b_2) \times \cdots \times (a_d, b_d)$ as the computational region, where $a_i = d_{a_i} - r$, $b_i = d_{b_i} - r$. Here d_{a_i} and d_{b_i} are the minimum and the maximum of \mathbf{x} in dimension i , and $r = 2 \left(\frac{\Gamma(d/2)d}{2\pi^{d/2}} \frac{\alpha+1}{\lambda} \log \frac{1}{\epsilon} \right)^{\frac{1}{d}}$, with $\epsilon = \exp \left\{ -\frac{\lambda}{\alpha+1} \frac{2\pi^{d/2}}{\Gamma(d/2)d} \left(\frac{r}{2} \right)^d \right\}$. See GS for justification of these choices.

7 Joint posterior and a briefing of TTMCMM for updating parameters in our variable dimensional modeling framework

Let k denote the random number of summands in

$$f_k(\mathbf{x}) = \sum_{i=1}^k K(\mathbf{x}, \boldsymbol{\theta}_{\pi_i(\mathbf{x})}) p_i(\mathbf{x}) \quad \forall \mathbf{x} \in D \subseteq \mathbb{R}^d. \quad (7.1)$$

Let $\mathbf{V} = (V_1, \dots, V_k)$, $\mathbf{z} = (z_1, \dots, z_k)$, $\boldsymbol{\theta} = (\boldsymbol{\theta}_1, \boldsymbol{\theta}_2)$, with $\boldsymbol{\theta}_1 = (\theta_{11}, \dots, \theta_{1k})$ and $\boldsymbol{\theta}_2 = (\theta_{21}, \dots, \theta_{2k})$. Let also $\boldsymbol{\psi}_1 = (\psi_1(\mathbf{s}_1), \dots, \psi_1(\mathbf{s}_n))$, $\boldsymbol{\psi}_2 = (\psi_2(\mathbf{s}_1), \dots, \psi_2(\mathbf{s}_n))$ and $\boldsymbol{\delta} = (\delta(t_1), \dots, \delta(t_n))$. The joint posterior is of the form

$$\begin{aligned} & \pi(k, \mathbf{V}, \mathbf{z}, \boldsymbol{\theta}_1, \boldsymbol{\theta}_2, \boldsymbol{\psi}_1, \boldsymbol{\psi}_2, \boldsymbol{\delta}, \tau, \sigma, \alpha, \lambda, b_\psi, a_\delta | \mathbf{Y}) \\ & \propto \pi(k) \pi(\mathbf{V}, \mathbf{z}, \boldsymbol{\theta}_1, \boldsymbol{\theta}_2 | k) \pi(\boldsymbol{\psi}_1, \boldsymbol{\psi}_2, \boldsymbol{\delta}) \pi(\tau, \varphi, b_\psi, a_\delta) \pi(\sigma) \pi(\alpha) \pi(\lambda | \alpha) \times L(\mathbf{V}, \mathbf{z}, \boldsymbol{\theta}_1, \boldsymbol{\theta}_2, \sigma | k, \mathbf{Y}), \end{aligned} \quad (7.2)$$

where $L(\mathbf{V}, \mathbf{z}, \boldsymbol{\theta}_1, \boldsymbol{\theta}_2, \sigma | k, \mathbf{Y})$ is the joint normal likelihood of $\mathbf{V}, \mathbf{z}, \boldsymbol{\theta}_1, \boldsymbol{\theta}_2, \sigma$ under the model

$$y_i = f_k(\mathbf{x}_i) + \epsilon_i; \quad \epsilon_i \stackrel{iid}{\sim} N(0, \sigma^2); \quad i = 1, \dots, n, \quad (7.3)$$

conditional on $f_k(\cdot)$.

For our applications, as the prior $\pi(k)$ on k we assume the discrete uniform prior on $\{1, 2, \dots, 30\}$; in our applications k never even reached 30. Under $\pi(\mathbf{V}, \mathbf{z}, \boldsymbol{\theta}_1, \boldsymbol{\theta}_2 | k)$,

$V_i \stackrel{iid}{\sim} \text{Beta}(1, \alpha)$; $i = 1, \dots, k$, \mathbf{z} are realizations from the Poisson process with intensity λ , and for $i = 1, \dots, k$, $(\theta_{1i}, \theta_{2i}) \stackrel{iid}{\sim} G_0$. Under $\pi(\boldsymbol{\psi}_1, \boldsymbol{\psi}_2, \boldsymbol{\delta})$, $\boldsymbol{\psi}_1, \boldsymbol{\psi}_2, \boldsymbol{\delta}$ are independent Gaussian processes, as detailed in Section 6. The prior distribution of $\tau, \varphi, b_\psi, a_\delta$, denoted by $\pi(\tau, \varphi, b_\psi, a_\delta)$, is already provided in Section 6. For the error standard deviation σ , the prior denoted by $\pi(\sigma)$ is the log-normal distribution with parameters 0 and 1, so that the mean and variance of σ are about 1.6 and 5, respectively. These quantities appear to be reasonable, and yielded adequate inference.

In order to obtain samples from the joint posterior (7.2) which involve the variable dimensional $f_k(\cdot)$, we implement the TTMCMM methodology. In a nutshell, TTMCMM updates all the parameters, both fixed and variable dimensional, as well as the number of parameters of the underlying posterior distribution in a single block using simple deterministic transformations of some low-dimensional random variable drawn from some fixed, but low-dimensional arbitrary distribution defined on some relevant support. The idea is an extension of Transformation based Markov Chain Monte Carlo (TMCMC) introduced by Dutta and Bhattacharya (2014) for updating high-dimensional parameters with known dimensionality in a single block using simple deterministic transformations of some low-dimensional (usually one-dimensional) random variable having arbitrary distribution on some relevant support. The strategy of updating high and variable dimensional parameters using very low-dimensional random variables clearly reduces dimensionality dramatically, thus greatly improving acceptance rate, mixing properties, and computational speed. In Section S-7 of the supplement we provide a detailed overview of TTMCMM, propose a general algorithm (Algorithm S-7.1) with certain advantages, and in Section S-8 of the supplement we specialize the algorithm to our spatio-temporal modeling set-up, providing full updating details (Algorithm S-8.1).

8 Simulation study

To illustrate the performance of our model we first create a synthetic data generating process which is nonstationary and non-Gaussian. One popular method to create such process is the kernel convolution approach. However, since we have developed our spatio-temporal model itself using the kernel convolution approach, it is perhaps desirable to obtain the synthetic data from some nonstationary, non-Gaussian process created using some approach independent of the kernel convolution method. In Section 8.1 we detail such an approach. Then we fit our proposed model to the data pretending that the data-generating process is unknown.

8.1 A nonstationary non-Gaussian data generating process

Let $X(\cdot)$ denote a stationary Gaussian process with mean function $\mu(t, \mathbf{s}) = \beta_0 + \beta_1 t + \beta_2 s_1 + \beta_3 s_2$, with $\mathbf{s} = (s_1, s_2)$, and covariance function

$$A(i, j) = c((t_i, \mathbf{s}_i), (t_j, \mathbf{s}_j)) = \exp \left\{ -0.5 \left(\sqrt{(t_i - t_j)^2 + (s_{1i} - s_{1j})^2 + (s_{2i} - s_{2j})^2} \right) \right\},$$

for any $t_i, t_j, \mathbf{s}_i = (s_{1i}, s_{2i}), \mathbf{s}_j = (s_{1j}, s_{2j})$.

Let $\mathbf{X} = (X(t_1, \mathbf{s}_1), \dots, X(t_n, \mathbf{s}_n))'$ denote observed data points from the Gaussian process X at the design points $\{(t_i, \mathbf{s}_i); i = 1, \dots, n\}$. Let $\mathbf{t} = (t_1, \dots, t_n)'$ and $\mathbf{S} = (\mathbf{s}'_1, \dots, \mathbf{s}'_n)'$. Further, let us denote by $\mathbf{A} = (A(i, j); i = 1, \dots, n; j = 1, \dots, n)$ the covariance matrix and $\boldsymbol{\mu} = (\mu(t_1, \mathbf{s}_1), \dots, \mu(t_n, \mathbf{s}_n))'$. Then the posterior process $[X(\cdot)|\mathbf{X}]$ is non-stationary Gaussian with mean function $\mu_X(t, \mathbf{s}) = \mu(t, \mathbf{s}) + \mathbf{A}_{12}\mathbf{A}_{22}^{-1}(\mathbf{X} - \boldsymbol{\mu})$ and variance $\mathbf{A}_{11} - \mathbf{A}_{12}\mathbf{A}_{22}^{-1}\mathbf{A}_{21}$, where $\mathbf{A} = \begin{pmatrix} \mathbf{A}_{11} & \mathbf{A}_{12} \\ \mathbf{A}_{21} & \mathbf{A}_{22} \end{pmatrix}$.

Let the posterior nonstationary Gaussian process $[X(\cdot)|\mathbf{X}]$ be denoted by $X^*(\cdot)$. Now, conditionally on the process $X^*(\cdot)$, consider another process $Y(\cdot)$ with mean function $\mu^*(t, \mathbf{s}) = X^*(t, \mathbf{s})$ and covariance function $c_Y((t_i, \mathbf{s}_i), (t_j, \mathbf{s}_j)) = \exp\{-0.5|X^*(t_i, \mathbf{s}_i) - X^*(t_j, \mathbf{s}_j)|\}$. Then marginally, $Y(\cdot)$ is a nonstationary non-Gaussian process.

For our illustration we will simulate the synthetic dataset from the process $Y(\cdot)$. The algorithm for generation of this synthetic data is provided in supplementary material (S-9.1).

8.2 Results of fitting our model to the simulated data

Note that for this problem the number of parameters to be updated ranges between 300 to 400. Our TTMC MC based model implementation took 35 mins to yield 900000 realizations following a burn-in of 100000. Quite encouragingly, TTMC MC exhibited satisfactory acceptance rate and mixing properties. Traceplots are shown in Figure S-9.1 of supplement.

8.2.1 Leave-one-out cross-validation

We assess the predictive power of our model with the leave-one-out cross validation method. All the 95 cases were included in the 95% highest posterior densities of the corresponding leave-one-out posterior predictive densities. Figure 8.1 displays the posterior predictive densities of six randomly selected space-time points, along with the true values, the latter denoted by the vertical lines. Thus, satisfactory performance of our proposed model is indicated by the results, particularly given the fact that our model does not assume knowledge of the true, data-generating, parametric model.

8.2.2 Correlation Analysis

Though our simulation mechanism is completely different from our proposed model, the simulated data do exhibit the pattern that the correlations are close to zero for two widely separated locations and/or times. Indeed, from the structure of the covariance matrix $\boldsymbol{\Sigma}_{(95|5)}$, it is easily seen that the (i, j) -th element ($i \neq j$) of $\boldsymbol{\Sigma}_{(95|5)}$ is close to zero whenever the distance between t_i and t_j and/or \mathbf{s}_i and \mathbf{s}_j is large.

We calculate the posterior densities of correlation for different pairs of space-time points. In formation of the pair, we select nearby locations, as well as locations which are widely separated, such that we obtain both high and low correlation values under the true, data-generating model. It is evident from Figure 8.2 that the true correlations, ranging from small to high values, lie well within their respective 95% credible intervals, vindicating reasonable performance of our model in terms of capturing the true correlation structure.

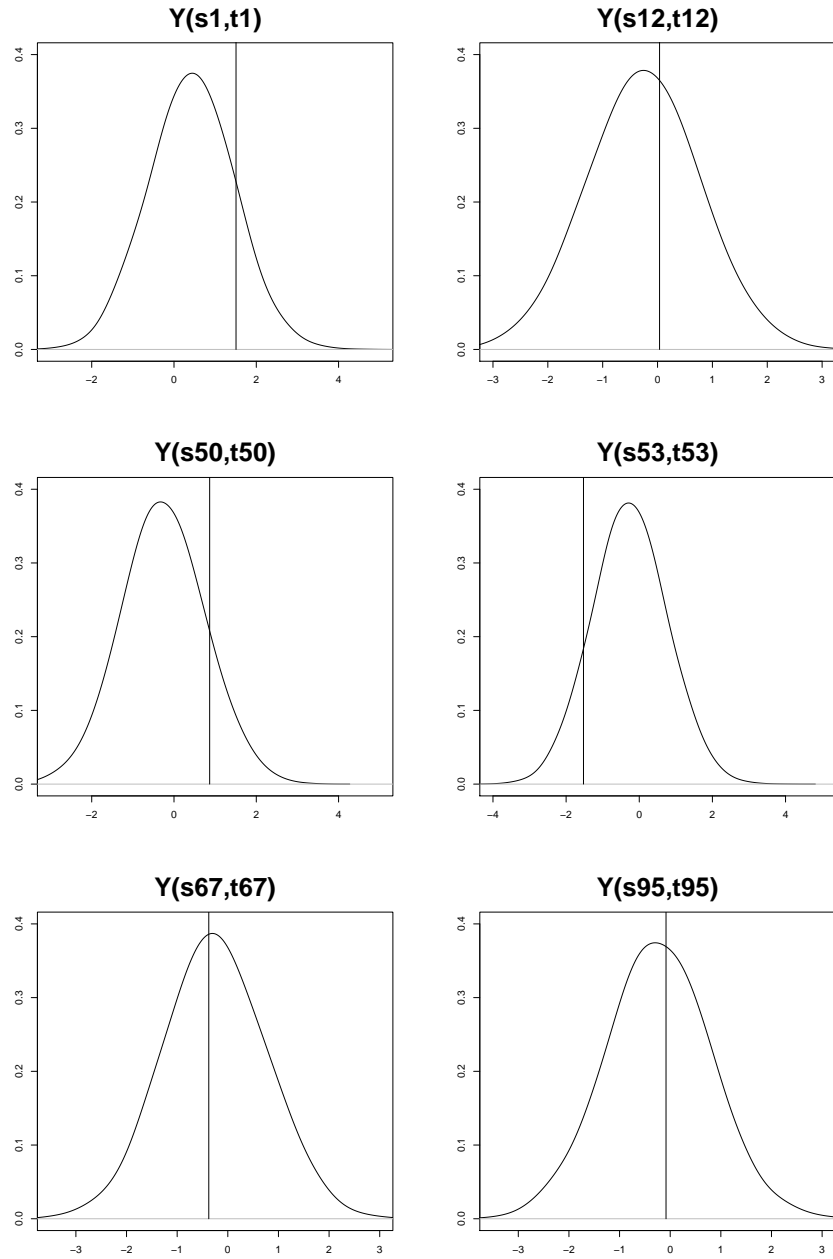


Figure 8.1: Simulation study: Posterior predictive densities of $Y(s, t)$ for the 6 different location-time pairs of our model – the corresponding true values are denoted by the vertical line.

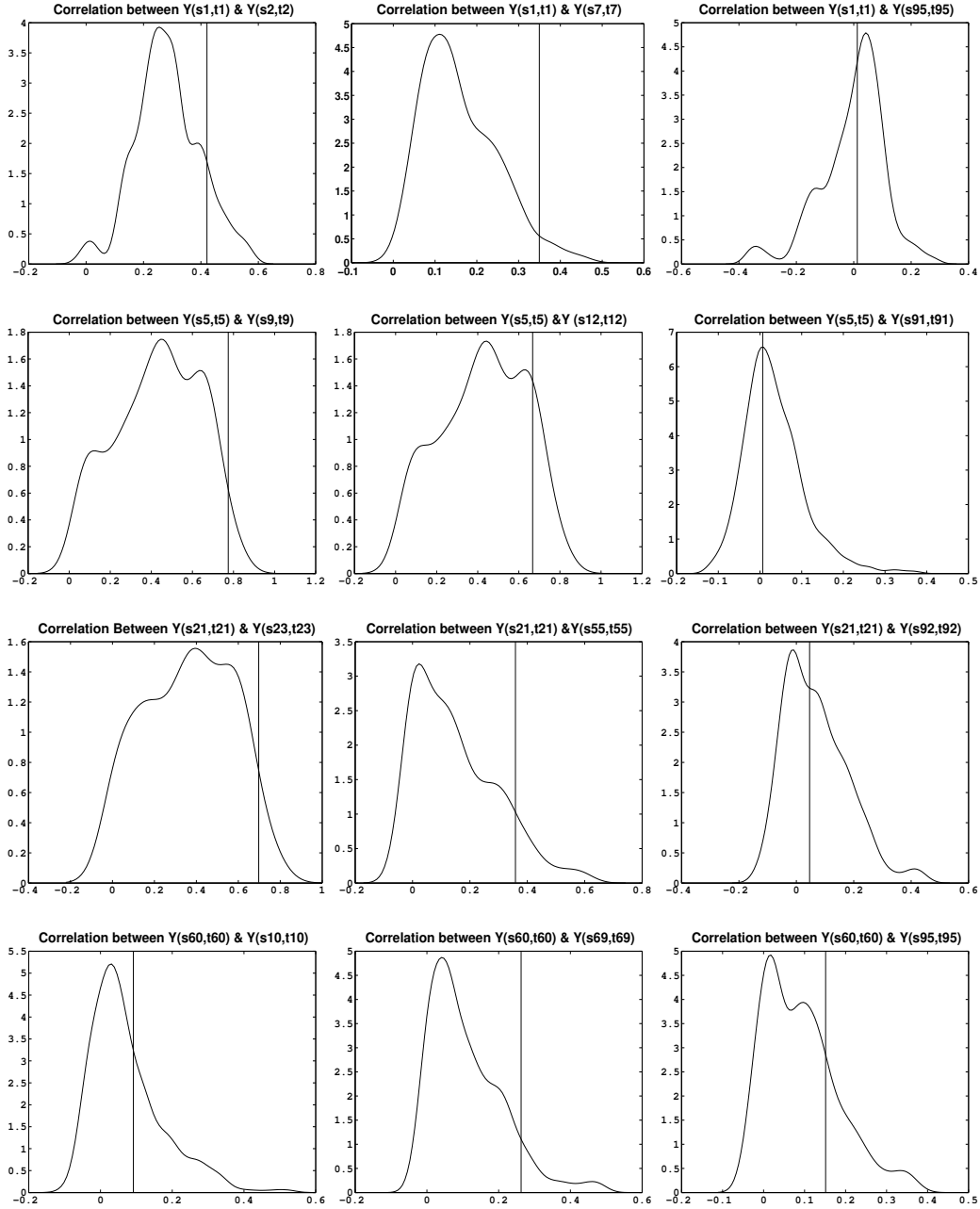


Figure 8.2: Simulation study: Posterior densities of the correlations for the 12 different pairs of spatio-temporal points of our model; the vertical lines indicate the true correlations.

8.3 Comparative study with respect to FR’s approach

We now compare the performance of our model with FR. For the purpose of comparison, we extended the exclusively spatial model of FR to space-time model, and apply the same to our simulated data.

We assess the predictive power of their model with the leave-one-out cross validation method. All the 95 cases were included in the 95% highest posterior densities of the corresponding leave-one-out posterior predictive densities. Figure 8.3 displays the posterior predictive densities along with the true values obtained by employing FR’s model for the same six locations that were investigated in our model. If we consider the CPO measure defined by $CPO_i = \pi(y_i^{obs}|y_{-i})$ (Conditional Predictive Ordinate) (Pettit (1990), Geisser (1993)), except for a few locations where the CPO measure for our model is slightly smaller than the model proposed by FR, our model performance is significantly better for most of the locations. Moreover, variabilities of the leave-one-out posterior predictive densities associated with the model of FR are substantially larger for all the locations.

8.3.1 Correlation Analysis

We calculate the posterior densities of the correlation for the same 12 pairs of space-time points. that were investigated in our model. The main features of the correlation analysis are the following :

- The posterior densities, which are highly multimodal in nature, are in keeping with the trace plots of the correlations (not shown), which clearly indicate convergence to multimodal distributions.
- Analogous to the CPO measure described above, here we evaluate the correlation based performance of the models in terms of the densities of the true correlations under the corresponding posterior distributions. From Figures 8.2 and 8.4, except for a few space-time pairs, our model significantly outperforms that of FR for all the remaining space-time pairs.
- Moreover, when the true correlations are close to zero, for all the space-time pairs, the densities of the true correlations under the corresponding posterior distributions are significantly higher than that of FR.
- The above facts strengthen our claim that, compared to other models, our correlation structure is sufficiently rich for capturing the actual correlations, specifically when the true correlation is close to zero for nonstationary models.

9 Real data analysis

9.1 Spatial data

According to the Clean Air Act certain air quality is to be maintained to protect the public health, and to maintain proper survival environment of animals and vegetations.

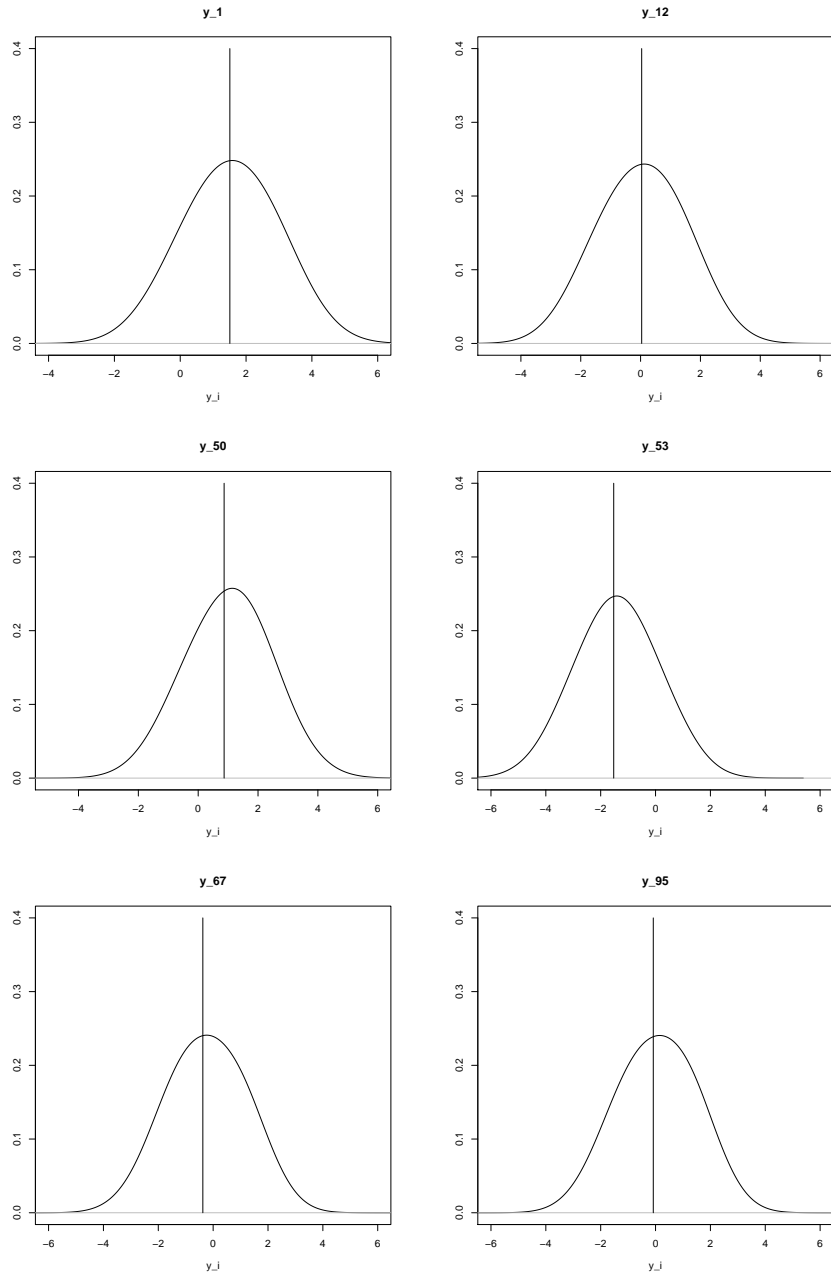


Figure 8.3: Simulation study: Posterior predictive densities of $Y(s, t)$ for the 6 different location-time pairs of FR – the corresponding true values are denoted by the vertical line.

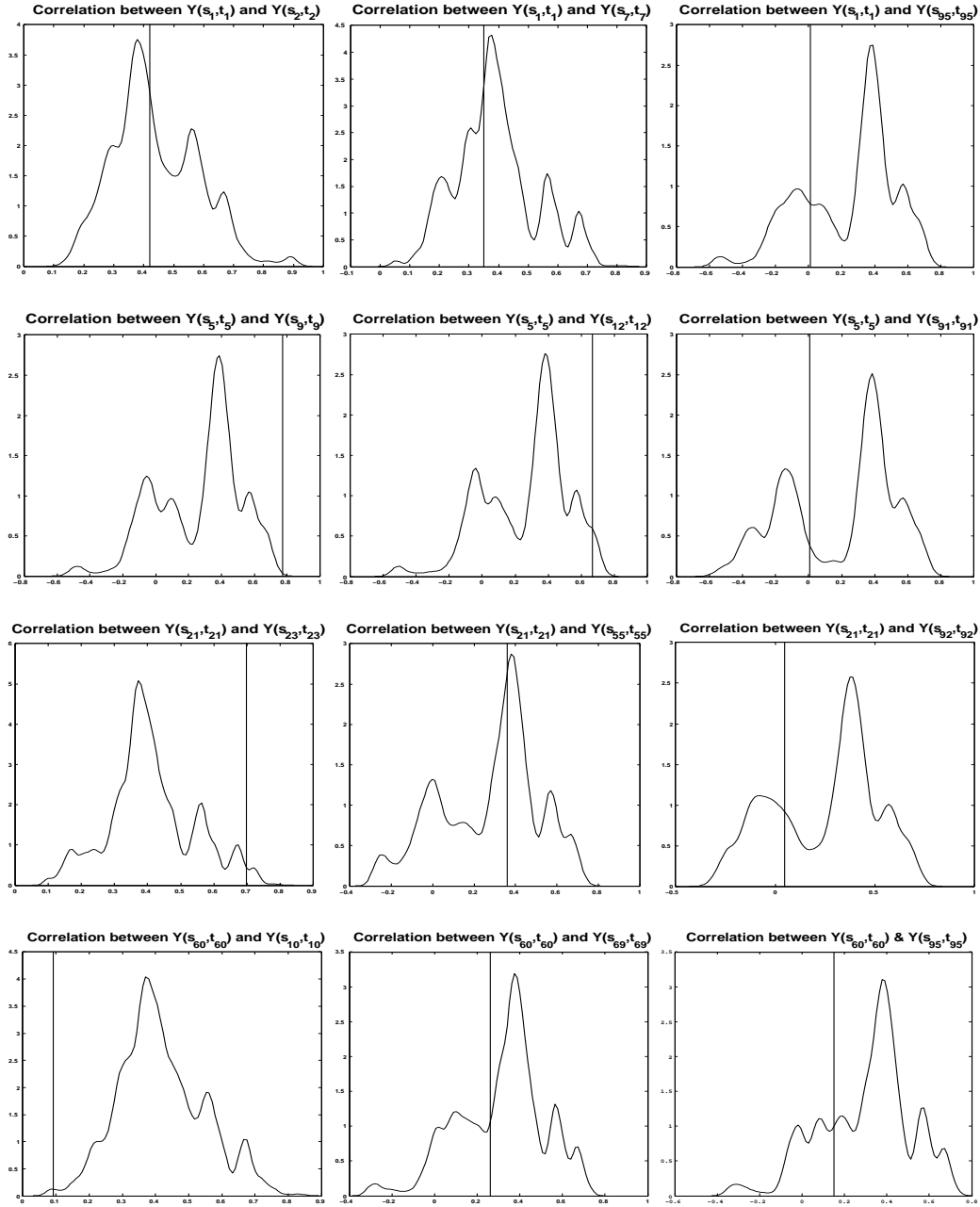


Figure 8.4: Simulation study: Posterior densities of the correlations for the 12 different pairs of spatio-temporal points of FR; the vertical lines indicate the true correlations.

As a measure of the quality of air, the Clean Air Act set standard limits for important air pollutants such as ozone. For our real data analysis we use the ozone metric called W126 metric. The impact of ozone exposure on trees, plants and ecosystems is often assessed using a seasonal index known as a “W126 index”, which is the annual maximum of consecutive three month running total of weighted sum of hourly concentrations observed between 8AM and 8PM on each day during the high ozone season of April through October. A fundamental principle behind W126 metric is that higher hourly average ozone concentrations should be weighted more than middle and lower values when assessing human and environmental effects. The cumulative W126 exposure index uses a sigmoidally weighted function. The W126 index is a cumulative exposure index and not an “average” value. As indicated above, it is a biology based index, which is supported by research results (i.e., under both experimental and ambient conditions) that show that the higher hourly average ozone concentrations should be weighted greater than the mid- and lower-level values. The US EPA reviewed the National Ambient Air Quality Standards (NAAQS) for ozone in 2015, and determined that a 3-month W126 index level of 17 ppm-hrs is sufficient to protect the public welfare based on the latest science on effects of ozone on vegetation (US Federal Register, 2015). Also, we have information on Community Multiscale Air Quality indices (CMAQ), which is highly correlated with ozone level, so that we can use CMAQ as a covariate in our model.

9.1.1 Calculating the W126 metric

Let $Q_l(\mathbf{s}, t)$ denote the observed ozone concentration level in parts per million (ppm) units at location \mathbf{s} at hour l on day t , for $t = 1, \dots, T$ and $l = 1, \dots, 12$, where $T = 214$ days between April 1 and October 31 in a given year. The hours are the 12 day light hours between 8AM and 7PM. The W126 metric for site \mathbf{s} is calculated as follows.

The weighted hourly metric is calculated using the transformation:

$$U_l(\mathbf{s}, t) = Q_l(\mathbf{s}, t) \times \left(\frac{1}{1 + 4403 \times \exp(-126 \times Q_l(\mathbf{s}, t))} \right).$$

This logistic transformation truncates the values smaller than 0.05ppm to zero, but does not alter the magnitude of values larger than 0.10ppm.

The daily index from the 12-hourly weighted values in each day is obtained as

$$Z(\mathbf{s}, t) = \sum_{l=1}^{12} U_l(\mathbf{s}, t).$$

The monthly index is calculated from the daily indices by summing and then adjusting for the number of days in the month as follows:

$$M_j(\mathbf{s}) = \sum_{t \in \text{month } j} Z(\mathbf{s}, t), j = 1, \dots, 7,$$

where the summation is over all the days l that fall within the calendar month j .

The three-month running totals are centered at the last month and are obtained as:

$$\bar{M}_j(\mathbf{s}) = \sum_{k=j-2}^j M_k(\mathbf{s}), j = 3, \dots, 7.$$

Finally, the annual W126 index value is calculated by:

$$Y(\mathbf{s}) = \max_{j=3}^7 \bar{M}_j(\mathbf{s}).$$

The secondary ozone standard is met at a site \mathbf{s} at a given year when the true value of $Y(\mathbf{s})$ is less than 21 ppm-hours.

Corresponding to each observed ozone concentration $Q_i(\mathbf{s}, t)$ we have a CMAQ model output $v_l(A, t)$, where the site \mathbf{s} is contained in the unique grid cell A . Using the output $v_l(A, t)$ and the above details daily and annual indices of CMAQ values namely $X(A, t)$ and $X(A)$ are constructed.

We have data on annual indices of ozone values (W126) $Y(\mathbf{s})$, and corresponding CMAQ $X(A)$ values for 76 locations in the US. Now we fit our model to this real data set. Here we model the data on the log scale; we also use the log transformation of the CMAQ values. In other words, we consider

$$\log(Y(\mathbf{s})) = \alpha_0 + \alpha_1 \log(X(A_i)) + f(\mathbf{s}_i) + \epsilon_i, \quad i = 1, \dots, 76,$$

where α_0 and α_1 are regression coefficients, $f(\mathbf{s}_i)$ is an annual level spatial random effect at location \mathbf{s}_i and ϵ_i is an independent nugget effect with variance σ^2 . Here $f(\mathbf{s}_i)$ is our proposed spatial model based on kernel convolution with ODPP.

It is worth mentioning that we had initially considered a stationary kernel for convolution, but obtained poor fit. This possibly suggested nonstationary process as an appropriate model, but until recently, we were not aware of any formal method for checking stationarity and nonstationarity in a completely nonparametric setup. Indeed, [Roy and Bhattacharya \(2020\)](#) proposed a novel recursive Bayesian methodology for characterizing stationarity and nonstationarity for general stochastic processes, among various other characterizations, and illustrated their ideas with ample examples in fields as varied as time series, MCMC convergence diagnosis, spatial and spatio-temporal setups, point processes, as well as (multiple) frequency determination of oscillating time series. With their ideas, they also analyse this ozone data to check stationarity. The details of their analyses and the results, presented in Section 13.7.1 of their paper, indicate that the ozone data is indeed nonstationary. Further, a simple quantile-quantile plot shows indicates non-normality of the data.

The above arguments justify our nonparametric model choice and nonstationary kernel used for convolution with ODDP. All the prior distributions are the same as mentioned before. For the additional parameters α_0 and α_1 , we use the vague prior distribution $N(0, 10^4)$, and for σ we use the log-normal prior with mean zero and variance 10^4 . The TTMC trace plots shown in Figure S-10.1 of supplement bear out adequate performance of our model and methodologies.

As before, we assess the predictive power of the model using leave-one-out cross validation. For all the locations, the true value of ozone concentration lies within the 95%

credible interval of the respective cross-validation posterior. This is summarized in the top panel of Figure 9.1, where the middle surface represents the observed data; the lower and the upper surfaces represent the lower and the upper 95% credible regions associated with the respective leave-one-out posterior predictive densities. The surface in the middle of the bottom panel are the posterior medians, while the lower and the upper surfaces denote the 95% credible intervals as before. For the convenience of visually comparing the observed data and the posterior medians, we include Figure 9.2, which also contains the 95% credible intervals. The plots clearly show that our proposed model is quite adequate for the ozone data.

Posterior densities of correlations, for 6 pairs of sites, are shown in Figure S-10.2 of supplement. All of them seem to give high posterior probability to the approximate range (0.1, 0.3).

9.2 Spatio-temporal data analysis

‘Particulate matter’ (PM) is the general term used for a mixture of solid particles and liquid droplets found in the air. Airborne PM comes from many different sources. “Primary” particles are released directly into the atmosphere from sources such as cars, trucks, heavy equipment, forest fires, and other burning activities. An extensive body of scientific evidence shows that there are adverse effects of this PM particles on health, including cardiovascular problems, premature death and many more. Ambient air monitoring stations generally measure air concentrations of different ranges of particles, but most monitoring station is for two size ranges: $PM_{2.5}$ and PM_{10} .

9.2.1 Data

Our data is a part of a big data set analysed by Paciorek *et al.* (2009) (Data Source: <http://www.stat.berkeley.edu/~paciorek/data/pm/>). They specify stationary spatial structures through the use of penalized thin plate splines. Assumption of stationarity leads to an important simplification in their model. The assumption of stationarity is particularly appropriate for $PM_{2.5}$ values, but there is evidence of nonstationarity for PM_{10} values. Indeed, Roy and Bhattacharya (2020) infer with their novel Bayesian recursive methodology that the PM_{10} data is strictly, as well as weakly nonstationary (Section 13.7.2 of their paper) and that the $PM_{2.5}$ data is strictly stationary (Section 13.7.3 of their paper).

For illustration purpose we fit a nonstationary spatio temporal model for a smaller section of the full data set. We analyse monthly average values of PM_{10} for the year 1988-2002 (180 time points) at 50 locations. There are few locations with fewer sample points. Our model will be appropriate for this kind of data, since we are using the spatial locations and time points as arguments of our proposed mean functional. Our data consists of total 3934 observations for monthly PM_{10} values. To increase the predictive performance of the model, we have used available covariate information for different spatial locations and time points. It is expected that inclusion of covariates may better explain the spatio-temporal heterogeneity. The details of the covariate selection are discussed in Yanosky *et al.* (2008b), Yanosky *et al.* (2008a). The non-time-varying covariates are as follows: distances to the nearest road within four road size classes; particulate point source emissions within 1 and

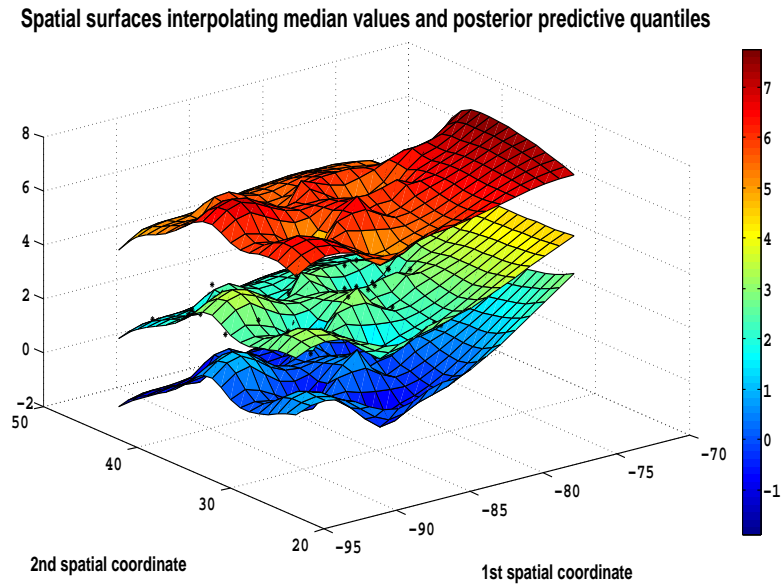
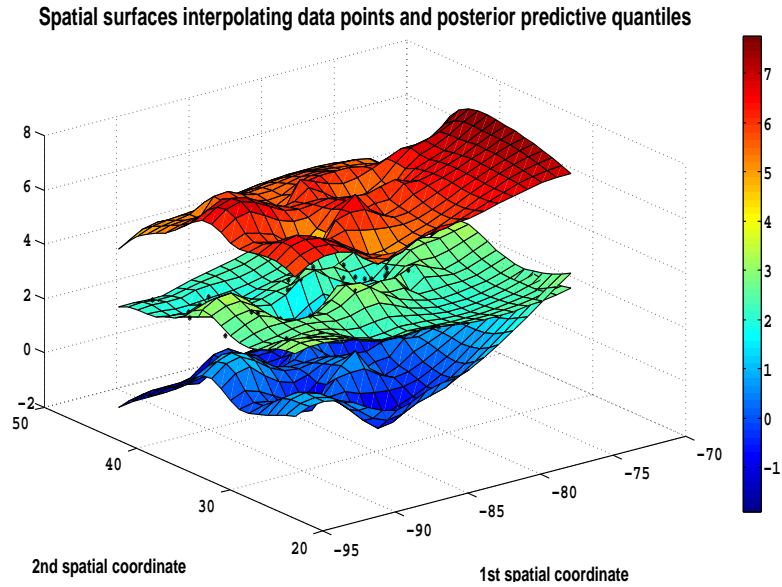


Figure 9.1: Real spatial data analysis: The top panel shows the surface plot of ozone concentrations (middle), the lower and the upper 95% credible intervals associated with the leave-one-out posterior predictive densities, denoted by the lower and the upper surfaces, respectively. The bottom panel shows the surface plot of the posterior medians (middle) along with the lower and the upper 95% credible intervals associated with the leave-one-out posterior predictive densities (lower and the upper surfaces, respectively). The observed data points are indicated by ‘*’.

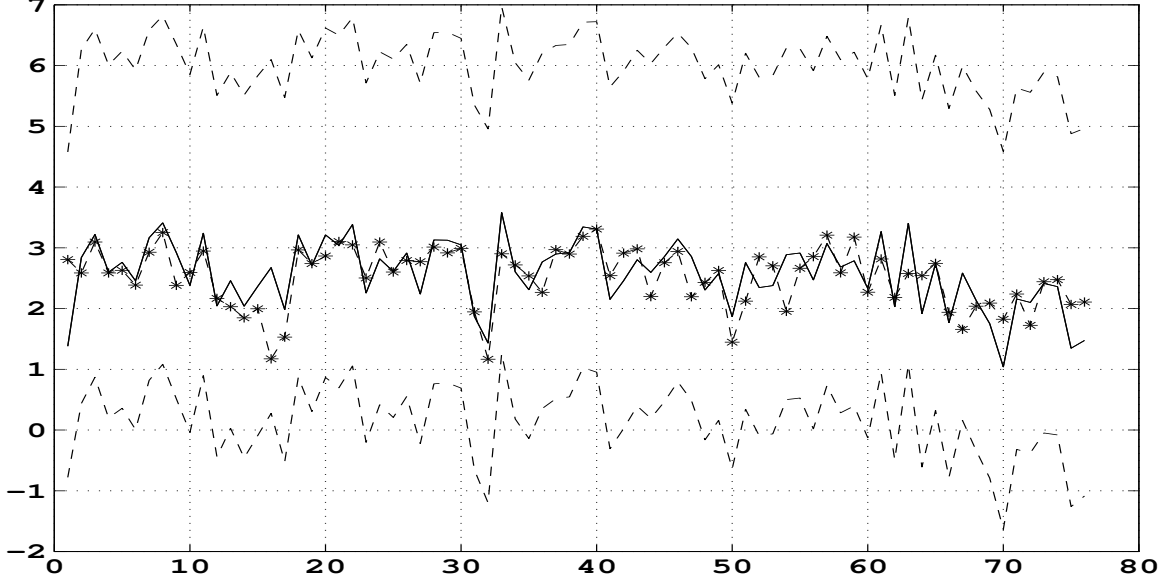


Figure 9.2: Real spatial data analysis: Posterior predictive distributions summarised by the median (middle line) and the 95% credible intervals as a function of \mathbf{s} . The observed data points are denoted by ‘*’.

10 km buffers; the proportion of urban land use of within 1 km; elevation; and block group, tract, and county population density from the 1990 US Census. The time varying covariates are wind speed, precipitation and barometric pressure, with hourly values averaged to the month at each station.

We also analyse the properties of the empirical correlations for increasing spatio-temporal lags with respect to the complete data set consisting of 70572 observations. Figure 9.3, obtained from the raw correlations after taking moving averages of length 50 for better visualization, shows that the correlations tend to zero with increasing lags, as realistically expected, in spite of the data being nonstationary. Moreover, a simple quantile-quantile plot (not shown for brevity) shows that the data is far from normality. These very much support our modeling idea.

9.2.2 Model

We propose the following model for the real data:

$$\log y_{it} = \alpha_0 + f(\mathbf{s}_i, t) + g_1(\tilde{\mathbf{z}}_i) + g_2(\mathbf{z}_{it}) + \epsilon_{it}, \quad i = 1, \dots, 50, t = 1, \dots, 180,$$

where α_0 is intercept term, $f(\mathbf{s}_i, t)$ is our proposed spatio-temporal model based on kernel convolution with ODDP. In the above, g_1 and g_2 are functionis of non-time varying covariates $\tilde{\mathbf{z}}_i$ and time varying covariates \mathbf{z}_{it} , respectively. We assume a Gaussian process prior on g_1 such that $\mu_1(\mathbf{z}) = E[g_1(\mathbf{z})] = \boldsymbol{\beta}'\mathbf{z}$ and $Cov(g_1(\mathbf{z}_i), g_1(\mathbf{z}_j)) = \exp(-\frac{1}{2}\|\mathbf{z}_i - \mathbf{z}_j\|)$.

We set g_2 as a linear function of time varying covariates: $g_2(\mathbf{z}) = \boldsymbol{\gamma}'\mathbf{z}$. The assumption of linearity in g_2 will simplify our computation to a great extent. Also there is evidence from the previous analysis that using linear terms in places of the unknown function led to only

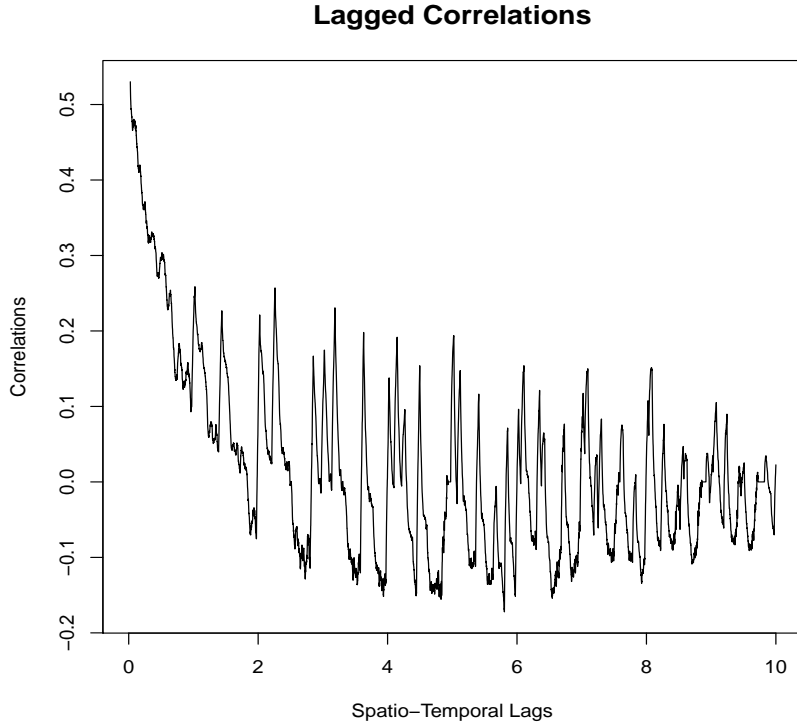


Figure 9.3: Empirical correlations for increasing spatio-temporal lags. The raw correlations are smoothed by taking moving averages of size 50 for better visualization.

negligible decrease in predictive ability. In our model, ϵ_{it} are independent nugget effects with variance σ^2 .

All the prior distributions are the same as mentioned before. For the additional parameters α_0, β, γ , we use the vague prior distribution $N(0, 10^4)$, and for σ we use the log-normal prior with mean zero and variance 10^4 .

9.2.3 Implementation

Note that here we have total 3934 number of observations. We have to update the number of parameters ranging between between 300 to 400. Our TTMCMM based algorithm took 25 minutes to generate 5000 observations following a burn in of 20000. As in the other cases, TTMCMM exhibited satisfactory acceptance rate and mixing properties, as evident from the trace plots displayed in S-10.3 of supplement.

9.2.4 Leave-one-out cross validation

As before, we assess the predictive power of the model using leave-one-out cross validation. For all the spatio-temporal points, the true value of PM_{10} lies within the 95% credible interval of the respective cross-validation posterior. Also we calculate the mean square prediction error ($MSPE$), given by $\frac{\sum(y_{it} - \hat{y}_{it})^2}{n}$, where \hat{y}_{it} is the median of the posterior predictive density at the spatial location (s_i, t) . In this case, we obtain $MSPE = 0.101$. Figure 9.4 displays the observed data and posterior medians for at three spatial locations having data for more than 10 years, which also contains 95% credible intervals. We have also reported $MSPE$ for these

three locations. The values are significantly lower than overall $MSPE$. It reveals the fact that our model have captured more precise information for the spatial locations, having larger number of time points. We also provide a visual representation of the model performance at 50 locations summarised over time points. In Figure 9.5, the surface represents the posterior median values, averaged over all month-specific predictions for 50 spatial locations. From the plots it is clear that our model performs quite satisfactorily for the data. Posterior densities of correlations, for 6 pairs of sites, are shown in Figure S-10.4 of the supplement.

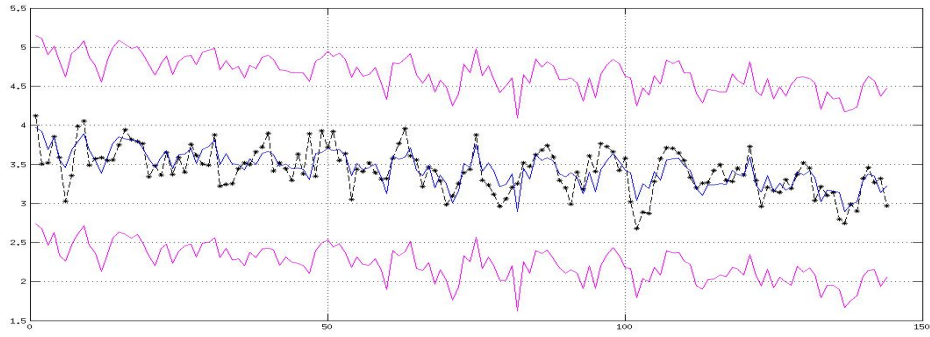
10 Summary and conclusion

In this article, we have developed a non stationary, non-Gaussian spatio-temporal model based on kernel convolution of ODDP. Dependence is induced in the weights through similarities in the ordering of the atoms. Using this property we could ensure that our model-based correlation between two random data points which are widely separated, will be close to zero. We incorporated non-stationarity via appropriate kernels, which would be convolved with ODDP. Although our proposed model is non stationary and non-separable, it includes stationarity and separability as special cases. Moreover, since our model is based on kernel convolution, replication is not necessary for inference. If one wishes to achieve different degrees of smoothness across space and across time, then that is also allowed by our model framework. For example, if we associate the ODDP prior only to the spatial locations, then the process will become smoother across time than across space depending on the choice of the kernel.

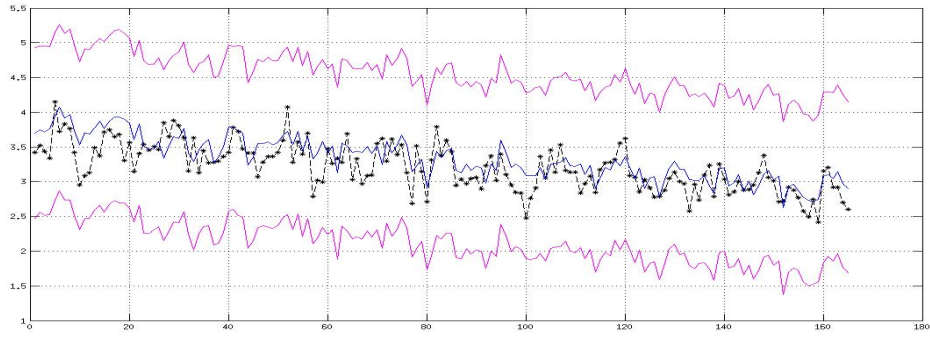
From the computational point of view, we have developed a fast and efficient TTMC MC based algorithm for implementing our variable dimensional spatio-temporal model. Indeed, our model consists of a large number of variables, where the number of variables associated with the summands is random. Using TTMC MC, we could update all the parameters, as well as number of the parameters simultaneously, using simple deterministic transformations of some a one-dimensional random variable.

We illustrated the performance of our model with a simulation study and have compared the performance of our model with the model of FR. The comparative study supports our claim that our model is capable of capturing the zero correlations between two widely separated data points (either in respect to space and/or time) more precisely. We have also applied our model and methods to two real data examples pertaining to spatial and spatio-temporal dependence. As illustrated in detail, in both cases our model exhibited excellent performance.

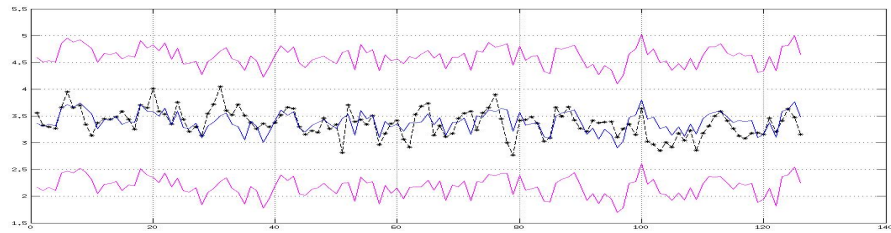
Although for the current paper we restricted ourselves to spatio-temporal applications only, our model is readily applicable in the functional data context. In fact, in the context of nonparametric function estimation, a new class of prior distributions can be introduced through our proposed model. Note that unknown functions can be modeled as a limit of a weighted sum of kernels or generator functions indexed by continuous parameters. In our model the weights will be the p_i 's of ODDP, and kernels are indexed by θ_i , where for $i = 1, 2, \dots$, $\theta_i \stackrel{iid}{\sim} G_0$. We have already obtained some sufficient conditions ensuring that our model converges in L_p norm and Besov semi-norm. These results make our proposed model a promising candidate for function estimation.



(a) spatial location:(38.270833 -85.740278), MSPE:0.0344



(b) spatial location:(41.600278 -87.334722), MSPE:0.051



(c) spatial location:(39.766111,-86.129167), MSPE:0.048

Figure 9.4: Real spatio-temporal data analysis: Posterior predictive distributions summarized by the median (middle line) and the 95% credible intervals as a function of t for three randomly chosen spatial locations. The observed data points are denoted by ‘*’.

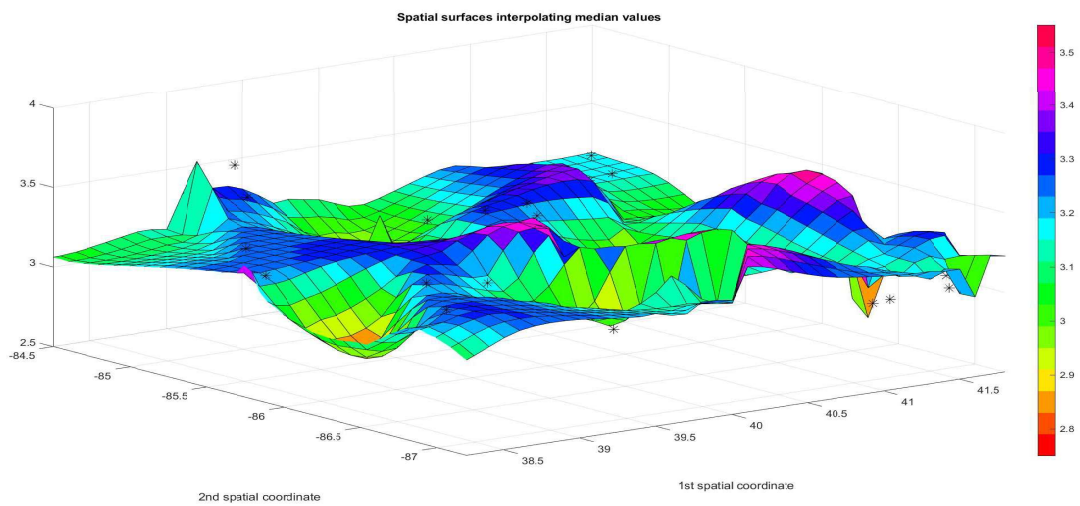


Figure 9.5: Real spatio-temporal data analysis: the surface plot of posterior median values at 50 locations, averaged over all month specific predictions from 1988-2002. The observed data points are indicated by '*'.

Acknowledgments

We are grateful to Prof. Sujit Sahu for kindly providing us with the ozone data set and to Mr. Suman Guha for helpful discussions.

Supplementary Material

S-1 Proof of Theorem 1

Note that

$$\int |K(\mathbf{x}, \boldsymbol{\theta})| dG_{\mathbf{x}}(\boldsymbol{\theta}) = \sum_{i=1}^{\infty} |K(\mathbf{x}, \boldsymbol{\theta}_{\pi_i(\mathbf{x})})| p_i, \quad (\text{S-1.1})$$

so that the monotone convergence theorem yields

$$\begin{aligned} E \left(\int |K(\mathbf{x}, \boldsymbol{\theta})| dG_{\mathbf{x}}(\boldsymbol{\theta}) \right) &= \sum_{i=1}^{\infty} E (|K(\mathbf{x}, \boldsymbol{\theta}_{\pi_i(\mathbf{x})})|) E(p_i) \\ &= \int |K(\mathbf{x}, \boldsymbol{\theta})| dG_0(\boldsymbol{\theta}) \sum_{i=1}^{\infty} E(p_i) \\ &= \int |K(\mathbf{x}, \boldsymbol{\theta})| dG_0(\boldsymbol{\theta}) \quad [\text{since } \sum_{i=1}^{\infty} p_i = 1]. \end{aligned}$$

Here we have used the fact that $\boldsymbol{\theta}_i$ and V_i 's are independent. Therefore $\int |K(\mathbf{x}, \boldsymbol{\theta})| dG_{\mathbf{x}}(\boldsymbol{\theta})$ is finite with probability one and hence

$$f(\mathbf{x}) = \int K(\mathbf{x}, \boldsymbol{\theta}) dG_{\mathbf{x}}(\boldsymbol{\theta}) = \sum_{i=1}^{\infty} K(\mathbf{x}, \boldsymbol{\theta}_{\pi_i(\mathbf{x})}) p_i(\mathbf{x})$$

is absolutely convergent with probability one. Since this series is bounded by (S-1.1), which is integrable, the bounded convergence theorem implies

$$\begin{aligned} E(f(\mathbf{x})) &= \sum_{i=1}^{\infty} E (K(\mathbf{x}, \boldsymbol{\theta}_{\pi_i(\mathbf{x})})) E(p_i) \\ &= \int K(\mathbf{x}, \boldsymbol{\theta}) dG_0(\boldsymbol{\theta}). \end{aligned}$$

■

S-2 Proof of Theorem 2

$$\begin{aligned} f(\mathbf{x}_1) f(\mathbf{x}_2) &= \int K(\mathbf{x}_1, \boldsymbol{\theta}) dG_{\mathbf{x}_1}(\boldsymbol{\theta}) \int K(\mathbf{x}_2, \boldsymbol{\theta}) dG_{\mathbf{x}_2}(\boldsymbol{\theta}) \\ &= \sum_i K(\mathbf{x}_1, \boldsymbol{\theta}_{\pi_i(\mathbf{x}_1)}) p_i(\mathbf{x}_1) \sum_j K(\mathbf{x}_2, \boldsymbol{\theta}_{\pi_j(\mathbf{x}_2)}) p_j(\mathbf{x}_2) \\ &= \sum_i \sum_j K(\mathbf{x}_1, \boldsymbol{\theta}_{\pi_i(\mathbf{x}_1)}) K(\mathbf{x}_2, \boldsymbol{\theta}_{\pi_j(\mathbf{x}_2)}) p_i(\mathbf{x}_1) p_j(\mathbf{x}_2) \quad (\text{S-2.1}) \end{aligned}$$

since both the series are absolutely convergent with probability one. This is bounded in absolute value by

$$\sum_i \sum_j |K(\mathbf{x}_1, \boldsymbol{\theta}_{\pi_i(\mathbf{x}_1)})K(\mathbf{x}_2, \boldsymbol{\theta}_{\pi_j(\mathbf{x}_2)})|p_i(\mathbf{x}_1)p_j(\mathbf{x}_2). \quad (\text{S-2.2})$$

Now if this is an integrable random variable, we may take the expectation of (S-2.1) inside the summation sign and obtain

$$\begin{aligned} E(f(\mathbf{x}_1)f(\mathbf{x}_2)) &= E\left(\int K(\mathbf{x}_1, \boldsymbol{\theta})dG_{\mathbf{x}_1}(\boldsymbol{\theta}) \int K(\mathbf{x}_2, \boldsymbol{\theta})dG_{\mathbf{x}_2}(\boldsymbol{\theta})\right) \\ &= \sum_i \sum_j E(K(\mathbf{x}_1, \boldsymbol{\theta}_{\pi_i(\mathbf{x}_1)})K(\mathbf{x}_2, \boldsymbol{\theta}_{\pi_j(\mathbf{x}_2)})) E(p_i(\mathbf{x}_1)p_j(\mathbf{x}_2)) \\ &= \sum_{\pi_i(\mathbf{x}_1) \neq \pi_j(\mathbf{x}_2)} E(K(\mathbf{x}_1, \boldsymbol{\theta}_{\pi_i(\mathbf{x}_1)})K(\mathbf{x}_2, \boldsymbol{\theta}_{\pi_j(\mathbf{x}_2)})) E(p_i(\mathbf{x}_1)p_j(\mathbf{x}_2)) \\ &\quad + \sum_{\pi_i(\mathbf{x}_1) = \pi_j(\mathbf{x}_2)} E(K(\mathbf{x}_1, \boldsymbol{\theta}_{\pi_i(\mathbf{x}_1)})K(\mathbf{x}_2, \boldsymbol{\theta}_{\pi_j(\mathbf{x}_2)})) E(p_i(\mathbf{x}_1)p_j(\mathbf{x}_2)) \\ &= \sum_{\pi_i(\mathbf{x}_1) \neq \pi_j(\mathbf{x}_2)} E(K(\mathbf{x}_1, \boldsymbol{\theta})) E(K(\mathbf{x}_2, \boldsymbol{\theta})) E(p_i(\mathbf{x}_1)p_j(\mathbf{x}_2)) \\ &\quad + \sum_{\pi_i(\mathbf{x}_1) = \pi_j(\mathbf{x}_2)} E(K(\mathbf{x}_1, \boldsymbol{\theta})K(\mathbf{x}_2, \boldsymbol{\theta})) E(p_i(\mathbf{x}_1)p_j(\mathbf{x}_2)) \\ &= E(K(\mathbf{x}_1, \boldsymbol{\theta})) E(K(\mathbf{x}_2, \boldsymbol{\theta})) \sum_{\pi_i(\mathbf{x}_1) \neq \pi_j(\mathbf{x}_2)} E(p_i(\mathbf{x}_1)p_j(\mathbf{x}_2)) \\ &\quad + E(K(\mathbf{x}_1, \boldsymbol{\theta})K(\mathbf{x}_2, \boldsymbol{\theta})) \sum_{\pi_i(\mathbf{x}_1) = \pi_j(\mathbf{x}_2)} E(p_i(\mathbf{x}_1)p_j(\mathbf{x}_2)) \\ &= E(K(\mathbf{x}_1, \boldsymbol{\theta})) E(K(\mathbf{x}_2, \boldsymbol{\theta})) \\ &\quad \left[\sum_{\pi_i(\mathbf{x}_1) \neq \pi_j(\mathbf{x}_2)} E(p_i(\mathbf{x}_1)p_j(\mathbf{x}_2)) + \sum_{\pi_i(\mathbf{x}_1) = \pi_j(\mathbf{x}_2)} E(p_i(\mathbf{x}_1)p_j(\mathbf{x}_2)) \right] \\ &\quad + E(K(\mathbf{x}_1, \boldsymbol{\theta})K(\mathbf{x}_2, \boldsymbol{\theta})) \sum_{\pi_i(\mathbf{x}_1) = \pi_j(\mathbf{x}_2)} E(p_i(\mathbf{x}_1)p_j(\mathbf{x}_2)) \\ &\quad - E(K(\mathbf{x}_1, \boldsymbol{\theta})) E(K(\mathbf{x}_2, \boldsymbol{\theta})) \sum_{\pi_i(\mathbf{x}_1) = \pi_j(\mathbf{x}_2)} E(p_i(\mathbf{x}_1)p_j(\mathbf{x}_2)) \\ &= \text{Cov}(K(\mathbf{x}_1, \boldsymbol{\theta}), K(\mathbf{x}_2, \boldsymbol{\theta})) \sum_{\pi_i(\mathbf{x}_1) = \pi_j(\mathbf{x}_2)} E(p_i(\mathbf{x}_1)p_j(\mathbf{x}_2)) \\ &\quad + E(K(\mathbf{x}_1, \boldsymbol{\theta})) E(K(\mathbf{x}_2, \boldsymbol{\theta})) \left[\sum_{\pi_i(\mathbf{x}_1), \pi_j(\mathbf{x}_2)} E(p_i(\mathbf{x}_1)p_j(\mathbf{x}_2)) \right] \\ &= \text{Cov}(K(\mathbf{x}_1, \boldsymbol{\theta}), K(\mathbf{x}_2, \boldsymbol{\theta})) \sum_{\pi_i(\mathbf{x}_1) = \pi_j(\mathbf{x}_2)} E(p_i(\mathbf{x}_1)p_j(\mathbf{x}_2)) \\ &\quad + E(K(\mathbf{x}_1, \boldsymbol{\theta})) E(K(\mathbf{x}_2, \boldsymbol{\theta})). \end{aligned}$$

An analogous equation shows that (S-2.2) is bounded, since, by our assumption

$$\int |K(\mathbf{x}, \boldsymbol{\theta})| dG_0(\boldsymbol{\theta}) < \infty \text{ and } \int |K(\mathbf{x}_1, \boldsymbol{\theta})K(\mathbf{x}_2, \boldsymbol{\theta})| dG_0(\boldsymbol{\theta}) < \infty.$$

To obtain the complete analytical expression of $E(f(\mathbf{x}_1)f(\mathbf{x}_2))$ we need to calculate $\sum_{\pi_i(\mathbf{x}_1)=\pi_j(\mathbf{x}_2)} E(p_i(\mathbf{x}_1)p_j(\mathbf{x}_2))$. Define

$$T(\mathbf{x}_1, \mathbf{x}_2) = \{k \mid \text{there exists } i, j \text{ such that } \pi_i(\mathbf{x}_1) = \pi_j(\mathbf{x}_2) = k\},$$

for $k \in T(\mathbf{x}_1, \mathbf{x}_2)$. We further define $A_{1k} = \{\pi_j(\mathbf{x}_1) \mid j < i \text{ where } \pi_i(\mathbf{x}_1) = k\}$, $S_k = A_{1k} \cap A_{2k}$ and $S'_k = A_{1k} \cup A_{2k} - S_k$.

Then it can be easily shown that

$$\sum_{\pi_i(\mathbf{x}_1)=\pi_j(\mathbf{x}_2)} E(p_i(\mathbf{x}_1)p_j(\mathbf{x}_2)) = \frac{2}{(\alpha+1)(\alpha+2)} \sum_{k \in T(\mathbf{x}_1, \mathbf{x}_2)} \left(\frac{\alpha}{\alpha+2}\right)^{\#S_k} \left(\frac{\alpha}{\alpha+1}\right)^{\#S'_k}.$$

Hence

$$\begin{aligned} \text{Cov}(f(\mathbf{x}_1), f(\mathbf{x}_2)) &= \text{Cov}_{G_0}(K(\mathbf{x}_1, \boldsymbol{\theta}), K(\mathbf{x}_2, \boldsymbol{\theta})) \times \frac{2}{(\alpha+1)(\alpha+2)} \\ &\times \sum_{k \in T(\mathbf{x}_1, \mathbf{x}_2)} \left(\frac{\alpha}{\alpha+2}\right)^{\#S_k} \left(\frac{\alpha}{\alpha+1}\right)^{\#S'_k}. \end{aligned}$$

■

S-3 Proof of Theorem 4

In this context, it is more convenient to deal with the notation used in the context of Theorem 2. Note that $\|\mathbf{x}_1 - \mathbf{x}_2\| \rightarrow 0$ implies that $\#S_k \rightarrow (k-1)$, $\#S'_k \rightarrow 0$, and hence, for any realization of the point process, $\text{Corr}(G_{\mathbf{x}_1}, G_{\mathbf{x}_2}) = \sum_{k \in T(\mathbf{x}_1, \mathbf{x}_2)} \left(\frac{\alpha}{\alpha+2}\right)^{\#S_k} \left(\frac{\alpha}{\alpha+1}\right)^{\#S'_k} \rightarrow \sum_{k=1}^{\infty} \left(\frac{\alpha}{\alpha+2}\right)^{k-1} = (\alpha+2)/2$. Since $\text{Corr}_{G_0}(K(\mathbf{x}_1, \boldsymbol{\theta}), K(\mathbf{x}_2, \boldsymbol{\theta})) \rightarrow 1$ as $\|\mathbf{x}_1 - \mathbf{x}_2\| \rightarrow 0$, it follows that $\text{Corr}(f(\mathbf{x}_1), f(\mathbf{x}_2)) \rightarrow 1$ as $\|\mathbf{x}_1 - \mathbf{x}_2\| \rightarrow 0$. On the other hand, as $\|\mathbf{x}_1 - \mathbf{x}_2\| \rightarrow \infty$, $\#T(\mathbf{x}_1, \mathbf{x}_2)$ is at most finite, $\#S_k \rightarrow 0$ and $\#S'_k \rightarrow \infty$. This implies that $\text{Corr}(G_{\mathbf{x}_1}, G_{\mathbf{x}_2}) \rightarrow 0$, and hence, $\text{Corr}(f(\mathbf{x}_1), f(\mathbf{x}_2)) \rightarrow 0$. Hence, by the dominated convergence theorem it follows that the unconditional correlation between $f(\mathbf{x}_1)$ and $f(\mathbf{x}_2)$ goes to 1 and 0, respectively, as $\|\mathbf{x}_1 - \mathbf{x}_2\| \rightarrow 0$ and $\|\mathbf{x}_1 - \mathbf{x}_2\| \rightarrow \infty$.

S-4 Proof of Theorem 7

Since for each \mathbf{x} , $f(\mathbf{x}) = \sum_{i=1}^{\infty} K(\mathbf{x}, \boldsymbol{\theta}_{\pi_i(\mathbf{x})})p_i(\mathbf{x})$, each \mathbf{x} must satisfy $\pi_k(\mathbf{x}) = i_k$, for every $k = 1, 2, \dots$, where $i_k \in \{1, 2, \dots\}$ ($i_k \neq i_{k'}$ for any $k \neq k'$), we must have $\mathbf{x} \in \bigcap_{k=1}^{\infty} A_{ki_k}$. For simplicity but without loss of generality let $i_k = k$ for $k = 1, 2, \dots$. Then for $\mathbf{x} \in \bigcap_{k=1}^{\infty} A_{ki_k}$

it holds that $K(\mathbf{x}, \boldsymbol{\theta}_{\pi_i(\mathbf{x})}) = K(\mathbf{x}, \boldsymbol{\theta}_i)$ and $p_i(\mathbf{x}) = V_i \prod_{j < i} (1 - V_j) = p_i$, say. Then, for any arbitrary \mathbf{x}_0 in the interior of $\cap_{k=1}^{\infty} A_{kk}$, it holds almost surely that

$$\lim_{\mathbf{x} \rightarrow \mathbf{x}_0} f(\mathbf{x}) = \lim_{\mathbf{x} \rightarrow \mathbf{x}_0} \sum_{i=1}^{\infty} K(\mathbf{x}, \boldsymbol{\theta}_i) p_i \quad (\text{S-4.1})$$

$$= \sum_{i=1}^{\infty} \lim_{\mathbf{x} \rightarrow \mathbf{x}_0} K(\mathbf{x}, \boldsymbol{\theta}_i) p_i$$

[using (A1) and the dominated convergence theorem

following from the facts that $K(\cdot, \cdot)$ is bounded and $\sum_{i=1}^{\infty} p_i = 1$.]

$$= \sum_{i=1}^{\infty} K(\mathbf{x}_0, \boldsymbol{\theta}_i) p_i \quad [\text{using (A2).}]$$

$$= f(\mathbf{x}_0). \quad (\text{S-4.2})$$

Hence $f(\cdot)$ is almost surely continuous in the interior of $\cap_{k=1}^{\infty} A_{kk}$.

To prove mean square continuity first note that the dominated convergence theorem can be applied as before, using boundedness of $K(\cdot, \cdot)$ and the fact that $\sum_{i=1}^{\infty} p_i = 1$ to guarantee that the following hold almost surely:

$$\lim_{\mathbf{x} \rightarrow \mathbf{x}_0} f(\mathbf{x})^2 = f(\mathbf{x}_0)^2, \quad (\text{S-4.3})$$

$$\lim_{\mathbf{x} \rightarrow \mathbf{x}_0} f(\mathbf{x}) f(\mathbf{x}_0) = f(\mathbf{x}_0)^2. \quad (\text{S-4.4})$$

Combining (S-4.2), (S-4.3) and (S-4.4) implies that $(f(\mathbf{x}) - f(\mathbf{x}_0))^2 \rightarrow 0$ almost surely. Now since $f(\cdot)$ is bounded almost surely by M (follows from (A1) and the fact that $\sum_{i=1}^{\infty} p_i = 1$), $f(\cdot)^2$ and $f(\cdot)f(\mathbf{x}_0)$ are almost surely bounded as well. Hence, taking expectations and using the dominated convergence theorem using the boundedness of $(f(\mathbf{x}) - f(\mathbf{x}_0))^2$, it follows that

$$\lim_{\mathbf{x} \rightarrow \mathbf{x}_0} E[f(\mathbf{x}) - f(\mathbf{x}_0)]^2 = 0.$$

Therefore, $f(\mathbf{x})$ is mean square continuous in the interior of $\cap_{k=1}^{\infty} A_{kk}$.

Let us now show that if $\mathbf{x}_0 \in \cap_{k=1}^{\infty} A_{kk}$ lies at the boundary of A_{kk} for some k , then $f(\cdot)$ is almost surely discontinuous at \mathbf{x}_0 . It is useful to note that for each k , $\pi_k(\cdot)$ is a step function and admits the representation

$$\pi_k(\mathbf{x}) = \sum_{i=1}^{\infty} i I_{A_{ki}}(\mathbf{x}).$$

For the sake of clarity, without loss of generality, let us assume that the dimensionality $d = 1$, so that $\mathbf{x}_0 = x_0$ is one-dimensional. Let us further assume, without loss of generality, that x_0 falls on the rightmost boundary of $A_{11} = \{x : \pi_1(x) = 1\}$, so that $x_0 = \sup\{x : \pi_1(x) = 1\}$.

Then, almost surely,

$$\lim_{x \downarrow x_0} f(x) = \sum_{i=1}^{\infty} K(x, \boldsymbol{\theta}_{i+1}) p_{i+1} \neq \sum_{i=1}^{\infty} K(x, \boldsymbol{\theta}_i) p_i = f(x_0),$$

showing that $f(\cdot)$ is almost surely discontinuous at x_0 . ■

S-5 Proof of Theorem 9

Without loss of generality, let \mathbf{x}_0 be an arbitrary point in the interior of $\cap_{k=1}^{\infty} A_{kk}$. Then, for any direction \mathbf{u} such that $\mathbf{x} = \mathbf{x}_0 + \mathbf{u} \in \mathcal{N}(\mathbf{x}_0) \cap \{\cap_{k=1}^{\infty} A_{kk}\}$, where $\mathcal{N}(\mathbf{x}_0)$ is any neighborhood of \mathbf{x}_0 ,

$$f(\mathbf{x}) = \sum_{i=1}^{\infty} K(\mathbf{x}, \boldsymbol{\theta}_i) p_i \tag{S-5.1}$$

and for each $i = 1, 2, \dots$, $K(\mathbf{x}, \boldsymbol{\theta}_i)$ admits the following (multivariate) Taylor's series expansion:

$$K(\mathbf{x}_0 + \mathbf{u}, \boldsymbol{\theta}_i) = K(\mathbf{x}_0, \boldsymbol{\theta}_i) + \mathbf{u}' \nabla K(\mathbf{x}_0, \boldsymbol{\theta}_i) + R(\mathbf{x}_0, \mathbf{u}, \boldsymbol{\theta}_i) \tag{S-5.2}$$

where, $|R(\mathbf{x}_0, \mathbf{u}, \boldsymbol{\theta}_i)| \leq c(\mathbf{x}_0, \boldsymbol{\theta}_i) \|\mathbf{u}\|^2$, for some function $c(\cdot, \cdot)$, independent of \mathbf{u} . The boundedness assumption (B1) guarantees that $c(\cdot, \cdot)$ is bounded above by some finite constant M_1 . Hence, for $i = 1, 2, \dots$,

$$R(\mathbf{x}_0, \mathbf{u}, \boldsymbol{\theta}_i) \leq M_1 \|\mathbf{u}\|^2. \tag{S-5.3}$$

It follows from (S-5.2) that

$$f(\mathbf{x}) = f(\mathbf{x}_0) + \mathbf{u}' \nabla f(\mathbf{x}_0) + R_2(\mathbf{x}_0, \mathbf{u}), \tag{S-5.4}$$

where

$$\begin{aligned} f(\mathbf{x}_0) &= \sum_{i=1}^{\infty} K(\mathbf{x}_0, \boldsymbol{\theta}_i) p_i \\ \nabla f(\mathbf{x}_0) &= \sum_{i=1}^{\infty} \nabla K(\mathbf{x}_0, \boldsymbol{\theta}_i) p_i \\ R_2(\mathbf{x}_0, \mathbf{u}) &= \sum_{i=1}^{\infty} R(\mathbf{x}_0, \mathbf{u}, \boldsymbol{\theta}_i) p_i \end{aligned}$$

In (S-5.4) $\mathbf{u}' \nabla f(\mathbf{x}_0)$ is clearly a process linear in \mathbf{u} . Moreover, since $\sum_{i=1}^{\infty} p_i = 1$, $|R_2(\mathbf{x}_0, \mathbf{u})|$ is bounded above by $M_1 \|\mathbf{u}\|^2$. Hence, almost surely, $\frac{|R_2(\mathbf{x}_0, \mathbf{u})|}{\|\mathbf{u}\|} \rightarrow 0$. Hence, using the dominated convergence theorem it follows that

$$\lim_{\|\mathbf{u}\| \rightarrow 0} E \left[\frac{f(\mathbf{x}_0 + \mathbf{u}) - f(\mathbf{x}_0) - \mathbf{u}' \nabla f(\mathbf{x}_0)}{\|\mathbf{u}\|} \right]^2 = \lim_{\|\mathbf{u}\| \rightarrow 0} E \left[\frac{R(\mathbf{x}_0, \mathbf{u})}{\|\mathbf{u}\|} \right]^2 = 0.$$

Hence, $f(\cdot)$ is mean square differentiable in the interior of $\cap_{k=1}^{\infty} A_{ki}$. ■

S-6 Proof of Theorem 10

For our purpose, we first state and prove a lemma.

Lemma 12. *Let p_k denote the random weights from an ODDP. For each positive integer $N \geq 1$ and each positive integer $r \geq 1$, let*

$$T_N(r, \alpha) = \left(\sum_{k=N}^{\infty} p_k \right)^r, \quad U_N(r, \alpha) = \sum_{k=N}^{\infty} p_k^r.$$

Then

$$E(T_N(r, \alpha)) = \left(\frac{\alpha}{\alpha + r} \right)^{N-1},$$

and

$$E(U_N(r, \alpha)) = \left(\frac{\alpha}{\alpha + r} \right)^{N-1} \frac{\Gamma(r)\Gamma(\alpha + 1)}{\Gamma(\alpha + r)}.$$

Proof. Let \mathcal{P} be a specific random measure from ODDP. Then

$$\mathcal{P}(\cdot) = V_{\pi_1} \delta_{\theta_{\pi_1}}(\cdot) + (1 - V_{\pi_1}) \left(V_{\pi_1}^* \delta_{\theta_{\pi_1}^*}(\cdot) + (1 - V_{\pi_1}^*) V_{\pi_2}^* \delta_{\theta_{\pi_2}^*}(\cdot) + (1 - V_{\pi_1}^*)(1 - V_{\pi_2}^*) V_{\pi_3}^* \delta_{\theta_{\pi_3}^*}(\cdot) + \dots \right),$$

where $V_{\pi_k}^* = V_{\pi_{k+1}}$ are independent $Beta(1, \alpha)$ random variables and $\theta_{\pi_k}^* = \theta_{\pi_{k+1}}$ are iid G_0 . So we have

$$\mathcal{P}(\cdot) \stackrel{\mathcal{D}}{=} V_{\pi_1} \delta_{\theta_{\pi_1}}(\cdot) + (1 - V_{\pi_1}) \mathcal{P}^*(\cdot),$$

where $V_{\pi_1}, \theta_{\pi_1}$ and $\mathcal{P}^*(\cdot)$ are independent and $\mathcal{P}^*(\cdot)$ is an ODDP.

Similarly we can show that

$$U_1(r, \alpha) \stackrel{\mathcal{D}}{=} V_{\pi_1}^r + (1 - V_{\pi_1})^r U_1(r, \alpha),$$

where on the right-hand side V_{π_1} and $U_1(r, \alpha)$ are mutually independent. Therefore taking expectations

$$E(U_1(r, \alpha)) = \frac{\Gamma(r+1)\Gamma(\alpha+1)}{\Gamma(\alpha+r+1)} + \frac{\alpha}{\alpha+r} E(U_1(r, \alpha)).$$

Then we have

$$E(U_1(r, \alpha)) = \frac{\Gamma(r)\Gamma(\alpha+1)}{\Gamma(\alpha+r)}. \tag{S-6.1}$$

Furthermore for $N \geq 2$, we have that

$$U_N(r, \alpha) = (1 - V_{\pi_1})^r \cdots (1 - V_{\pi_{(N-1)}})^r (U_1(r, \alpha)),$$

where all the variables on the right hand side are mutually independent. Taking expectations, we have

$$E(U_N(r, \alpha)) = \left(\prod_{k=1}^{N-1} E(1 - V_{\pi_k})^r \right) E((U_1(r, \alpha))).$$

Then using (S-6.1) we have

$$E(U_N(r, \alpha)) = \left(\frac{\alpha}{\alpha + r} \right)^{N-1} \frac{\Gamma(r)\Gamma(\alpha + 1)}{\Gamma(\alpha + r)}.$$

Now, similarly we can show that

$$\begin{aligned} T_N(r, \alpha) &\stackrel{\mathcal{D}}{=} (1 - V_{\pi_1})^r \cdots (1 - V_{\pi_{(N-1)}})^r (T_1(r, \alpha)) \\ &= (1 - V_{\pi_1})^r \cdots (1 - V_{\pi_{(N-1)}})^r \\ &= \left(\frac{\alpha}{\alpha + r} \right)^{N-1}. \end{aligned}$$

Hence, the lemma is proved. \square

We now proceed to the proof of Theorem 10. Note that

$$\begin{aligned} &|m_N(\mathbf{y}) - m_\infty(\mathbf{y})| \\ &= \left| \int_{\Theta} [\mathbf{y}|P_N][P]d\Theta - \int_{\Theta} [\mathbf{y}|P][P]d\Theta \right| \\ &\leq \int_{\Theta} |[\mathbf{y}|P_N] - [\mathbf{y}|P]| [P]d\Theta \end{aligned} \tag{S-6.2}$$

Now we expand $[\mathbf{y}|P_N]$ around P using multivariate Taylor's series expansion up to the second order:

$$[\mathbf{y}|P_N] = [\mathbf{y}|P] + \frac{\partial[\mathbf{y}|P_N]}{\partial P_N} \Big|_{P_N=P} (P_N - P) + (P_N - P)' \frac{\partial^2[\mathbf{y}|P_N]}{\partial P_N^2} \Big|_{P_N=P^*} (P_N - P),$$

[where P^* lies between P and P_N , that is, $\|P - P^*\| \leq \|P - P_N\|$.]

Noting that $[\mathbf{y}|P_N]$ and $[\mathbf{y}|P]$ are multivariate normal densities with mean P_N and P respectively and variance $\sigma^2 I$, where I is the $n \times n$ identity matrix, we have

$$\begin{aligned} \frac{\partial[\mathbf{y}|P_N]}{\partial P_N} \Big|_{P_N=P} &= [\mathbf{y}|P](\mathbf{y} - P)', \quad \text{and} \\ \frac{\partial^2[\mathbf{y}|P_N]}{\partial P_N^2} \Big|_{P_N=P^*} &= [\mathbf{y}|P^*]I(\mathbf{y} - P^*)(\mathbf{y} - P^*)'I - [\mathbf{y}|P^*]I. \end{aligned}$$

Therefore (S-6.2) becomes

$$\begin{aligned} &\int |[\mathbf{y}|P](\mathbf{y} - P)'(P_N - P) + (P_N - P)'[\mathbf{y}|P^*](\mathbf{y} - P^*)(\mathbf{y} - P^*)'(P_N - P) \\ &\quad - (P_N - P)'[\mathbf{y}|P^*]I(P_N - P)| [P]d\Theta. \end{aligned}$$

So, we have

$$\begin{aligned} &\int_{\mathbb{R}^n} |m_N(\mathbf{y}) - m_\infty(\mathbf{y})| d\mathbf{y} \\ &\leq \int_{\mathbb{R}^n} \int |[\mathbf{y}|P](\mathbf{y} - P)'(P_N - P) + (P_N - P)'[\mathbf{y}|P^*](\mathbf{y} - P^*)(\mathbf{y} - P^*)'(P_N - P) \\ &\quad - (P_N - P)'[\mathbf{y}|P^*]I(P_N - P)| [P]d\Theta. \end{aligned}$$

Now, using Fubini's theorem we can interchange the order of integration. Finally we have

$$\begin{aligned}
& \int_{\mathbb{R}^n} \int |[\mathbf{y}|P](\mathbf{y}-P)'(P_N-P) + (P_N-P)'[\mathbf{y}|P^*](\mathbf{y}-P^*)(\mathbf{y}-P^*)'(P_N-P) \\
& \quad - (P_N-P)'[\mathbf{y}|P^*]I(P_N-P)| [P]d\Theta d\mathbf{y} \\
&= \int \int_{\mathbb{R}^n} |[\mathbf{y}|P](\mathbf{y}-P)'(P_N-P) + (P_N-P)'[\mathbf{y}|P^*](\mathbf{y}-P^*)(\mathbf{y}-P^*)'(P_N-P) \\
& \quad - (P_N-P)'[\mathbf{y}|P^*]I(P_N-P)| d\mathbf{y}[P]d\Theta \\
&\leq \int \left[\int_{\mathbb{R}^n} [\mathbf{y}|P] |(\mathbf{y}-P)'(P_N-P)| d\mathbf{y} \right. \\
& \quad \left. + \int_{\mathbb{R}^n} (P_N-P)' \{[\mathbf{y}|P^*](\mathbf{y}-P^*)(\mathbf{y}-P^*)' + [\mathbf{y}|P^*]I\} (P_N-P) d\mathbf{y} \right] [P]d\Theta \\
&= \int \left[\sqrt{\frac{2}{\pi}} \mathbf{1}'_{n \times 1} |P_N - P| + 2(P_N - P)'I(P_N - P) \right] [P]d\Theta \\
&= E_{\Theta} \left[\sqrt{\frac{2}{\pi}} \mathbf{1}'_{n \times 1} |P_N - P| + 2(P_N - P)'(P_N - P) \right] \\
&= 2E_{\Theta} \left[\sqrt{\frac{2}{\pi}} \sum_{i=1}^n |P_N(\mathbf{x}_i) - P(\mathbf{x}_i)| + \sum_{i=1}^n (P_N(\mathbf{x}_i) - P(\mathbf{x}_i))^2 \right]. \tag{S-6.3}
\end{aligned}$$

In the above, $\mathbf{1}_{n \times 1}$ denotes the n -component vector with each element 1. Now,

$$|P_N(\mathbf{x}_i) - P(\mathbf{x}_i)| \leq M \left| p_N^N(\mathbf{x}_i) - p_N^\infty(\mathbf{x}_i) - \sum_{i=N+1}^{\infty} p_i(\mathbf{x}_i) \right|,$$

where $p_N^N(\mathbf{x}_i) = 1 - \sum_{k=1}^{N-1} p_k(\mathbf{x}_i) = 1 - \sum_{k=1}^{N-1} V_{\pi_k(\mathbf{x}_i)} \prod_{j < k} (1 - V_{\pi_j(\mathbf{x}_i)})$ and $p_N^\infty(\mathbf{x}_i) = V_{\pi_N(\mathbf{x}_i)} \prod_{j < N} (1 - V_{\pi_j(\mathbf{x}_i)})$ are the random weights corresponding to the N -th coefficient in the Sethuraman construction of truncated ODDP and the original ODDP respectively. We also have

$$\begin{aligned}
& (P_N(\mathbf{x}_i) - P(\mathbf{x}_i))^2 \\
& \leq M^2 \left(p_N^N(\mathbf{x}_i) - p_N^\infty(\mathbf{x}_i) - \sum_{i=N+1}^{\infty} p_i(\mathbf{x}_i) \right)^2 \\
& = M^2 \left[(p_N^N(\mathbf{x}_i) - p_N^\infty(\mathbf{x}_i))^2 + \left(\sum_{i=N+1}^{\infty} p_i(\mathbf{x}_i) \right)^2 + 2(p_N^N(\mathbf{x}_i) - p_N^\infty(\mathbf{x}_i)) \left(\sum_{i=N}^{\infty} p_i(\mathbf{x}_i) \right) \right].
\end{aligned}$$

Therefore

$$\begin{aligned}
& E_{\Theta} \left[\sum_{i=1}^n |P_N(\mathbf{x}_i) - P(\mathbf{x}_i)| \right] \\
& \leq \sum_{i=1}^n E_{\Theta} M \left[|p_N^N(\mathbf{x}_i) - p_N^\infty(\mathbf{x}_i)| + \sum_{i=N+1}^{\infty} p_i(\mathbf{x}_i) \right],
\end{aligned}$$

and

$$\begin{aligned}
& E_{\Theta} \left[\sum_{i=1}^n (P_N(\mathbf{x}_i) - P(\mathbf{x}_i))^2 \right] \\
& \leq \sum_{i=1}^n E_{\Theta} M^2 \left[(p_N^N(\mathbf{x}_i) - p_N^{\infty}(\mathbf{x}_i))^2 + \left(\sum_{i=N+1}^{\infty} p_i(\mathbf{x}_i) \right)^2 + 2 (p_N^N(\mathbf{x}_i) - p_N^{\infty}(\mathbf{x}_i)) \left(\sum_{i=N+1}^{\infty} p_i(\mathbf{x}_i) \right) \right]
\end{aligned}$$

Now,

$$\begin{aligned}
E(|p_N^N(\mathbf{x}_i) - p_N^{\infty}(\mathbf{x}_i)|) &= E[(1 - V_{\pi_1})(1 - V_{\pi_2}) \cdots (1 - V_{\pi_N})] \\
&= \left(\frac{\alpha}{\alpha + 1} \right)^N \text{ Since } V_i\text{'s are } iid \text{ Beta}(1, \alpha) \text{ random variables.}
\end{aligned} \tag{S-6.4}$$

Similarly, we have

$$\begin{aligned}
E(p_N^N(\mathbf{x}_i) - p_N^{\infty}(\mathbf{x}_i))^2 &= E[(1 - V_{\pi_1})(1 - V_{\pi_2}) \cdots (1 - V_{\pi_N})]^2 \\
&= \left(\frac{\alpha}{\alpha + 2} \right)^N.
\end{aligned} \tag{S-6.5}$$

Now, using Theorem 12 we have

$$E_{\Theta} \left(\sum_{i=N+1}^{\infty} p_i(\mathbf{x}_i) \right) = \left(\frac{\alpha}{\alpha + 1} \right)^N, \tag{S-6.6}$$

and

$$E_{\Theta} \left(\sum_{i=N+1}^{\infty} p_i(\mathbf{x}_i) \right)^2 = \left(\frac{\alpha}{\alpha + 2} \right)^N. \tag{S-6.7}$$

Now,

$$\begin{aligned}
& E_{\Theta} \left[2 (p_N^N(x_i) - p_N^{\infty}(x_i)) \left(\sum_{i=N+1}^{\infty} p_i(x_i) \right) \right] \\
&= 2E(1 - V_{\pi_1})(1 - V_{\pi_2}) \cdots (1 - V_{\pi_N}) \sum_{i=N+1}^{\infty} (1 - V_{\pi_1})(1 - V_{\pi_2}) \cdots (1 - V_{\pi_N}) \cdots (1 - V_{\pi_{i-1}}) V_{\pi_i} \\
&= 2 \left(\frac{\alpha}{\alpha + 2} \right)^N \sum_{i=N}^{\infty} \left(\frac{\alpha}{\alpha + 1} \right)^{i-N-1} \left(\frac{1}{\alpha + 1} \right) \\
&= 2 \left(\frac{\alpha}{\alpha + 2} \right)^N.
\end{aligned} \tag{S-6.8}$$

So, combining (S-6.5), (S-6.6), (S-6.7) and (S-6.8) we have

$$\begin{aligned} & \sum_{i=1}^n E_{\Theta} M^2 \left[(p_N^N(\mathbf{x}_i) - p_N^{\infty}(\mathbf{x}_i))^2 + \left(\sum_{i=N+1}^{\infty} p_i(\mathbf{x}_i) \right)^2 + 2 (p_N^N(\mathbf{x}_i) - p_N^{\infty}(\mathbf{x}_i)) \left(\sum_{i=N+1}^{\infty} p_i(\mathbf{x}_i) \right) \right] \\ & = 4M^2 n \left(\frac{\alpha}{\alpha + 2} \right)^N. \end{aligned} \quad (\text{S-6.9})$$

Therefore, combining (S-6.4) and (S-6.7) with (S-6.9) finally we have

$$\int_{\mathbb{R}^n} |m_N(\mathbf{y}) - m_{\infty}(\mathbf{y})| d\mathbf{y} \leq 4M^2 n \left(\frac{\alpha}{\alpha + 2} \right)^N + 2\sqrt{\frac{2}{\pi}} Mn \left(\frac{\alpha}{\alpha + 1} \right)^N,$$

thus completing the proof. ■

S-7 Transdimensional transformation based Markov chain Monte Carlo (TTMCMC)

In order to obtain a valid algorithm based on transformations, [Dutta and Bhattacharya \(2014\)](#) design appropriate “move types” so that detailed balance and irreducibility hold. We first illustrate the basic idea on transformation based moves with a simple example. Given that we are in the current state x , we may propose the “forward move” $x' = x + \epsilon$, where $\epsilon > 0$ is a simulation from some arbitrary density $g(\cdot)$ which is supported on the positive part of the real line. To move back to x from x' , we need to apply the “backward transformation” $x' - \epsilon$. In general, given ϵ and the current state x , we shall denote the forward transformation by $T(x, \epsilon)$, and the backward transformation by $T^b(x, \epsilon)$. For fixed ϵ the forward and the backward transformations must be one to one and onto, and satisfy $T^b(T(x, \epsilon), \epsilon) = x = T(T^b(x, \epsilon), \epsilon)$; see [Dutta and Bhattacharya \(2014\)](#) for a detailed discussion regarding these.

The simple idea discussed above has been generalized to the multi-dimensional situation by [Dutta and Bhattacharya \(2014\)](#). Remarkably, for any dimension, the moves can be constructed by simple deterministic transformations of the one-dimensional random variable ϵ , which is simulated from any arbitrary distribution on some relevant support.

The idea based on transformations has been generalized to the case of variable dimensionality by [Das and Bhattacharya \(2019b\)](#). In other words, [Das and Bhattacharya \(2019b\)](#) show that using simple deterministic transformations and a single ϵ (or just a few ϵ 's) it is possible to devise an effective dimension-hopping algorithm which changes dimension as well as updates the other parameters, all in a single block, while maintaining, at the same time, high acceptance rate. In this sense this new methodology accomplishes automation of move-types. [Das and Bhattacharya \(2019b\)](#) refer to this dimension changing methodology as Transdimensional Transformation based Markov Chain Monte Carlo (TTMCMC).

Before we illustrate the key concept of TTMCMC with a simple example, it is necessary to define some requisite notation, borrowed from [Dutta and Bhattacharya \(2014\)](#).

S-7.1 Notation

Suppose now that \mathcal{X} is a k -dimensional space of the form $\mathcal{X} = \prod_{i=1}^k \mathcal{X}_i$ so that $T = (T_1, \dots, T_k)$ where each $T_i : \mathcal{X}_i \times \mathcal{D} \rightarrow \mathcal{X}_i$, for some set \mathcal{D} , are the component-wise transformations. Let $\zeta = (\zeta_1, \dots, \zeta_k)$ be a vector of indicator variables, where, for $i = 1, \dots, k$, $\zeta_i = 1$ and $\zeta_i = -1$ indicate, respectively, application of forward transformation and backward transformation to x_i , and let $\zeta_i = 0$ denote no change to x_i . Given any such indicator vector ζ , let us define $T_\zeta = (g_{1,\zeta_1}, g_{2,\zeta_2}, \dots, g_{k,\zeta_k})$ where

$$g_{i,\zeta_i} = \begin{cases} T_i^b & \text{if } \zeta_i = -1 \\ x_i & \text{if } \zeta_i = 0 \\ T_i & \text{if } \zeta_i = 1. \end{cases}$$

Corresponding to any given ζ , we also define the following ‘conjugate’ vector $\zeta^c = (\zeta_1^c, \zeta_2^c, \dots, \zeta_k^c)$, where

$$\zeta_i^c = \begin{cases} 1 & \text{if } \zeta_i = -1 \\ 0 & \text{if } \zeta_i = 0 \\ -1 & \text{if } \zeta_i = 1. \end{cases}$$

With this definition of ζ^c , T_{ζ^c} can be interpreted as the conjugate of T_ζ .

Since 3^k values of ζ are possible, it is clear that T , via ζ , induces 3^k many types of ‘moves’ of the forms $\{T_{\zeta_i}; i = 1, \dots, 3^k\}$ on the state-space. Suppose now that there is a subset \mathcal{Y} of \mathcal{D} such that the sets $T_{\zeta_i}(\mathbf{x}, \mathcal{Y})$ and $T_{\zeta_j}(\mathbf{x}, \mathcal{Y})$ are disjoint for every $\zeta_i \neq \zeta_j$. In fact, \mathcal{Y} denotes the support of the distribution $g(\cdot)$ from which ϵ is simulated.

S-7.2 Illustration of TTMC MC with a simple example

Let us now illustrate the main idea of TTMC MC informally using the additive transformation. Although the example we illustrate TTMC MC with is borrowed from [Das and Bhattacharya \(2019b\)](#), the algorithm we now present is somewhat different from that of [Das and Bhattacharya \(2019b\)](#). Assume that the current state is $\mathbf{x} = (x_1, x_2) \in \mathbb{R}^2$. We first randomly select $u = (u_1, u_2, u_3) \sim \text{Multinomial}(w_b, w_d, w_{nc})$, where $w_b, w_d, w_{nc} (> 0)$ such that $w_b + w_d + w_{nc} = 1$ are the probabilities of birth, death, and no-change moves, respectively. That is, if $u_1 = 1$, then we increase the dimensionality from 2 to 3; if $u_2 = 1$, then we decrease the dimensionality from 2 to 1, and if $u_3 = 1$, then we keep the dimensionality unchanged. In the latter case, when the dimensionality is unchanged, the acceptance probability remains the same as in TMC MC, as provided in Algorithm 3.1 of [Dutta and Bhattacharya \(2014\)](#).

If $u_1 = 1$, we can increase the dimensionality by first selecting one of x_1 and x_2 with probability $1/2$ – assuming for clarity that x_1 has been selected, we then construct the move-type $T_{b,\zeta}(\mathbf{x}, \epsilon) = (x_1 + a_1\epsilon, x_1 - a_1\epsilon, x_2 + \zeta_2 a_2\epsilon) = (g_{1,\zeta_1=1}(x_1, \epsilon), g_{1,\zeta_1^c=-1}(x_1, \epsilon), g_{2,\zeta_2}(x_2, \epsilon))$, say. Here, as in TMC MC, we draw $\epsilon \sim g(\cdot)$, where $g(\cdot)$ is supported on the positive part of the real line, and draw $\zeta_2 = 1$ with probability p_2 and $\zeta_2 = -1$ with probability $1 - p_2$. Note that the value $\zeta_2 = 0$ is redundant for additive transformation (see [Dutta and Bhattacharya \(2014\)](#) for the details) and so is omitted here. We re-label $\mathbf{x}' = T_{b,\zeta}(\mathbf{x}, \epsilon) = (x_1 + a_1\epsilon, x_1 - a_1\epsilon, x_2 + \zeta_2 a_2\epsilon)$ as (x'_1, x'_2, x'_3) . Thus, $T_{b,\zeta}(\mathbf{x}, \epsilon)$ increases the dimension from 2 to 3.

We accept this birth move with probability

$$a_b(\mathbf{x}, \epsilon) = \min \left\{ 1, \frac{w_d}{w_b} \times \frac{p_2^{I_{\{1\}}(\zeta_2^c)} q_2^{I_{\{-1\}}(\zeta_2^c)}}{p_2^{I_{\{1\}}(\zeta_2)} q_2^{I_{\{-1\}}(\zeta_2)}} \times \frac{\pi(x_1 + a_1\epsilon, x_1 - a_1\epsilon, x_2 + \zeta_2 a_2\epsilon)}{\pi(x_1, x_2)} \times \left| \frac{\partial(T_{b,\zeta}(\mathbf{x}, \epsilon))}{\partial(\mathbf{x}, \epsilon)} \right| \right\}. \quad (\text{S-7.1})$$

In (S-7.1),

$$\left| \frac{\partial(T_{b,\zeta}(\mathbf{x}, \epsilon))}{\partial(\mathbf{x}, \epsilon)} \right| = \left| \frac{\partial(x_1 + a_1\epsilon, x_1 - a_1\epsilon, x_2 + \zeta_2 a_2\epsilon)}{\partial(x_1, x_2, \epsilon)} \right| = \left| \begin{pmatrix} 1 & 1 & 0 \\ 0 & 0 & 1 \\ a_1 & -a_1 & \zeta_2 a_2 \end{pmatrix} \right| = 2a_1. \quad (\text{S-7.2})$$

Now let us illustrate the problem of returning to $(x_1, x_2) \in \mathbb{R}^2$ from $T_{b,\zeta}(\mathbf{x}, \epsilon) = (x_1 + a_1\epsilon, x_1 - a_1\epsilon, x_2 + \zeta_2 a_2\epsilon) \in \mathbb{R}^3$. For our purpose, in this paper, we select one of the first two elements of $T_{b,\zeta}(\mathbf{x}, \epsilon)$ with the same probability. Suppose that we select $x_1 + a_1\epsilon$ with probability 1/2. We then deterministically choose its right-adjacent $x_1 - a_1\epsilon$, and form the average $x_1^* = ((x_1 + a_1\epsilon) + (x_1 - a_1\epsilon))/2 = x_1$. For non-additive transformations we can consider the averages of the backward moves of the selected element and its right-adjacent. Even in this additive transformation example, after simulating ϵ as before we can consider the respective backward moves of $x_1 + a_1\epsilon$ and $x_1 - a_1\epsilon$, both yielding x_1 , and then take the average denoted by x_1^* . For the remaining element $x_2 + \zeta_2 a_2\epsilon$, we need to simulate ζ_2^c and then consider the move $(x_2 + \zeta_2 a_2\epsilon) + \zeta_2^c a_2\epsilon = x_2$. Thus, we can return to (x_1, x_2) using this strategy.

Letting $\mathbf{x}' = (x'_1, x'_2, x'_3) = (x_1 + a_1\epsilon, x_1 - a_1\epsilon, x_2 + \zeta_2 a_2\epsilon)$, and denoting the average involving the first two elements by x_1^* , the death move is then given by $\mathbf{x}'' = T_{d,\zeta}(\mathbf{x}', \epsilon) = (x_1^*, x'_3 + \zeta_2^c a_2\epsilon) = (\frac{x'_1 + x'_2}{2}, x'_3 + \zeta_2^c a_2\epsilon)$. Now observe that for returning to (x'_1, x'_2) from x_1^* , we must have $x^* + a_1\epsilon^* = x'_1$ and $x^* - a_1\epsilon^* = x'_2$, which yield $\epsilon^* = (x'_1 - x'_2)/2a_1$. Hence, the Jacobian associated with the death move in this case is given by

$$\left| \frac{\partial(T_{d,\zeta}(\mathbf{x}', \epsilon), \epsilon^*, \epsilon)}{\partial(\mathbf{x}', \epsilon)} \right| = \left| \frac{\partial\left(\frac{x'_1 + x'_2}{2}, x'_3 + \zeta_2^c a_2\epsilon, \frac{x'_1 - x'_2}{2a_1}, \epsilon\right)}{\partial(x'_1, x'_2, x'_3, \epsilon)} \right| = \left| \begin{pmatrix} \frac{1}{2} & 0 & \frac{1}{2a_1} & 0 \\ \frac{1}{2} & 0 & -\frac{1}{2a_1} & 0 \\ 0 & 1 & 0 & 0 \\ 0 & \zeta_2^c a_2 & 0 & 1 \end{pmatrix} \right| = \frac{1}{2a_1}. \quad (\text{S-7.3})$$

We accept this death move with probability

$$a_d(\mathbf{x}'', \epsilon, \epsilon^*) = \min \left\{ 1, \frac{w_b}{w_d} \times \frac{P(\zeta^c)}{P(\zeta)} \frac{\pi(\mathbf{x}'')}{\pi(\mathbf{x}'^{(t)})} \left| \frac{\partial(T_{d,\zeta}(\mathbf{x}', \epsilon), \epsilon^*, \epsilon)}{\partial(\mathbf{x}', \epsilon)} \right| \right\} \\ = \min \left\{ 1, 3 \times \frac{w_b}{w_d} \times \frac{p_2^{I_{\{1\}}(\zeta_2^c)} q_2^{I_{\{-1\}}(\zeta_2^c)}}{p_2^{I_{\{1\}}(\zeta_2)} q_2^{I_{\{-1\}}(\zeta_2)}} \times \frac{\pi(\mathbf{x}'')}{\pi(\mathbf{x}')} \times \frac{1}{2a_1} \right\}.$$

In general, $\mathbf{x} \in \mathbb{R}^{mk}$ may be of the form $(\mathbf{x}_1, \mathbf{x}_2, \dots, \mathbf{x}_m)$, where $\mathbf{x}_\ell = (x_{\ell,1}, x_{\ell,2}, \dots, x_{\ell,k})$ for $\ell = 1, 2, \dots, m$, where $m \geq 1$ is an integer. Let us assume that if the dimension of any one

\mathbf{x}_ℓ is changed, then the dimensions of all other $\mathbf{x}_{\ell'}$; $\ell' \neq \ell$ must also change accordingly. For instance, in our model, where we have summands with unknown number of components and the i -th component is characterized by the parameters associated with ODDP $(\boldsymbol{\theta}_{1i}, \boldsymbol{\theta}_{2i}, V_i, z_i)$, when the dimension of the current k -dimensional vector of the location parameter of the central distribution $(\theta_{11}, \dots, \theta_{1k})$ is increased by one, then one must simultaneously increase the dimension of the other set of the current k -dimensional location parameter $(\theta_{21}, \dots, \theta_{2k})$, the k -dimensional vector of the associated point process (z_1, \dots, z_k) , as well as the k -dimensional mass vector (V_1, \dots, V_k) by one. In Section S-7.3 we present a TTMC algorithm (Algorithm S-7.1) for situations of this kind, and show that detailed balance holds (irreducibility and aperiodicity hold by the same arguments provided in Das and Bhattacharya (2019b)). It is worth mentioning that although Das and Bhattacharya (2019b) provide a TTMC algorithm for these situations (Algorithm 5.1 of their paper), their algorithm is somewhat different from ours in that, for the death move, we select only one element randomly; then we choose the right-adjacent element; take backward transformations of both of them, finally taking the average. On the other hand, Das and Bhattacharya (2019b) select two elements randomly without replacement. This difference between the algorithm is reflected in the acceptance ratios – our algorithm is slightly simpler in that the random selection probabilities do not appear in our acceptance ratio, unlike that of Das and Bhattacharya (2019b).

S-7.3 General TTMC algorithm for jumping more than one dimensions at a time when several sets of parameters are related

Algorithm S-7.1. *General TTMC algorithm for jumping m dimensions with m related sets of co-ordinates.*

- Let the initial value be $\mathbf{x}^{(0)} \in \mathbb{R}^{mk}$, where $k \geq m$.
- For $t = 0, 1, 2, \dots$
 1. Generate $u = (u_1, u_2, u_3) \sim \text{Multinomial}(1; w_{b,k}, w_{d,k}, w_{nc,k})$.
 2. If $u_1 = 1$ (increase dimension from mk to $(m+1)k$), then
 - (a) Randomly select one co-ordinate from $\mathbf{x}_1^{(t)} = (x_{11}^{(t)}, \dots, x_{1k}^{(t)})$ without replacement. Let j denote the chosen co-ordinate.
 - (b) Generate $\boldsymbol{\epsilon}_m = (\epsilon_1, \dots, \epsilon_m) \stackrel{iid}{\sim} g(\cdot)$ and for $i \in \{1, \dots, k\} \setminus \{j\}$ simulate $\zeta_{\ell,i} \sim \text{Multinomial}(1; p_{\ell,i}, q_{\ell,i}, 1 - p_{\ell,i} - q_{\ell,i})$ independently, for every $\ell = 1, \dots, m$.
 - (c) Propose the birth move as follows: for each $\ell = 1, \dots, m$, apply the transformation $x_{\ell,i}^{(t)} \rightarrow g_{i, \zeta_{\ell,i}}(x_{\ell,i}^{(t)}, \epsilon_1)$ for $i \in \{1, \dots, k\} \setminus \{j\}$ and, for each $\ell \in \{1, \dots, m\}$, split $x_{\ell,j}^{(t)}$ into $g_{\ell, \zeta_{\ell,j}=1}(x_{\ell,j}^{(t)}, \epsilon_\ell)$ and $g_{\ell, \zeta_{\ell,j}=-1}(x_{\ell,j}^{(t)}, \epsilon_\ell)$. In other words, let $\mathbf{x}' = T_{b, \zeta}(\mathbf{x}^{(t)}, \boldsymbol{\epsilon}_m) = (\mathbf{x}'_1, \dots, \mathbf{x}'_m)$ denote the complete

birth move, where, for $\ell = 1, \dots, m$, \mathbf{x}'_ℓ is given by

$$\begin{aligned} \mathbf{x}'_\ell = & (g_{\ell, \zeta_{\ell, 1}}(x_{\ell, 1}^{(t)}, \epsilon_1), \dots, g_{j-1, \zeta_{\ell, j-1}}(x_{\ell, j-1}^{(t)}, \epsilon_1), \\ & g_{j, \zeta_{\ell, j}=1}(x_{\ell, j}^{(t)}, \epsilon_\ell), g_{j, \zeta_{\ell, j}^c=-1}(x_{\ell, j}^{(t)}, \epsilon_\ell), g_{j+1, \zeta_{\ell, j+1}}(x_{\ell, j+1}^{(t)}, \epsilon_1), \dots, \\ & \dots, g_{k, \zeta_{\ell, k}}(x_{\ell, k}^{(t)}, \epsilon_1)). \end{aligned}$$

Re-label the $k+1$ elements of \mathbf{x}'_ℓ as $(x'_{\ell, 1}, x'_{\ell, 2}, \dots, x'_{\ell, k+1})$.

(d) Calculate the acceptance probability of the birth move \mathbf{x}' :

$$a_b(\mathbf{x}^{(t)}, \boldsymbol{\epsilon}_m) = \min \left\{ 1, \frac{w_{d, k+1}}{w_{b, k}} \times \frac{P_{(j)}(\boldsymbol{\zeta}^c)}{P_{(j)}(\boldsymbol{\zeta})} \frac{\pi(\mathbf{x}')}{\pi(\mathbf{x}^{(t)})} \left| \frac{\partial(T_{b, \boldsymbol{\zeta}}(\mathbf{x}^{(t)}, \boldsymbol{\epsilon}_m))}{\partial(\mathbf{x}^{(t)}, \boldsymbol{\epsilon}_m)} \right| \right\},$$

where

$$P_{(j)}(\boldsymbol{\zeta}) = \prod_{\ell=1}^m \prod_{i \in \{1, \dots, k\} \setminus \{j\}} p_{\ell, i}^{I_{\{1\}}(\zeta_{\ell, i})} q_{\ell, i}^{I_{\{-1\}}(\zeta_{\ell, i})},$$

and

$$P_{(j)}(\boldsymbol{\zeta}^c) = \prod_{\ell=1}^m \prod_{i \in \{1, \dots, k\} \setminus \{j\}} p_{\ell, i}^{I_{\{1\}}(\zeta_{\ell, i}^c)} q_{\ell, i}^{I_{\{-1\}}(\zeta_{\ell, i}^c)}.$$

(e) Set

$$\mathbf{x}^{(t+1)} = \begin{cases} \mathbf{x}' & \text{with probability } a_b(\mathbf{x}^{(t)}, \boldsymbol{\epsilon}_m) \\ \mathbf{x}^{(t)} & \text{with probability } 1 - a_b(\mathbf{x}^{(t)}, \boldsymbol{\epsilon}_m). \end{cases}$$

3. If $u_2 = 1$ (decrease dimension from k to $k - m$, for $k \geq 2m$), then

(a) Generate $\boldsymbol{\epsilon}_m = (\epsilon_1, \dots, \epsilon_m) \stackrel{iid}{\sim} g(\cdot)$.

(b) Randomly select one co-ordinate (say, the j -th co-ordinate) from $\mathbf{x}_1 = (x_{1, 1}, \dots, x_{1, k-1})$. For $\ell = 1, \dots, m$, let

$$x_{\ell, j}^* = \left(g_{j, \zeta_{\ell, j}^c=-1}(x_{\ell, j}, \epsilon_\ell) + g_{j', \zeta_{\ell, j'+1}=1}(x_{\ell, j+1}, \epsilon_\ell) \right) / 2;$$

replace the co-ordinate $x_{\ell, j}$ by the average $x_{\ell, j}^*$ and delete $x_{\ell, j+1}$.

(c) Simulate $\boldsymbol{\zeta}$ by generating independently, for $\ell = 1, \dots, m$ and for $i \in \{1, \dots, k\} \setminus \{j, j+1\}$, $\zeta_{\ell, i} \sim \text{Multinomial}(1; p_{\ell, i}, q_{\ell, i}, 1 - p_{\ell, i} - q_{\ell, i})$.

(d) For $\ell = 1, \dots, m$ and for $i \in \{1, \dots, k\} \setminus \{j, j+1\}$, apply the transformation $x'_{\ell, i} = g_{i, \zeta_{\ell, i}}(x_{\ell, i}^{(t)}, \epsilon_1)$.

(e) Propose the following death move $\mathbf{x}' = T_{d, \boldsymbol{\zeta}}(\mathbf{x}^{(t)}, \boldsymbol{\epsilon}_m) = (\mathbf{x}'_1, \dots, \mathbf{x}'_m)$ where for $\ell = 1, \dots, m$, \mathbf{x}_ℓ is given by

$$\begin{aligned} \mathbf{x}'_\ell = & (g_{1, \zeta_{\ell, 1}}(x_{\ell, 1}^{(t)}, \epsilon_1), \dots, g_{j-1, \zeta_{\ell, j-1}}(x_{\ell, j-1}^{(t)}, \epsilon_1), x_{\ell, j}^*, g_{j+1, \zeta_{\ell, j+1}}(x_{\ell, j+1}^{(t)}, \epsilon_1), \\ & \dots, g_{k, \zeta_{\ell, k}}(x_{\ell, k}^{(t)}, \epsilon_1)). \end{aligned}$$

Re-label the elements of \mathbf{x}'_ℓ as $(x'_{\ell, 1}, x'_{\ell, 2}, \dots, x'_{\ell, k-1})$.

(f) For $\ell = 1, \dots, m$, solve for ϵ_ℓ^* from the equations $g_{\ell, \zeta_{\ell, j}=1}(x_{\ell, j}^*, \epsilon_\ell^*) = x_{\ell, j}$ and $g_{\ell, \zeta_{\ell, j}=-1}(x_{\ell, j}^*, \epsilon_\ell^*) = x_{\ell, j+1}$ and express ϵ_ℓ^* in terms of $x_{\ell, j}$ and $x_{\ell, j+1}$. Let $\boldsymbol{\epsilon}_m^* = (\epsilon_1^*, \dots, \epsilon_m^*)$.

(g) Calculate the acceptance probability of the death move:

$$a_d(\mathbf{x}^{(t)}, \boldsymbol{\epsilon}_m, \boldsymbol{\epsilon}_m^*) = \min \left\{ 1, \frac{w_{b, k-m}}{w_{d, k}} \times \frac{P_{(j, j+1)}(\boldsymbol{\zeta}^c)}{P_{(j, j+1)}(\boldsymbol{\zeta})} \frac{\pi(\mathbf{x}')}{\pi(\mathbf{x}^{(t)})} \left| \frac{\partial(T_{d, \boldsymbol{\zeta}}(\mathbf{x}^{(t)}, \boldsymbol{\epsilon}_m), \boldsymbol{\epsilon}_m^*, \boldsymbol{\epsilon}_m)}{\partial(\mathbf{x}^{(t)}, \boldsymbol{\epsilon}_m)} \right| \right\},$$

where

$$P_{(j, j+1)}(\boldsymbol{\zeta}) = \prod_{\ell=1}^m \prod_{i \in \{1, \dots, k\} \setminus \{j, j+1\}} p_{\ell, i}^{I_{\{1\}}(\zeta_{\ell, i})} q_{\ell, i}^{I_{\{-1\}}(\zeta_{\ell, i})},$$

and

$$P_{(j, j+1)}(\boldsymbol{\zeta}^c) = \prod_{\ell=1}^m \prod_{i \in \{1, \dots, k\} \setminus \{j, j+1\}} p_{\ell, i}^{I_{\{1\}}(\zeta_{\ell, i}^c)} q_{\ell, i}^{I_{\{-1\}}(\zeta_{\ell, i}^c)}.$$

(h) Set

$$\mathbf{x}^{(t+1)} = \begin{cases} \mathbf{x}' & \text{with probability } a_d(\mathbf{x}^{(t)}, \boldsymbol{\epsilon}_m, \boldsymbol{\epsilon}_m^*) \\ \mathbf{x}^{(t)} & \text{with probability } 1 - a_d(\mathbf{x}^{(t)}, \boldsymbol{\epsilon}_m, \boldsymbol{\epsilon}_m^*). \end{cases}$$

4. If $u_3 = 1$ (dimension remains unchanged), then implement steps (1), (2), (3) of Algorithm 3.1 of [Dutta and Bhattacharya \(2014\)](#).

• End for

S-7.4 Detailed balance

To see that detailed balance is satisfied for the birth and death moves, note that associated with the birth move, the probability of transition $\mathbf{x} \in \mathbb{R}^k \mapsto T_{b, z}(\mathbf{x}, \boldsymbol{\epsilon}_m) \in \mathbb{R}^{k+m}$, with $k \geq m$, is given by:

$$\begin{aligned} & \pi(\mathbf{x}) \times \frac{1}{k} \times w_{b, k} \times \prod_{\ell=1}^m g(\epsilon_\ell) \times \prod_{\ell=1}^m \prod_{i \in \{1, \dots, k\} \setminus \{j\}} p_{\ell, i}^{I_{\{1\}}(\zeta_{\ell, i})} q_{\ell, i}^{I_{\{-1\}}(\zeta_{\ell, i})} \\ & \times \min \left\{ 1, \frac{w_{d, k+m}}{w_{b, k}} \times \frac{\prod_{\ell=1}^m \prod_{i \in \{1, \dots, k\} \setminus \{j\}} p_{\ell, i}^{I_{\{1\}}(\zeta_{\ell, i}^c)} q_{\ell, i}^{I_{\{-1\}}(\zeta_{\ell, i}^c)}}{\prod_{\ell=1}^m \prod_{i \in \{1, \dots, k\} \setminus \{j\}} p_{\ell, i}^{I_{\{1\}}(\zeta_{\ell, i})} q_{\ell, i}^{I_{\{-1\}}(\zeta_{\ell, i})}} \right. \\ & \quad \left. \times \frac{\pi(T_{b, \boldsymbol{\zeta}}(\mathbf{x}, \boldsymbol{\epsilon}_m))}{\pi(\mathbf{x})} \times \left| \frac{\partial(T_{b, \boldsymbol{\zeta}}(\mathbf{x}^{(t)}, \boldsymbol{\epsilon}_m))}{\partial(\mathbf{x}^{(t)}, \boldsymbol{\epsilon}_m)} \right| \right\} \\ & = \frac{1}{k} \times \prod_{i=1}^m g(\epsilon_i) \times \min \left\{ \pi(\mathbf{x}) \times w_{b, k} \times \prod_{\ell=1}^m \prod_{i \in \{1, \dots, k\} \setminus \{j\}} p_{\ell, i}^{I_{\{1\}}(\zeta_{\ell, i})} q_{\ell, i}^{I_{\{-1\}}(\zeta_{\ell, i})}, \right. \\ & \quad \left. \times w_{d, k+m} \times \prod_{\ell=1}^m \prod_{i \in \{1, \dots, k\} \setminus \{j\}} p_{\ell, i}^{I_{\{1\}}(\zeta_{\ell, i}^c)} q_{\ell, i}^{I_{\{-1\}}(\zeta_{\ell, i}^c)} \pi(T_{b, \boldsymbol{\zeta}}(\mathbf{x}, \boldsymbol{\epsilon}_m)) \times \left| \frac{\partial(T_{b, \boldsymbol{\zeta}}(\mathbf{x}^{(t)}, \boldsymbol{\epsilon}_m))}{\partial(\mathbf{x}^{(t)}, \boldsymbol{\epsilon}_m)} \right| \right\}. \end{aligned} \tag{S-7.4}$$

The transition probability of the reverse death move is given by:

$$\begin{aligned}
& \pi(\mathbf{x}) \times w_{d,k+m} \times \frac{1}{k} \times \prod_{\ell=1}^m g(\epsilon_\ell) \times \prod_{\ell=1}^m \prod_{i \in \{1, \dots, k\} \setminus \{j\}} p_{\ell,i}^{I_{\{1\}}(\zeta_{\ell,i}^c)} q_{\ell,i}^{I_{\{-1\}}(\zeta_{\ell,i}^c)} \times \left| \frac{\partial(T_{d,\zeta}^{-1}(\mathbf{x}^{(t)}, \boldsymbol{\epsilon}_m), \boldsymbol{\epsilon}_m^*, \boldsymbol{\epsilon}_m)}{\partial(\mathbf{x}^{(t)}, \boldsymbol{\epsilon}_m)} \right| \\
& \times \min \left\{ 1, \frac{w_{b,k}}{w_{d,k+m}} \times \frac{\prod_{\ell=1}^m \prod_{i \in \{1, \dots, k\} \setminus \{j\}} p_{\ell,i}^{I_{\{1\}}(\zeta_{\ell,i})} q_{\ell,i}^{I_{\{-1\}}(\zeta_{\ell,i})}}{\prod_{\ell=1}^m \prod_{i \in \{1, \dots, k\} \setminus \{j\}} p_{\ell,i}^{I_{\{1\}}(\zeta_{\ell,i}^c)} q_{\ell,i}^{I_{\{-1\}}(\zeta_{\ell,i}^c)}} \right. \\
& \quad \left. \times \frac{\pi(\mathbf{x})}{\pi(T_{b,\zeta}(\mathbf{x}, \boldsymbol{\epsilon}_m))} \times \left| \frac{\partial(T_{d,\zeta}(\mathbf{x}^{(t)}, \boldsymbol{\epsilon}_m), \boldsymbol{\epsilon}_m^*, \boldsymbol{\epsilon}_m)}{\partial(\mathbf{x}^{(t)}, \boldsymbol{\epsilon}_m)} \right| \right\} \\
& = \frac{1}{k} \times \prod_{\ell=1}^m g(\epsilon_\ell) \times \min \left\{ \pi(T_{b,\zeta}(\mathbf{x}, \boldsymbol{\epsilon}_m)) \times w_{d,k+m} \times \prod_{\ell=1}^m \prod_{i \in \{1, \dots, k\} \setminus \{j\}} p_{\ell,i}^{I_{\{1\}}(\zeta_{\ell,i}^c)} q_{\ell,i}^{I_{\{-1\}}(\zeta_{\ell,i}^c)} \right. \\
& \quad \left. \times \left| \frac{\partial(T_{d,\zeta}^{-1}(\mathbf{x}^{(t)}, \boldsymbol{\epsilon}_m), \boldsymbol{\epsilon}_m^*, \boldsymbol{\epsilon}_m)}{\partial(\mathbf{x}^{(t)}, \boldsymbol{\epsilon}_m)} \right|, w_{b,k} \times \prod_{\ell=1}^m \prod_{i \in \{1, \dots, k\} \setminus \{j\}} p_{\ell,i}^{I_{\{1\}}(\zeta_{\ell,i})} q_{\ell,i}^{I_{\{-1\}}(\zeta_{\ell,i})} \times \pi(\mathbf{x}) \right\}. \tag{S-7.5}
\end{aligned}$$

Noting that $\left| \frac{\partial(T_{d,\zeta}^{-1}(\mathbf{x}^{(t)}, \boldsymbol{\epsilon}_m), \boldsymbol{\epsilon}_m^*, \boldsymbol{\epsilon}_m)}{\partial(\mathbf{x}^{(t)}, \boldsymbol{\epsilon}_m^*, \boldsymbol{\epsilon}_m)} \right| = \left| \frac{\partial(T_{b,\zeta}(\mathbf{x}^{(t)}, \boldsymbol{\epsilon}_m))}{\partial(\mathbf{x}^{(t)}, \boldsymbol{\epsilon}_m)} \right|$, it follows that (S-7.4) = (S-7.5), showing that detailed balance holds for the birth and the death moves.

S-8 TTMCMC algorithm for our spatio-temporal model

We now specialize the general TTMCMC algorithm (Algorithm S-7.1) provided in Section S-7.3 in our spatio-temporal context. For our spatio-temporal model, we need to update the variable dimensional mass parameter $\mathbf{V} = (V_1, \dots, V_k)$, the point process variables $\mathbf{z} = (z_1, \dots, z_k)$, location parameters $\boldsymbol{\theta}_1 = (\theta_{11}, \dots, \theta_{1k})$, the other set of location parameters $\boldsymbol{\theta}_2 = (\theta_{21}, \dots, \theta_{2k})$, and fixed dimensional parameters α , λ , error variance σ and the parameters related to the kernel, namely, φ , a_δ , b_ψ , $(\psi_1(\mathbf{s}_1), \dots, \psi_1(\mathbf{s}_n))$, $(\psi_2(\mathbf{s}_1), \dots, \psi_2(\mathbf{s}_n))$, $(\delta(t_1), \dots, \delta(t_n))$, and τ . For updating the variable dimensional parameters we use proposed TTMCMC algorithm, and for fixed dimension we use the TMCMC algorithm of [Dutta and Bhattacharya \(2014\)](#). We denote by $\boldsymbol{\xi} = (\mathbf{V}, \mathbf{z}, \boldsymbol{\theta}_1, \boldsymbol{\theta}_2)$ the collection of all variable dimensional parameters and by $\boldsymbol{\eta} = (\varphi, a_\delta, b_\psi, \psi_1(\mathbf{s}_1), \dots, \psi_1(\mathbf{s}_n), \psi_2(\mathbf{s}_1), \dots, \psi_2(\mathbf{s}_n), \delta(t_1), \dots, \delta(t_n), \tau, \alpha, \lambda)$, the collection of all fixed dimensional parameters. The detailed updating procedure is provided as Algorithm S-8.1.

Algorithm S-8.1. *Detailed updating procedure of our spatio-temporal model*

- Initialise the number of components k ; let $k^{(0)}$ be the chosen initial value (we chose $k^{(0)} = 15$ as the initial value for our applications).
- Given $k = k^{(0)}$, let $\boldsymbol{\xi}^{(0)}$ denote the initial value of $\boldsymbol{\xi}$. Also, let $\boldsymbol{\eta}^{(0)}$ denote the initial value of $\boldsymbol{\eta}$.

- Since z and V are constrained random variables, we consider updating the reparameterized versions $V^* = \log(V)$ and $z^* = \log\left(\frac{z-a}{b-a}\right)$. After every iteration we invert the transformations to store the original variables V and z . For the sake of convenience of presentation of our algorithm we slightly abuse notation by referring to V^* and z^* as V and z respectively.
- For $t = 0, 1, 2, \dots$

1. Generate $u = (u_1, u_2, u_3) \sim \text{Multinomial}\left(1; \frac{1}{3}, \frac{1}{3}, \frac{1}{3}\right)$.

2. If $u_1 = 1$ (increase dimension from k to $k+1$ for each of the variables V, z, θ_1, θ_2), then

(a) Randomly select one co-ordinate from $\{1, \dots, k\}$. Let j denote the chosen co-ordinate.

(b) Generate $\epsilon_5 = (\epsilon_1, \dots, \epsilon_5) \stackrel{iid}{\sim} N(0, 1)\mathbb{I}_{\{\epsilon > 0\}}$ ($\mathbb{I}_{\{\epsilon > 0\}}$ denoting the indicator function). For updating the variable dimensional parameters, simulate

$$\zeta_{\ell,i}^{(1)} = \begin{cases} 1 & \text{w.p.} & \frac{1}{2} \\ -1 & \text{w.p.} & \frac{1}{2} \end{cases} \text{ for } i \in \{1, \dots, k\} \setminus \{j\} \text{ and } \ell = 1, \dots, 4,$$

and for updating the fixed one dimensional parameters, simulate

$$\zeta_{\ell}^{(2)} = \begin{cases} 1 & \text{w.p.} & \frac{1}{2} \\ -1 & \text{w.p.} & \frac{1}{2} \end{cases} \text{ for } \ell = 5, \dots, 10.$$

For updating fixed multi-dimensional parameters, simulate

$$\zeta_{\ell,i}^{(3)} = \begin{cases} 1 & \text{w.p.} & \frac{1}{2} \\ -1 & \text{w.p.} & \frac{1}{2} \end{cases} \text{ for } i \in \{1, \dots, n\} \text{ and } \ell = 11, 12, 13, 14.$$

(c) Propose the birth move as follows. For $i \in \{1, \dots, k\} \setminus \{j\}$, apply the additive transformation:

$$V_i^{(t)} \rightarrow (V_i^{(t)} + \zeta_{1,i}^{(1)} a_1 \epsilon_1)$$

$$z_i^{(t)} \rightarrow (z_i^{(t)} + \zeta_{2,i}^{(1)} a_2 \epsilon_2)$$

$$\theta_{1i}^{(t)} \rightarrow (\theta_{1i}^{(t)} + \zeta_{3,i}^{(1)} a_3 \epsilon_3)$$

$$\theta_{2i}^{(t)} \rightarrow (\theta_{2i}^{(t)} + \zeta_{4,i}^{(1)} a_4 \epsilon_4)$$

and split:

$$V_j^{(t)} \text{ into } (V_j^{(t)} + a_1 \epsilon_1) \text{ and } (V_j^{(t)} - a_1 \epsilon_1)$$

$$z_j^{(t)} \text{ into } (z_j^{(t)} + a_2 \epsilon_2) \text{ and } (z_j^{(t)} - a_2 \epsilon_2)$$

$$\theta_{1j}^{(t)} \text{ into } (\theta_{1j}^{(t)} + a_3 \epsilon_3) \text{ and } (\theta_{1j}^{(t)} - a_3 \epsilon_3)$$

$$\theta_{2j}^{(t)} \text{ into } (\theta_{2j}^{(t)} + a_4 \epsilon_4) \text{ and } (\theta_{2j}^{(t)} - a_4 \epsilon_4)$$

In other words, let $\mathbf{x}' = T_{b, \zeta^{(1)}}(\mathbf{x}^{(t)}, \epsilon_m) = (V', z', \theta'_1, \theta'_2)$ denote the complete birth move, where,

$$\begin{aligned} V' = & ((V_1^{(t)} + \zeta_{1,1}^{(1)} a_1 \epsilon_1) \dots (V_{j-1}^{(t)} + \zeta_{1,j-1}^{(1)} a_1 \epsilon_1), (V_j^{(t)} + a_1 \epsilon_1), (V_j^{(t)} - a_1 \epsilon_1) \\ & \dots (V_k^{(t)} + \zeta_{1,k}^{(1)} a_1 \epsilon_1)) \end{aligned}$$

(S-8.1)

$$\begin{aligned} \mathbf{z}' = & ((z_1^{(t)} + \zeta_{2,1}^{(1)} a_2 \epsilon_2) \dots (z_{j-1}^{(t)} + \zeta_{2,j-1}^{(1)} a_2 \epsilon_2), (z_j^{(t)} + a_2 \epsilon_2), (z_j^{(t)} - a_2 \epsilon_2) \\ & \dots (z_k^{(t)} + \zeta_{2,k}^{(1)} a_2 \epsilon_2)) \end{aligned} \quad (\text{S-8.2})$$

$$\begin{aligned} \boldsymbol{\theta}'_1 = & ((\theta_{1,1}^{(t)} + \zeta_{3,1}^{(1)} a_3 \epsilon_3) \dots (\theta_{1,j-1}^{(t)} + \zeta_{3,j-1}^{(1)} a_3 \epsilon_3), (\theta_{1,j}^{(t)} + a_3 \epsilon_3), (\theta_{1,j}^{(t)} - a_3 \epsilon_3) \\ & \dots (\theta_{1,k}^{(t)} + \zeta_{3,k}^{(1)} a_3 \epsilon_3)) \end{aligned} \quad (\text{S-8.3})$$

$$\begin{aligned} \boldsymbol{\theta}'_2 = & ((\theta_{2,1}^{(t)} + \zeta_{4,1}^{(1)} a_4 \epsilon_4) \dots (\theta_{2,j-1}^{(t)} + \zeta_{4,j-1}^{(1)} a_4 \epsilon_4), (\theta_{2,j}^{(t)} + a_4 \epsilon_4), (\theta_{2,j}^{(t)} - a_4 \epsilon_4) \\ & \dots (\theta_{2,k}^{(t)} + \zeta_{4,k}^{(1)} a_4 \epsilon_4)) \end{aligned} \quad (\text{S-8.4})$$

Re-label the $k+1$ elements of \mathbf{V}' as $(V'_1, V'_2, \dots, V'_{k+1})$,

\mathbf{z}' as $(z'_1, z'_2, \dots, z'_{k+1})$, $\boldsymbol{\theta}'_1$ as $(\theta'_{1,1}, \theta'_{1,2}, \dots, \theta'_{1,k+1})$, $\boldsymbol{\theta}'_2$ as $(\theta'_{2,1}, \theta'_{2,2}, \dots, \theta'_{2,k+1})$.

- (d) We apply the additive transformation based on the single ϵ_5 to update all the fixed dimensional parameter $\boldsymbol{\eta}$ as follows:

$$\begin{aligned} \varphi^{(t)} & \rightarrow (\varphi^{(t)} + \zeta_5^{(2)} a_5 \epsilon_5) \\ a_\delta^{(t)} & \rightarrow (a_\delta^{(t)} + \zeta_6^{(2)} a_6 \epsilon_5) \\ b_\psi^{(t)} & \rightarrow (b_\psi^{(t)} + \zeta_7^{(2)} a_7 \epsilon_5) \\ \alpha^{(t)} & \rightarrow (\alpha^{(t)} + \zeta_8^{(2)} a_8 \epsilon_5) \\ \lambda^{(t)} & \rightarrow (\lambda^{(t)} + \zeta_9^{(2)} a_9 \epsilon_5) \\ \tau^{(t)} & \rightarrow (\tau^{(t)} + \zeta_{10}^{(2)} a_{10} \epsilon_5) \\ \sigma^{(t)} & \rightarrow (\sigma^{(t)} + \zeta_{11}^{(2)} a_{11} \epsilon_5) \\ \psi_1^{(t)}(\mathbf{s}_i) & \rightarrow (\psi_1^{(t)}(\mathbf{s}_i) + \zeta_{12,i}^{(3)} a_{12} \epsilon_5) \\ \psi_2^{(t)}(\mathbf{s}_i) & \rightarrow (\psi_2^{(t)}(\mathbf{s}_i) + \zeta_{13,i}^{(3)} a_{13} \epsilon_5) \\ \delta^{(t)}(t_i) & \rightarrow (\delta^{(t)}(t_i) + \zeta_{14,i}^{(3)} a_{14} \epsilon_5) \end{aligned}$$

Let $\boldsymbol{\eta}' = T_{b,\zeta^{(2)}}(\boldsymbol{\eta}^{(t)}, \epsilon_5) = (\varphi', a'_\delta, b'_\psi, \psi'_1(\mathbf{s}_1), \dots, \psi'_1(\mathbf{s}_n), \psi'_2(\mathbf{s}_1), \dots, \psi'_2(\mathbf{s}_n), \delta'(t_1), \dots, \delta'(t_n), \tau', \alpha', \lambda', \sigma')$ denote the complete move type for fixed dimensional parameters.

In the above transformations the a_i 's are the scaling constants to be chosen appropriately; see [Das and Bhattacharya \(2019b\)](#) and [Dey and Bhattacharya \(2018\)](#) (see also [Dey and Bhattacharya \(2019\)](#)) for the details. In our applications we choose the scales on the basis of pilot runs of our TTMC algorithm.

- (e) Calculate the acceptance probability:

$$a_{b,\zeta}(\boldsymbol{\xi}^{(t)}, \boldsymbol{\eta}^{(t)}, \boldsymbol{\epsilon}_5) = \min \left\{ 1, \frac{\pi(\boldsymbol{\xi}', \boldsymbol{\eta}')}{\pi(\boldsymbol{\xi}^{(t)}, \boldsymbol{\eta}^{(t)})} \left| \frac{\partial(T_{b,\zeta^{(1)}}(\boldsymbol{\xi}^{(t)}, \boldsymbol{\epsilon}_4))}{\partial(\boldsymbol{\xi}^{(t)}, \boldsymbol{\epsilon}_4)} \right| \left| \frac{\partial(T_{b,\zeta^{(2)}}(\boldsymbol{\eta}^{(t)}, \boldsymbol{\epsilon}_5))}{\partial(\boldsymbol{\eta}^{(t)}, \boldsymbol{\epsilon}_5)} \right| \right\},$$

where

$$\frac{\partial(T_{b,\zeta^{(1)}}(\boldsymbol{\xi}^{(t)}, \boldsymbol{\epsilon}_4))}{\partial(\boldsymbol{\xi}^{(t)}, \boldsymbol{\epsilon}_4)} = 2^4 a_1 a_2 a_3 a_4$$

and

$$\frac{\partial(T_{b,\zeta^{(2)}}(\boldsymbol{\eta}^{(t)}, \boldsymbol{\epsilon}_5))}{\partial(\boldsymbol{\eta}^{(t)}, \boldsymbol{\epsilon}_5)} = 1.$$

(f) Set

$$(\boldsymbol{\xi}^{(t+1)}, \boldsymbol{\eta}^{(t+1)}) = \begin{cases} (\boldsymbol{\xi}', \boldsymbol{\eta}') & \text{with probability } a_{b,\zeta}(\boldsymbol{\xi}^{(t)}, \boldsymbol{\eta}^{(t)}, \boldsymbol{\epsilon}_5), \\ (\boldsymbol{\xi}^{(t)}, \boldsymbol{\eta}^{(t)}) & \text{with probability } 1 - a_{b,\zeta}(\boldsymbol{\xi}^{(t)}, \boldsymbol{\eta}^{(t)}, \boldsymbol{\epsilon}_5). \end{cases}$$

3. If $u_2 = 1$ (decrease dimension from k to $k-1$ for each of the variables $\mathbf{V}, \mathbf{z}, \boldsymbol{\theta}_1, \boldsymbol{\theta}_2$), then

(a) Generate $\boldsymbol{\epsilon}_5 = (\epsilon_1, \dots, \epsilon_5) \stackrel{iid}{\sim} N(0, 1) \mathbb{I}_{\{\epsilon > 0\}}$.

(b) Randomly select one co-ordinate from $\{1, 2, \dots, k-1\}$. Let j be the selected co-ordinate. Then let

$$V_j^* = ((V_j + a_1 \epsilon_1) + (V_{j+1} - a_1 \epsilon_1)) / 2;$$

replace the co-ordinate V_j by the average V_j^* and delete V_{j+1} . Similarly, let

$$z_j^* = ((z_j + a_2 \epsilon_2) + (z_{j+1} - a_2 \epsilon_2)) / 2;$$

replace the co-ordinate z_j by the average z_j^* and delete z_{j+1} . Form

$$\theta_{1,j}^* = ((\theta_{1,j} + a_3 \epsilon_3) + (\theta_{1,j+1} - a_3 \epsilon_3)) / 2;$$

and replace the co-ordinate $\theta_{1,j}$ by the average $\theta_{1,j}^*$ and delete $\theta_{1,j+1}$; create

$$\theta_{2,j}^* = ((\theta_{2,j} + a_4 \epsilon_4) + (\theta_{2,j+1} - a_4 \epsilon_4)) / 2;$$

and replace the co-ordinate $\theta_{2,j}$ by the average $\theta_{2,j}^*$ and delete $\theta_{2,j+1}$.

(c) Simulate ζ similarly as in the case of the birth move.

(d) For the co-ordinates other than j and $j+1$ apply the additive transformation

$$\begin{aligned} V_i^{(t)} &\rightarrow (V_i^{(t)} + \zeta_{1,i}^{(1)} a_1 \epsilon_1) \\ z_i^{(t)} &\rightarrow (z_i^{(t)} + \zeta_{2,i}^{(1)} a_2 \epsilon_2) \\ \theta_{1i}^{(t)} &\rightarrow (\theta_{1i}^{(t)} + \zeta_{3,i}^{(1)} a_3 \epsilon_3) \\ \theta_{2i}^{(t)} &\rightarrow (\theta_{2i}^{(t)} + \zeta_{4,i}^{(1)} a_4 \epsilon_4) \\ &\text{for } i \in \{1, \dots, k\} \setminus \{j, j+1\}. \end{aligned}$$

(e) In other words, let $\boldsymbol{\xi}' = T_{d,\zeta^{(1)}}(\boldsymbol{\xi}^{(t)}, \boldsymbol{\epsilon}_4) = (\mathbf{V}', \mathbf{z}', \boldsymbol{\theta}'_1, \boldsymbol{\theta}'_2)$ denote the complete death move, where,

$$\begin{aligned} \mathbf{V}' &= ((V_1^{(t)} + \zeta_{1,1}^{(1)} a_1 \epsilon_1) \dots (V_{j-1}^{(t)} + \zeta_{1,j-1}^{(1)} a_1 \epsilon_1), V_j^*, (V_{j+2}^{(t)} + \zeta_{1,j+2}^{(1)} a_1 \epsilon_1) \\ &\quad \dots (V_k^{(t)} + \zeta_{1,k}^{(1)} a_1 \epsilon_1)) \end{aligned}$$

(S-8.5)

$$\mathbf{z}' = ((z_1^{(t)} + \zeta_{2,1}^{(1)} a_2 \epsilon_2) \dots (z_{j-1}^{(t)} + \zeta_{2,j-1}^{(1)} a_2 \epsilon_2), z_j^*, (z_{j+21}^{(t)} + \zeta_{2,j+21}^{(1)} a_2 \epsilon_2), \dots (z_k^{(t)} + \zeta_{2,k}^{(1)} a_2 \epsilon_2)) \quad (\text{S-8.6})$$

$$\boldsymbol{\theta}'_1 = ((\theta_{1,1}^{(t)} + \zeta_{3,1}^{(1)} a_3 \epsilon_3) \dots (\theta_{1,j-1}^{(t)} + \zeta_{3,j-1}^{(1)} a_3 \epsilon_3), \theta_{1,j}^*, (\theta_{1,j+2}^{(t)} + \zeta_{3,j+2}^{(1)} a_3 \epsilon_3) \dots (\theta_{1,k}^{(t)} + \zeta_{3,k}^{(1)} a_3 \epsilon_3)) \quad (\text{S-8.7})$$

$$\boldsymbol{\theta}'_2 = ((\theta_{2,1}^{(t)} + \zeta_{4,1}^{(1)} a_4 \epsilon_4) \dots (\theta_{2,j-1}^{(t)} + \zeta_{4,j-1}^{(1)} a_4 \epsilon_4), \theta_{2,j}^*, (\theta_{2,j+2}^{(t)} + \zeta_{4,j+2}^{(1)} a_4 \epsilon_4) \dots (\theta_{2,k}^{(t)} + \zeta_{4,k}^{(1)} a_4 \epsilon_4)) \quad (\text{S-8.8})$$

Re-label the $k-1$ elements of \mathbf{V}' as $(V'_1, V'_2, \dots, V'_{k-1})$, \mathbf{z}' as $(z'_1, z'_2, \dots, z'_{k-1})$, $\boldsymbol{\theta}'_1$ as $(\theta'_{1,1}, \theta'_{1,2}, \dots, \theta'_{1,k-1})$, and $\boldsymbol{\theta}'_2$ as $(\theta'_{2,1}, \theta'_{2,2}, \dots, \theta'_{2,k-1})$.

- (f) Solve for ϵ_1^* from the equations $V_j^* + a_1 \epsilon_1^* = V_j$ and $V_j^* - a_1 \epsilon_1^* = V_{j+1}$, which yield $\epsilon_1^* = \frac{(V_j - V_{j+1})}{2a_1}$. Similarly, we have $\epsilon_2^* = \frac{(z_j - z_{j+1})}{2a_2}$, $\epsilon_3^* = \frac{(\theta_{1,j} - \theta_{1,j+1})}{2a_3}$ and $\epsilon_4^* = \frac{(\theta_{2,j} - \theta_{2,j+1})}{2a_4}$. Let $\boldsymbol{\epsilon}_4^* = (\epsilon_1^*, \dots, \epsilon_4^*)$.
- (g) For updating the fixed dimensional parameters $\boldsymbol{\eta} = (\varphi, a_\delta, b_\psi, \psi_1(\mathbf{s}_1), \dots, \psi_1(\mathbf{s}_n), \psi_2(\mathbf{s}_1), \dots, \psi_2(\mathbf{s}_n), \delta(t_1), \dots, \delta(t_n), \tau, \alpha, \lambda, \sigma)$ implement step 2 (d).
- (h) Calculate the acceptance probability of the death move:

$$a_{d,\zeta}(\boldsymbol{\xi}^{(t)}, \boldsymbol{\eta}^{(t)}, \boldsymbol{\epsilon}_5, \boldsymbol{\epsilon}_4^*) = \min \left\{ 1, \frac{\pi(\boldsymbol{\xi}', \boldsymbol{\eta}')}{\pi(\boldsymbol{\xi}^{(t)}, \boldsymbol{\eta}^{(t)})} \left| \frac{\partial(T_{d,\zeta(1)}(\boldsymbol{\xi}^{(t)}, \boldsymbol{\epsilon}_4), \boldsymbol{\epsilon}_4^*, \boldsymbol{\epsilon}_4)}{\partial(\boldsymbol{\xi}^{(t)}, \boldsymbol{\epsilon}_4)} \right| \left| \frac{\partial(T_{d,\zeta(2)}(\boldsymbol{\eta}^{(t)}, \boldsymbol{\epsilon}_5))}{\partial(\boldsymbol{\eta}^{(t)}, \boldsymbol{\epsilon}_5)} \right| \right\},$$

where

$$\left| \frac{\partial(T_{d,\zeta(1)}(\boldsymbol{\xi}^{(t)}, \boldsymbol{\epsilon}_4), \boldsymbol{\epsilon}_4^*, \boldsymbol{\epsilon}_4)}{\partial(\boldsymbol{\xi}^{(t)}, \boldsymbol{\epsilon}_4)} \right| = \frac{1}{2^4 a_1 a_2 a_3 a_4}$$

and

$$\frac{\partial(T_{d,\zeta(2)}(\boldsymbol{\eta}^{(t)}, \boldsymbol{\epsilon}_5))}{\partial(\boldsymbol{\eta}^{(t)}, \boldsymbol{\epsilon}_5)} = 1.$$

- (i) Set

$$(\boldsymbol{\xi}^{(t+1)}, \boldsymbol{\eta}^{(t+1)}) = \begin{cases} (\boldsymbol{\xi}', \boldsymbol{\eta}') & \text{with probability } a_{d,\zeta}(\boldsymbol{\xi}^{(t)}, \boldsymbol{\eta}^{(t)}, \boldsymbol{\epsilon}_5, \boldsymbol{\epsilon}_4^*), \\ (\boldsymbol{\xi}^{(t)}, \boldsymbol{\eta}^{(t)}) & \text{with probability } 1 - a_{d,\zeta}(\boldsymbol{\xi}^{(t)}, \boldsymbol{\eta}^{(t)}, \boldsymbol{\epsilon}_5, \boldsymbol{\epsilon}_4^*). \end{cases}$$

4. If $u_3 = 1$ (dimension remains unchanged), then update $(\boldsymbol{\xi}^{(t)}, \boldsymbol{\eta}^{(t)})$ by implementing steps (1), (2), (3) of Algorithm 3.1 of [Dutta and Bhattacharya \(2014\)](#).

• End for

S-9 Simulation study

S-9.1 Algorithm for generating the synthetic data

We have performed the following steps to simulate a non stationary 95×1 vector:

1. We first take a grid of size 100.
2. We generate one random number t_i from each interval $(i - 1, i]$; $i = 1, \dots, 100$ as 100 time points. We store the time points in a vector which we denote by $\mathbf{t} = (t(1), \dots, t(100))'$.
3. Next we generate 100 random points of the form $\{\mathbf{s}_i = (s(1, i), s(2, i)); i = 1, \dots, 100\}$ from $[0, 50] \times [0, 50]$ as locations. We store the locations in a 100×2 matrix $\mathbf{S} = (\mathbf{s}'_1, \dots, \mathbf{s}'_{100})'$.
4. Then we randomly choose 5 time points from \mathbf{t} and 5 locations from \mathbf{S} and omit these random points from \mathbf{t} and \mathbf{S} . So, we obtain a new time vector of length 95, say \mathbf{t}_{95} and a new matrix of locations of order 95×2 , say \mathbf{S}_{95} . We store the omitted time points in a separate vector, \mathbf{t}_5 , and the locations in a separate matrix, \mathbf{S}_5 , for future use.
5. Next we calculate the covariance matrix $\mathbf{A} = (\mathbf{A}(i, j))$ of order 100×100 based on \mathbf{t} and \mathbf{S} , where (i, j) -th element of \mathbf{A} is given by

$$\mathbf{A}(i, j) = \begin{cases} 1 & \text{if } i = j \\ \exp\left(-0.5\sqrt{(t(i) - t(j))^2 + (s(1, i) - s(1, j))^2 + (s(2, i) - s(2, j))^2}\right) & \text{if } i \neq j \end{cases}$$

6. We partition the above covariance function \mathbf{A} consisting of four component matrices $\mathbf{A}_{11}, \mathbf{A}_{12}, \mathbf{A}_{21}$ and \mathbf{A}_{22} , where \mathbf{A}_{11} is a 5×5 covariance matrix based on \mathbf{t}_5 and \mathbf{S}_5 ; \mathbf{A}_{22} is a 95×95 covariance matrix based on \mathbf{t}_{95} and \mathbf{S}_{95} (the form of the (i, j) -th element being the same as for the matrix \mathbf{A} , except now \mathbf{t}, \mathbf{S} are replaced with \mathbf{t}_5 and \mathbf{S}_5 for \mathbf{A}_{11} ; for \mathbf{A}_{22} , \mathbf{t}, \mathbf{S} are replaced with \mathbf{t}_{95} and \mathbf{S}_{95}); $\mathbf{A}_{12} = \mathbf{A}_{21}^T$ is a 5×95 matrix, containing the covariances between the deleted points and existing points. The (i, j) -th element of \mathbf{A}_{12} is given by

$$\mathbf{A}_{12}(i, j) = \left(-0.5\sqrt{(t_5(i) - t_{95}(j))^2 + (s_5(1, i) - s_{95}(1, j))^2 + (s_5(2, i) - s_{95}(2, j))^2}\right),$$

for $i = 1, \dots, 5$ and $j = 1, \dots, 95$.

7. Next we generate one 5 dimensional random sample, \mathbf{x}_5 , from a 5 variate normal distribution with mean function

$$\boldsymbol{\mu}_5^T = \mathbf{D}_5 \boldsymbol{\beta},$$

and covariance matrix \mathbf{A}_{11} , where $\boldsymbol{\beta}_5^T = (0.1, 0.01, 0.02)$ and $\mathbf{D}_5 = (\mathbf{t}_5; \mathbf{S}_5)$ is the design matrix. Note that \mathbf{D}_5 is a 5×3 matrix.

8. Given \mathbf{x}_5 we simulate a 95×1 random vector, $\mathbf{x}_{(95|5)}$ from a conditional 95 variate normal distribution with mean

$$\boldsymbol{\mu}_{(95|5)}^T = \mathbf{D}_{95}\boldsymbol{\beta} + (\mathbf{x}_5 - \boldsymbol{\mu}_5)^T \mathbf{A}_{11}^{-1} \mathbf{A}_{12}$$

and covariance

$$\boldsymbol{\Sigma}_{(95|5)} = \mathbf{A}_{22} - \mathbf{A}_{21} \mathbf{A}_{11}^{-1} \mathbf{A}_{12},$$

where \mathbf{D}_{95} is obtained exactly same as \mathbf{D}_5 , only \mathbf{t}_5 and \mathbf{S}_5 are replaced with \mathbf{t}_{95} and \mathbf{S}_{95} , respectively.

9. The last step is to simulate a 95×1 vector, $\mathbf{y}_{(95|\mathbf{x}_{(95|5)})}$, conditionally on $\mathbf{x}_{(95|5)}$. We simulate $\mathbf{y}_{(95|\mathbf{x}_{(95|5)})}$ from a 95 variate normal distribution with mean

$$\boldsymbol{\mu}_{\mathbf{y}}^T = 0.01(\mathbf{x}_{(95|5)})^T$$

and covariance matrix

$$\boldsymbol{\Sigma}_{\mathbf{y}} = \begin{cases} 1 & \text{if } i = j \\ \exp(-0.5(|x_{(95|5)}(i) - x_{(95|5)}(j)|)) & \text{if } i \neq j, \end{cases}$$

for $i = 1, \dots, 95$ and $j = 1, \dots, 95$.

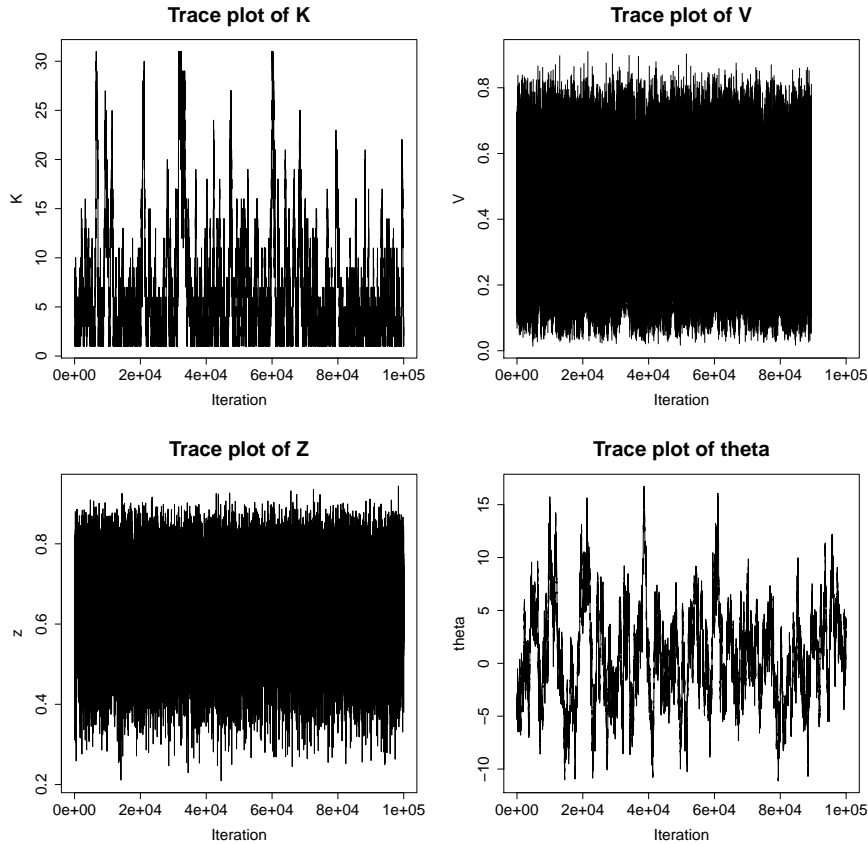


Figure S-1: Simulation study: Traceplots of variable dimensional parameters.

S-10 Real data analysis

S-10.1 Spatial Data

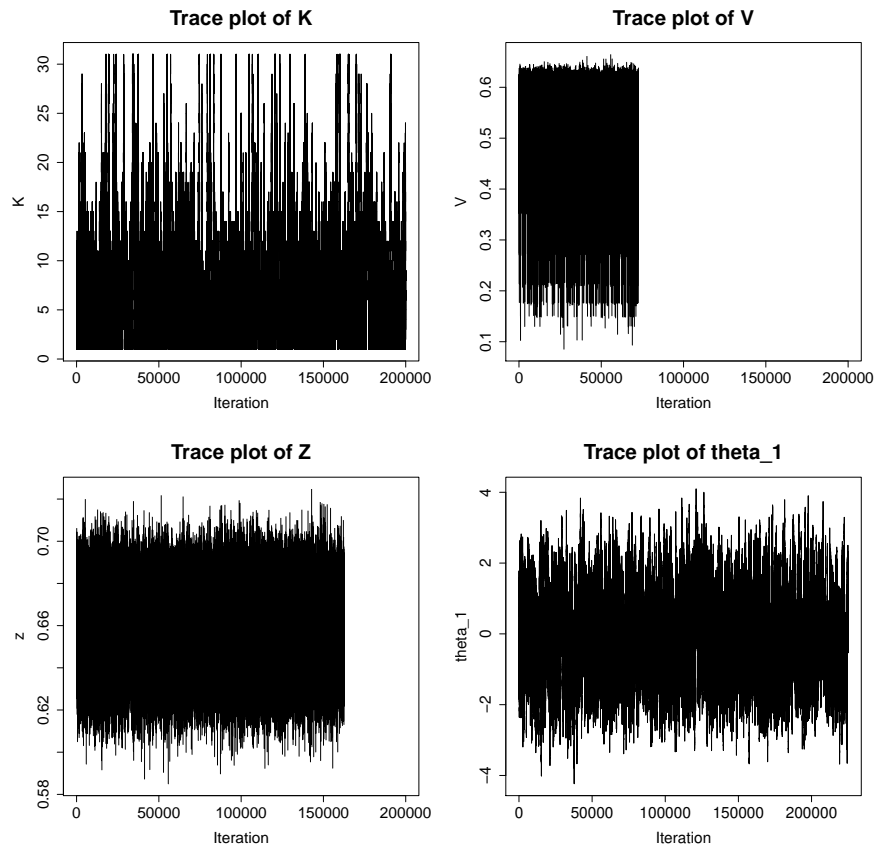


Figure S-1: Real spatial data analysis: Traceplots of variable dimensional parameters.

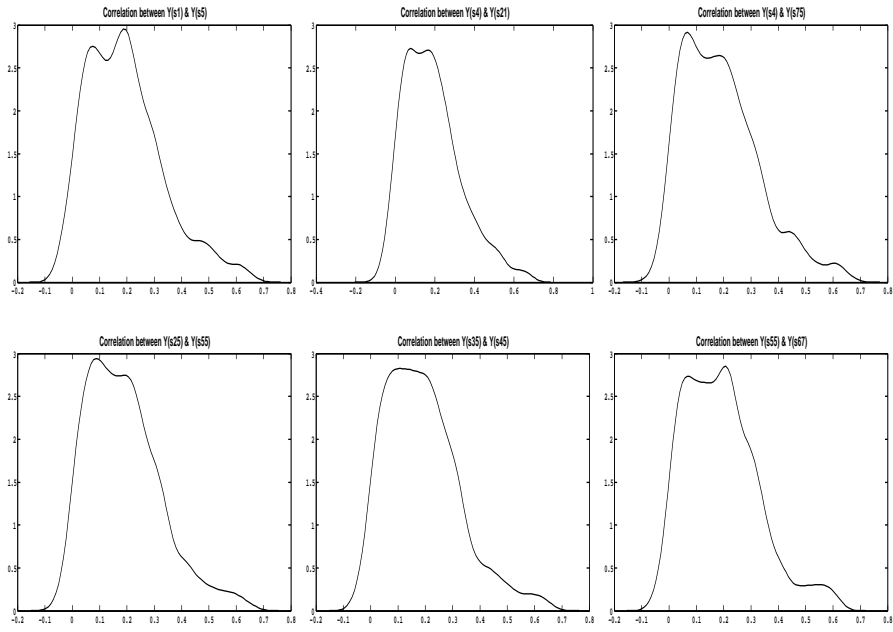


Figure S-2: Real spatial data analysis: Posterior densities of correlations for 6 different pairs of locations.

S-10.2 Spatio-temporal Data

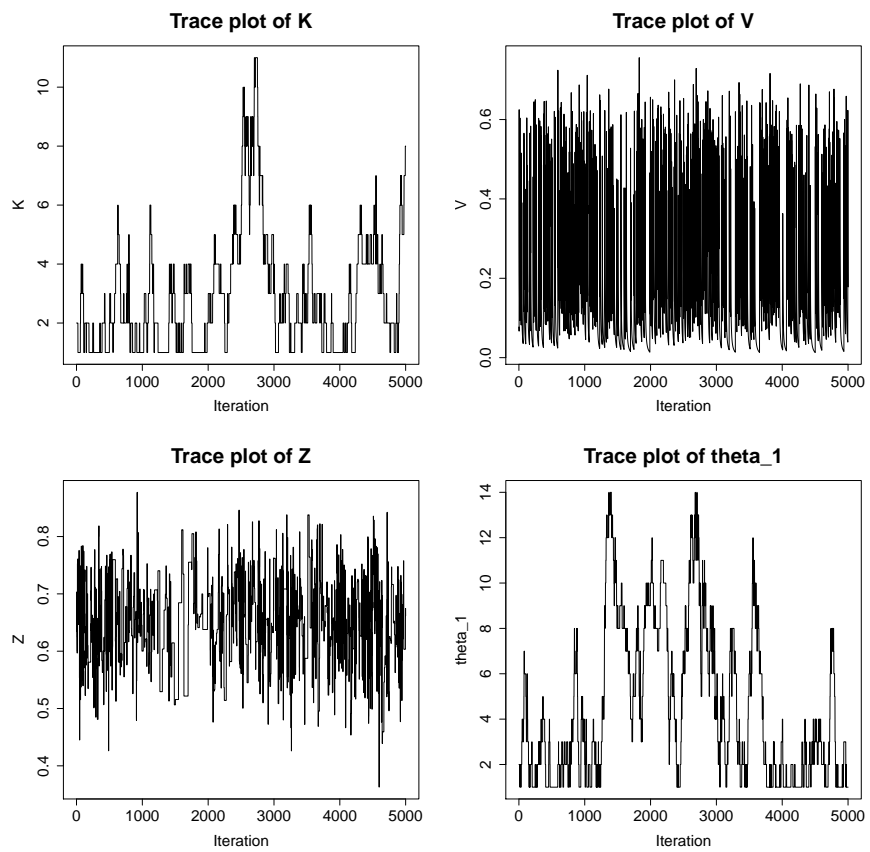
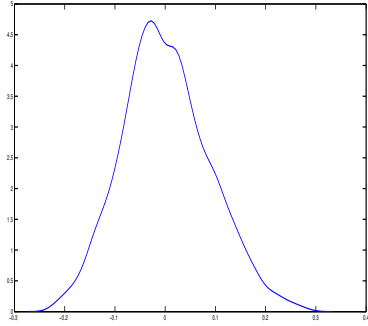
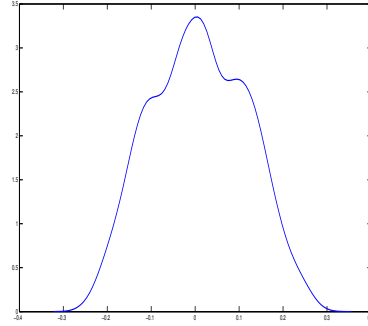


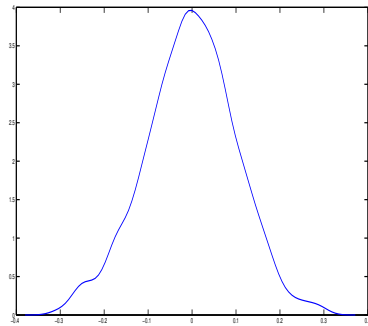
Figure S-3: Real spatio-temporal data analysis: Traceplots of variable dimensional parameters.



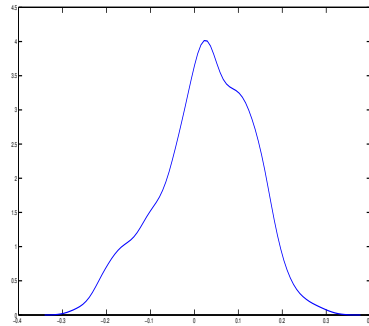
(a) Correlation between $(y_{1,21}, y_{2,21})$



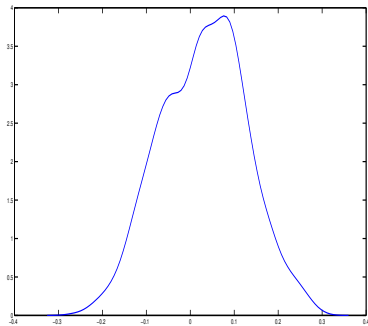
(b) Correlation between $(y_{1,21}, y_{7,21})$



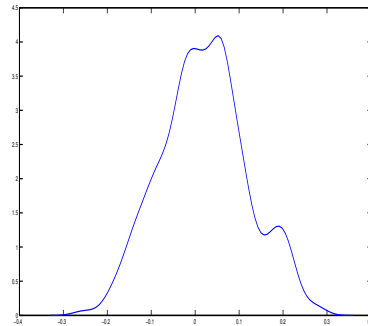
(c) Correlation between $(y_{2,21}, y_{7,21})$



(d) Correlation between $(y_{24,15}, y_{40,15})$



(e) Correlation between $(y_{24,15}, y_{49,15})$



(f) Correlation between $(y_{40,15}, y_{49,15})$

Figure S-4: Real spatio-temporal data analysis: Posterior densities of correlations for 6 different pairs of spatio-temporal points.

Bibliography

- Banerjee, S. and Gelfand, A. E. (2003). On Smoothness Properties of Spatial Processes. *Journal of Multivariate Analysis*, **84**, 85100.
- Chang, Y.-M., Hsu, N.-J., and Huang, H.-C. (2011). Semiparametric Estimation and Selection for Nonstationary Spatial Covariance Functions. *Journal of Computational and Graphical Statistics*, **19**, 117–139.
- Cressie, N. A. C. and Wikle, C. K. (2011). *Statistics for Spatio-Temporal Data*. Wiley, New York.
- Damian, D., Sampson, P. D., and Guttorp, P. (2001). Bayesian Estimation of Semi-Parametric Non-stationary Spatial Covariance Structures. *Environmetrics*, **12**, 161–178.
- Das, M. and Bhattacharya, S. (2019a). Supplement to “Nonstationary, Nonparametric, Nonseparable Bayesian Spatio-Temporal Modeling Using Kernel Convolution of Order Based Dependent Dirichlet Process”. arXiv preprint.
- Das, M. and Bhattacharya, S. (2019b). Transdimensional Transformation Based Markov Chain Monte Carlo. *Brazilian Journal of Probability and Statistics*, **33**, 87–138.
- Dey, K. K. and Bhattacharya, S. (2018). A Brief Tutorial on Transformation Based Markov Chain Monte Carlo and Optimal Scaling of the Additive Transformation. *Brazilian Journal of Probability and Statistics*, **31**, 569–617.
- Dey, K. K. and Bhattacharya, S. (2019). A Brief Review of Optimal Scaling of the Main MCMC Approaches and Optimal Scaling of Additive TMCMC Under Non-Regular Cases. *Brazilian Journal of Probability and Statistics*, **33**, 222–266.
- Duan, J. A., Guindani, M., and Gelfand, A. E. (2007). Generalized Spatial Dirichlet Process Models. *Biometrika*, **94**, 809–825.
- Duan, J. A., Gelfand, A. E., and Sirmans, C. F. (2009). Modeling Space-Time Data Using Stochastic Differential Equations. *Bayesian Analysis*, **4**, 733–758.
- Dutta, S. and Bhattacharya, S. (2014). Markov Chain Monte Carlo Based on Deterministic Transformations. *Statistical Methodology*, **16**, 100–116. Also available at <http://arxiv.org/abs/1106.5850>. Supplement available at <http://arxiv.org/abs/1306.6684>.

- Ferguson, T. S. (1973). A Bayesian Analysis of Some Nonparametric Problems. *The Annals of Statistics*, **1**, 209–230.
- Ferguson, T. S. (1974). Prior Distributions on Spaces of Probability Measures. *The Annals of Statistics*, **2**, 615–629.
- Fuentes, M. (2002). Spectral Methods for Nonstationary Spatial Processes. *Biometrika*, **89**, 197–210.
- Fuentes, M. and Reich, B. (2013). Multivariate Spatial Nonparametric Modelling via Kernel Process Mixing. *Statistica Sinica*, **23**, 75–97.
- Fuentes, M. and Smith, R. L. (2001). A New Class of Nonstationary Spatial Models. Technical Report, Department of Statistics, North Carolina State University.
- Geisser, S. (1993). *Predictive Inference : An for Introduction*. Chapman & Hall, London.
- Gelfand, A. E., Kottas, A., and MacEachern, S. N. (2005). Bayesian Nonparametric Spatial Modeling With Dirichlet Process Mixing. *Journal of the American Statistical Association*, **100**, 1021–1035.
- Gilani, O., Berrocal, V. J., and Batterman, S. A. (2016). Non-stationary Spatio-temporal Modeling of Traffic-related Pollutants in Near-road Environments. *Spatial and Spatio-temporal Epidemiology*, **18**, 24–37.
- Griffin, J. E. and Steel, M. F. J. (2004). Semiparametric Bayesian Inference for Stochastic Frontier Models. *Journal of Econometrics*, **123**, 121–152.
- Griffin, J. E. and Steel, M. F. J. (2006). Order-Based Dependent Dirichlet Processes. *Journal of the American Statistical Association*, **101**, 179–194.
- Guttorp, P. and Sampson, P. D. (1994). Methods for Estimating Heterogeneous Spatial Covariance Functions with Environmental Applications. In G. P. Patil and C. R. Rao, editors, *Handbook of Statistics XII: Environmental Statistics*, pages 663–690, New York. Elsevier/North Holland.
- Guttorp, P., Schmidt, A. M., Bartlett, M., and Besag, J. (2013). Covariance Structure of Spatial and Spatiotemporal Processes. *WIREs Comput Stat*, pages 279–287.
- Haas, T. C. (1995). Local Prediction of a Spatio-Temporal Process with an Application to Wet Sulfate Deposition. *Journal of the American Statistical Association*, **90**, 1189–1199.

- Higdon, D. (1998). A Process-Convolution Approach to Modeling Temperatures in the North Atlantic Ocean. *Environmental and Ecological Statistics*, **5**, 173190.
- Higdon, D. (2001). Space and Space-Time Modeling Using Process Convolutions. In C. W. A. V. Barnett, P. C. Chatwin, and A. H. El-Sharaawi, editors, *Quantitative Methods for Current Environmental Issues*, pages 37–56, London. Springer-Verlag.
- Higdon, D., Swall, J., and Kern, J. (1999). Non-Stationary Spatial Modeling. In J. M. Bernardo, J. O. Berger, A. P. Dawid, and A. F. M. Smith, editors, *Bayesian Statistics 6*, pages 761–768, Oxford. Oxford University Press.
- Ingebrigtsen, R., Lindgren, F., and Steinsland, I. (2014). Spatial Models with Explanatory Variables in the Dependence Structure. *Spatial Statistics*, **8**, 20–38.
- Ishwaran, H. and James, L. F. (2001). Gibbs Sampling Methods for Stick-Breaking Prior. *Journal of the American Statistical Association*, **96**, 161–173.
- Kim, H.-m., Mallick, B. K., and Holmes, C. C. (2005). Analyzing Nonstationary Spatial Data using Piecewise Gaussian Processes. *Journal of the American Statistical Association*, pages 653–668.
- Kottas, A., Duan, J. A., and Gelfand, A. E. (2007). Modeling Disease Incidence Data with Spatial and Spatio-Temporal Dirichlet Process Mixtures. *Biometrical Journal*, **49**, 1–14.
- Neto, J. H. V., Schmidt, A. M., and Guttorp, P. (2014). Accounting for Spatially Varying Directional Effects in Spatial Covariance Structures. *Journal of the Royal Statistical Society. Series C (Applied Statistics)*, **63**, 103–122.
- Nott, D. J. and Dunsmuir, W. T. M. (2002). Estimation of Nonstationary Spatial Covariance Structure. *Biometrika*, **89**, 819–829.
- Paciorek, C. J. (2003). *Nonstationary Gaussian Process for Regression and Spatial Modeling*. Doctoral thesis, Carnegie Mellon University.
- Paciorek, C. J., Yanosky, J. D., and Puett, R. C. (2009). Practical Large-scale Spatio-Temporal Modeling of Particulate Matter Concentrations. *The Annals of Applied Statistics*, **3**, 370–397.
- Petrone, S., Guindani, M., and Gelfand, A. E. (2009). Hybrid Dirichlet Mixture Models for Functional Data. *Journal of the Royal Statistical Society. Series B*, **71**, 755–782.

- Pettit, L. (1990). The Conditional of Predictive-Ordinate for the Normal Distribution. *Journal of the Royal Statistical Society: Series B*, **52**, 175–184.
- Reich, B. J., Fuentes, M., and Dunson, D. B. (2011). Bayesian Spatial Quantile Regression. *Journal of the American Statistical Association*, **106**, 6–20.
- Risser, M. D. and Calder, C. A. (2015). Regression-based Covariance Functions for Nonstationary Spatial Modeling. *Environmetrics*, **26**, 284–297.
- Risser, M. D., Calder, C. A., Berrocal, V. J., and Berrett, C. (2019). Nonstationary Spatial Prediction of Soil Organic Carbon: Implications for Stock Assessment Decision Making. *The Annals of Applied Statistics*, **13**, 165–188.
- Roy, S. and Bhattacharya, S. (2020). Bayesian Characterizations of Properties of Stochastic Processes with Applications. ArXiv Preprint.
- Sampson, P. D. and Guttorp, P. (1992). Nonparametric Estimation of Nonstationary Spatial Covariance Structure. *Journal of the American Statistical Association*, **87**, 1081–109.
- Schmidt, A. M. and O’Hagan, A. (2003). Bayesian Inference for Nonstationary Spatial Covariance Structure via Spatial Deformations. *Journal of the Royal Statistical Society: Series B*, **65**, 743–758.
- Schmidt, A. M., Guttorp, P., and O’Hagan, A. (2011). Considering Covariates in the Covariance Structure of Spatial Processes. *Environmetrics*, **22**, 487–500.
- Sethuraman, J. (1994). A constructive definition of Dirichlet priors. *Statistica Sinica*, **4**, 639–650.
- Stein, M. L. (1999). *Interpolation of Spatial Data: Some Theory for Kriging*. Springer-Verlag, New York.
- Wolpert, R. L., Clyde, M. A., and Tu, C. (2011). Stochastic Expansions Using Continuous Dictionaries: Lévy Adaptive Regression Kernels. *Annals of Statistics (to appear)*.
- Yaglom, A. M. (1987a). *Correlation Theory of Stationary and Related Random Functions—Volume-I: Basic Results*. Springer-Verlag, New York.
- Yaglom, A. M. (1987b). *Correlation Theory of Stationary and Related Random Functions—Volume-II: Supplementary Notes and References*. Springer-Verlag, New York.

Yanosky, J. D., Paciorek, C. J., and Suh, H. H. (2008a). Predicting Chronic Fine Particulate Exposures Using Spatio-temporal Models for the Northeastern and Midwestern U.S. *Environmental Health Perspectives*, **117**, 522–529.

Yanosky, J. D., Paciorek, C. J., Schwartz, J., Laden, F., Puett, R. C., and Suh, H. H. (2008b). Spatio-temporal Modeling of Chronic Pm10 Exposures of Nurses Health Study. *Atmospheric Environment*, **47**, 4047–4062.